Discovering and imaging mineral systems at all scales using natural-source electromagnetic methods

Dr. Alan G. Jones

ManoTick GeoSolutions Ltd.

Presented to SAGA
13th November, 2025

MTGS

MT Short Course

I give a 2-day lecture course on MT, or 4-5 days with hands-on components

- can be run in-house over 2-4/5 days
- or virtually over 2-4/5 days, or 4-8/10 half-days over 2-4/5 weeks
- contact me for details: alan.jones@manotick-geosolutions.com

Magnetotellurics Course:
From Theory to Interpretation

Alan G. Jones

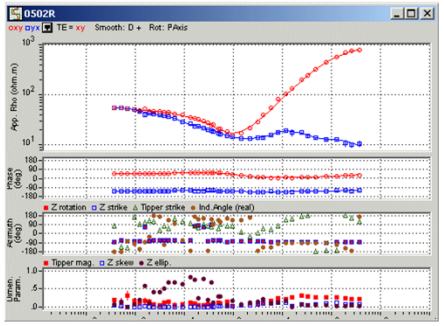

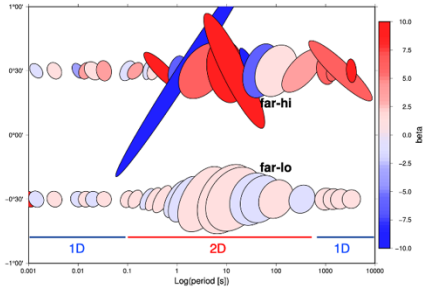

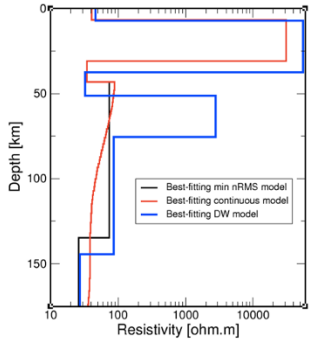

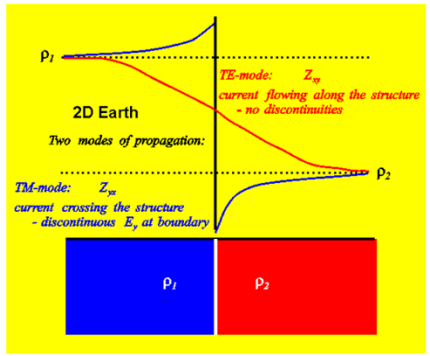

$$div\ \mathbf{B} = 0$$
$$div\ \mathbf{D} = q$$
$$curl\ \mathbf{E} = -\partial \mathbf{B} / \partial t$$
$$curl\ \mathbf{H} = \mathbf{J} + \partial \mathbf{D} / \partial t$$

EMIW – 2 - 8 August, St. John's, NL

Division 6 of IAGA has been running a very successful series of workshops since 1972 on EM Induction – EM Induction Workshops (EMIWs)

These EMIWs have been all over the world, including twice before in Canada (Ottawa, 1974; Victorian, 1982).

And will return to Canada next year!

"The 27th international Workshop on Electromagnetic Induction in the Earth and Planetary Bodies (EMIW2026) will be held from August 2–8, 2026, in the vibrant city of St. John's, Newfoundland and Labrador, Canada."

Make sure to put this on your calendar!!!

MT3DINV4 – 31 July – 2 August, St. John's, NL

I have been running a series of workshops on MT data inversion in 3-D, called MT3DINV.

The results from the first two were presented in Miensopust et al. (2013)

Magnetotelluric 3-D inversion—a review of two successful workshops on forward and inversion code testing and comparison

Marion P. Miensopust,[1,2,*] Pilar Queralt,[3] Alan G. Jones[1] and the 3D MT modellers[†]

[1]*Dublin Institute for Advanced Studies, School of Cosmic Physics, Dublin, Ireland. E-mail: Marion.Miensopust@bgr.de*
[2]*Institut für Geophysik, Westfälische Wilhelms-Universität Münster, Germany*
[3]*Deptartment Geodinàmica i Geofisica, Universitat de Barcelona, Spain*

A fourth workshop will take place for 2 ½ days in St. John's, NL, on 31 July – 2 August just prior to the EM Induction Workshop (2-8 August, 2026)

Three parts:

1) A model that you have to calculate the fields and responses for
2) A secret model that you have to invert for structure
3) Real data that you have to invert for structure ← New

Natural Source EM

Dominantly ground-based “magnetotellurics”, but also “tippers” and encouraging airborne methods (ZTEM, MobileMT, QAMT)

Two signal sources:

>8 Hz: Global lightning storms

<8 Hz: Solar activity

Magnetotellurics - MT

Formally local 2-horizontal component **E** (Ex, Ey) and local 3-component **H** (Hx, Hy, Hz)

Relate the fields by:

$$\begin{bmatrix} Ex \\ Ey \\ Hz \end{bmatrix} = \begin{bmatrix} Zxx\ Zxy \\ Zyx\ Zyy \\ Tzx\ Tzy \end{bmatrix} \begin{bmatrix} Hx \\ Hy \end{bmatrix}$$

E = **Z** **H**

Also Tippers (Geomagnetic Transfer Function)

Hz = Tzx Hx + Tzy Hy

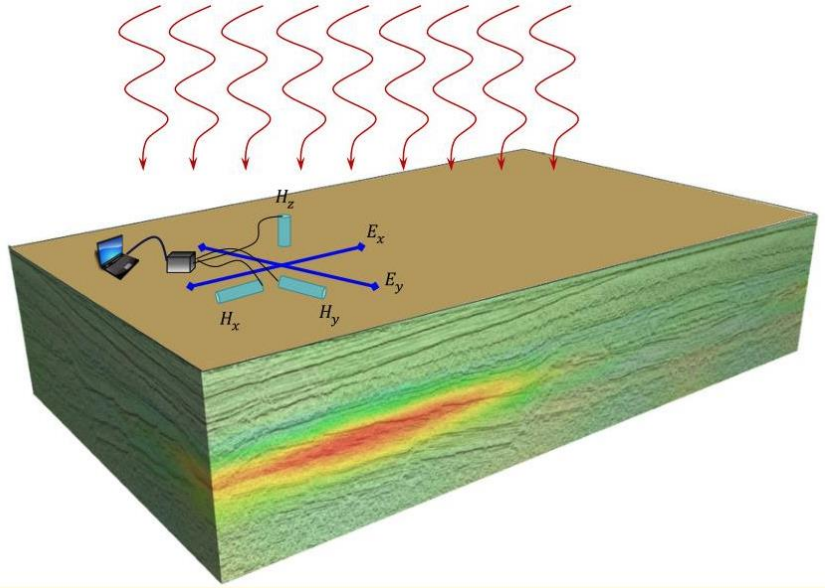

MT - Five components

Two electric dipoles nominally 90 deg apart measuring Ex, Ey

Three magnetometers measuring Hx, Hy, Hz

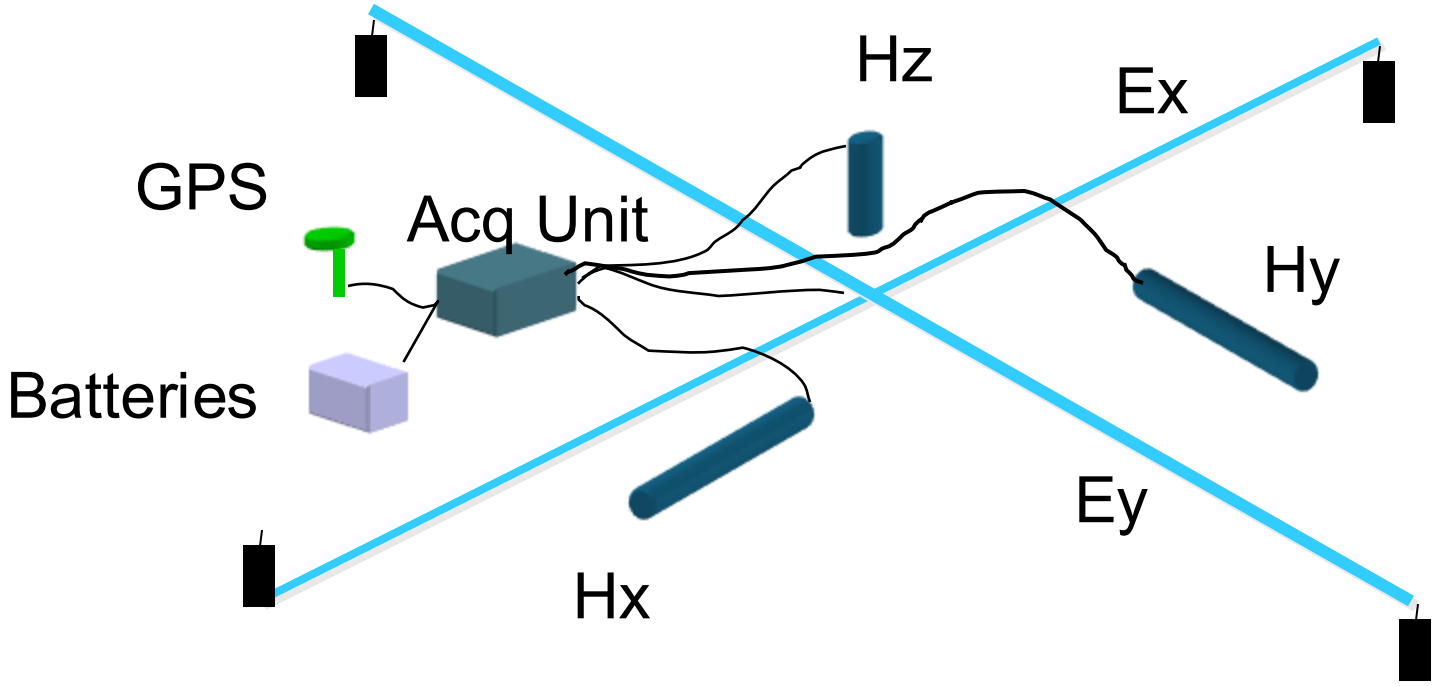

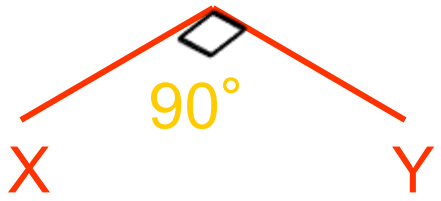

Advantages of NSEM

Natural source EM advantages over controlled-source EM

- simpler logistics (do not need a source)
- always in the far-field
- sophisticated data processing and analysis methods
- full tensor information
  - strike variation with depth
  - dimensionality
- surficial distortion removal
- Rapid well-developed 2-D & 3-D inversion codes

The early papers

Three people are credited with establishing MT

Hirayama (1934) and Rikitake (1948) – global studies
Tikhonov (1950) – very short theoretical paper (in Russian)
Cagniard (1953) – Geophysics paper, very accessible

It was Cagniard, a CGG seismologist, who named the method and developed "magneto-tellurics" as a potential geophysical mapping tool

BASIC THEORY OF THE MAGNETO-TELLURIC METHOD OF GEOPHYSICAL PROSPECTING*†‡

LOUIS CAGNIARD§

MT in the medieval times – the equipment

"Sticky-tape and plaster" MT systems were built by many academic institutions through the late-1950s to late-1970s

The Edinburgh 1970s MT system:

- Off-the shelf Keithley amps
- "Trigg" tellurics
- Jolivet magnetometers for high freqs and 3-comp EDA fluxgate for low freqs
- Recording on Watenabe paper chart with coloured pens
- Hand digitised the time series

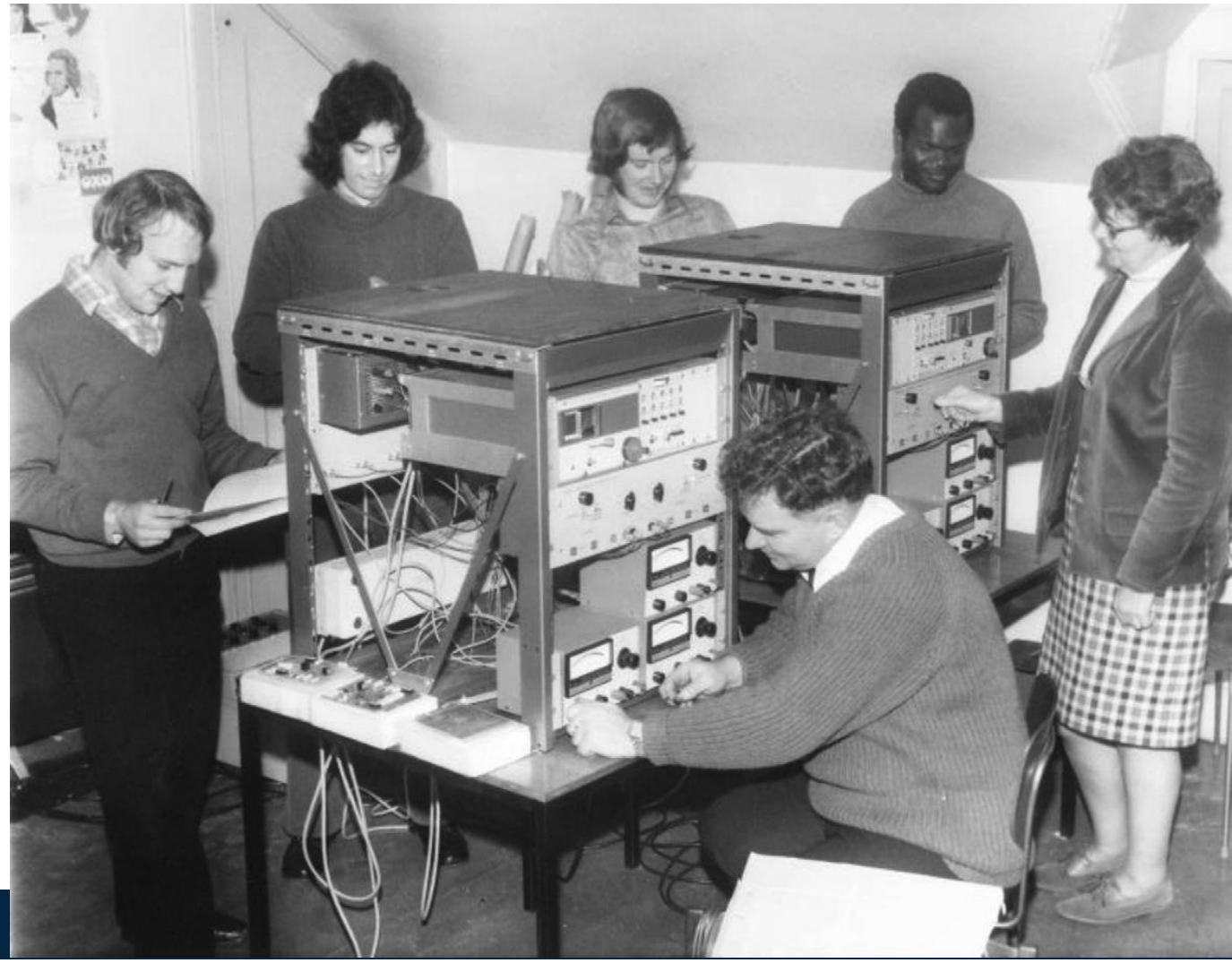

MT in the medieval times – example time series

Example time series:

a) Pi2 activity around local midnight
b) Pc3 activity at local midday
c) Bay-type activity
d) Pc5 pulsation

No-one looks at time series any more... 🙁

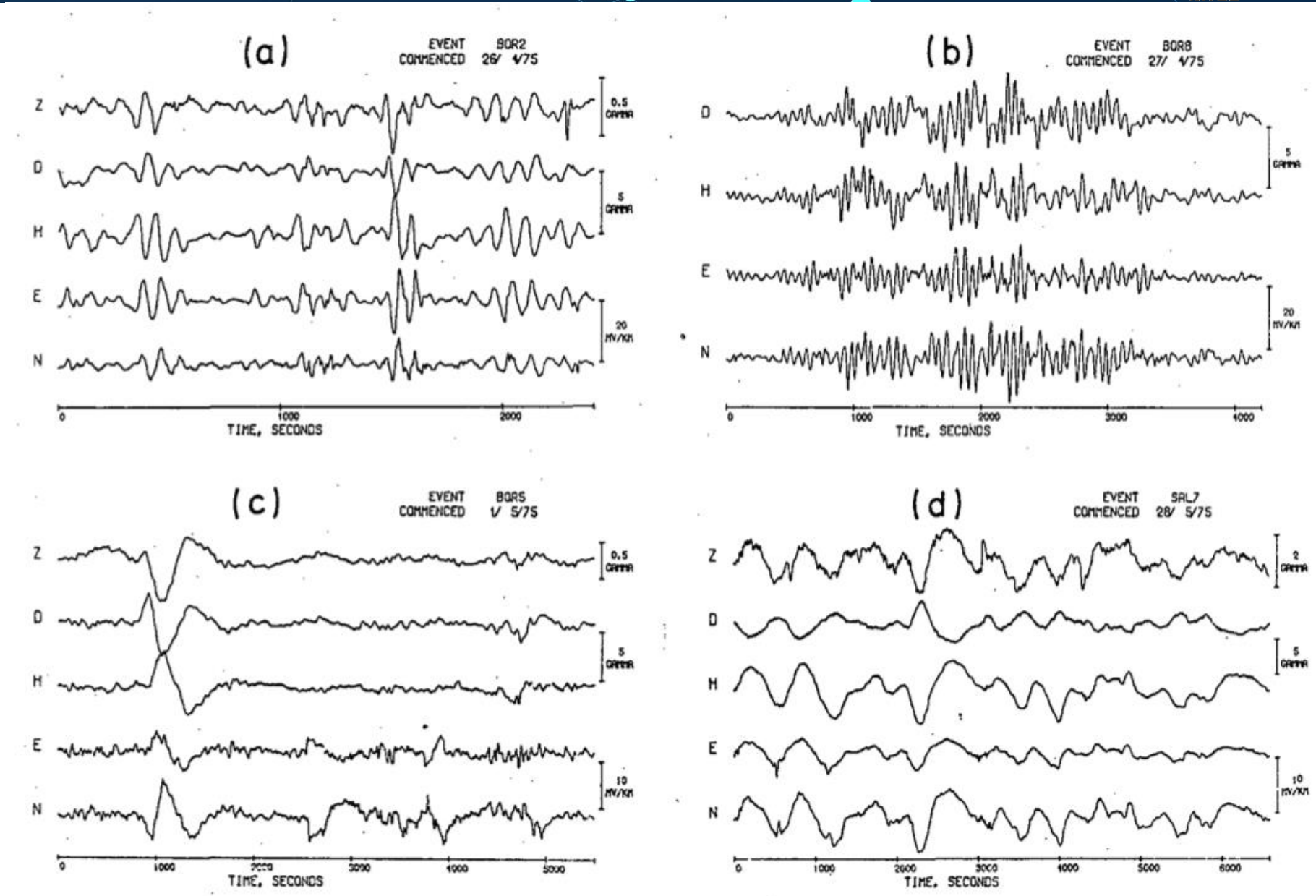

MT in the medieval times – 1-D Monte-Carlo inversion

Modelling of MT data at the time (1976) was mostly by forward trial-and-error 1-D or 2-D.
I developed a brute-force 1-D Monte-Carlo approach

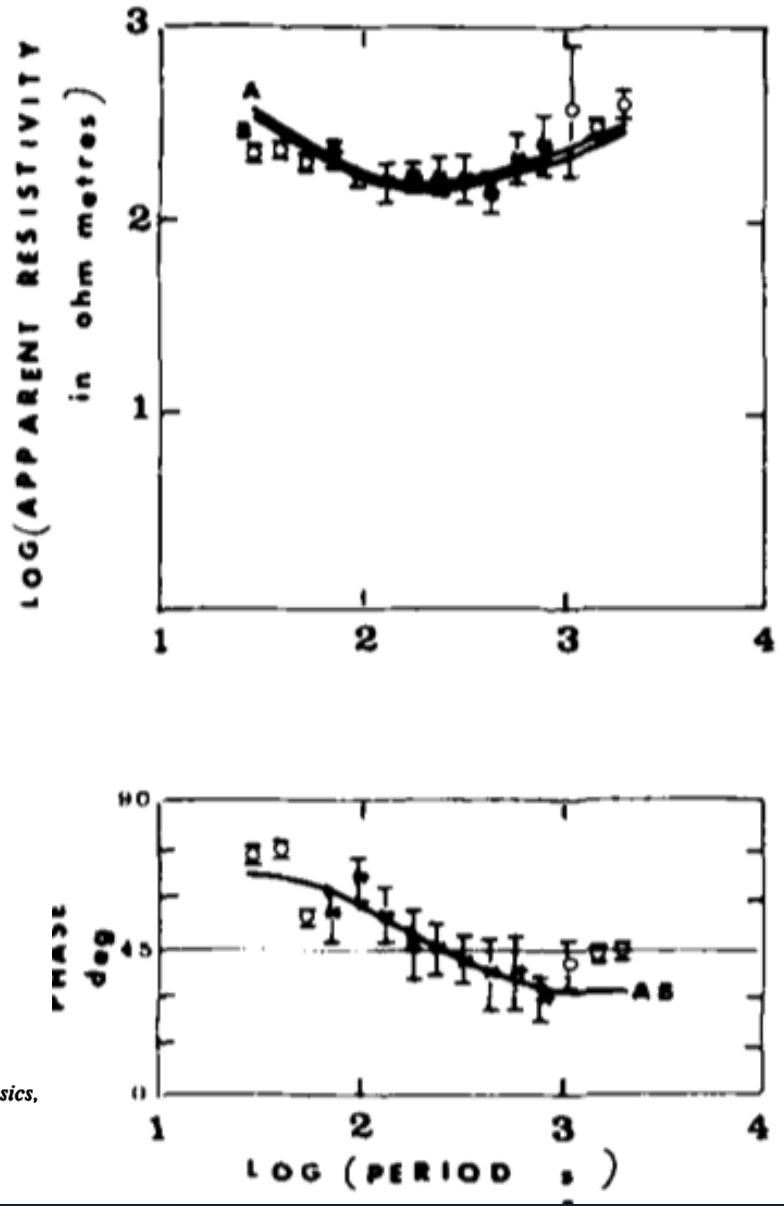

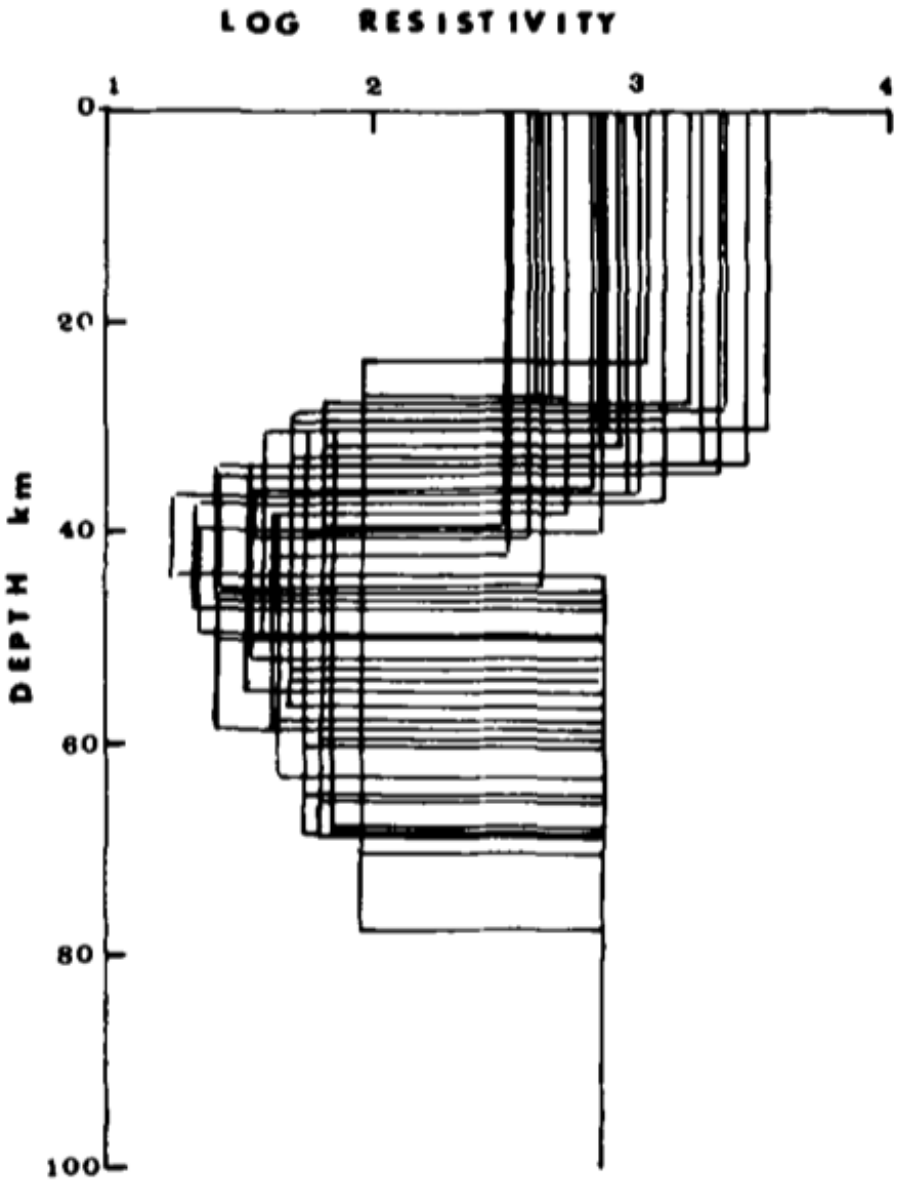

A multi-station magnetotelluric study in southern Scotland – II. Monte-Carlo inversion of the data and its geophysical and tectonic implications

Alan G. Jones* and Rosemary Hutton *Department of Geophysics, University of Edinburgh*

Modern MT – the easy life...

Fabulous commercial equipment – 32bit, GPS, satellite data upload

Fabulous processing codes – especially robust codes developed in 1980s

Fabulous analysis approaches – especially understanding galvanic effects

Fabulous inversion codes – 1D, 2D, 3D, isotropic, some anisotropic

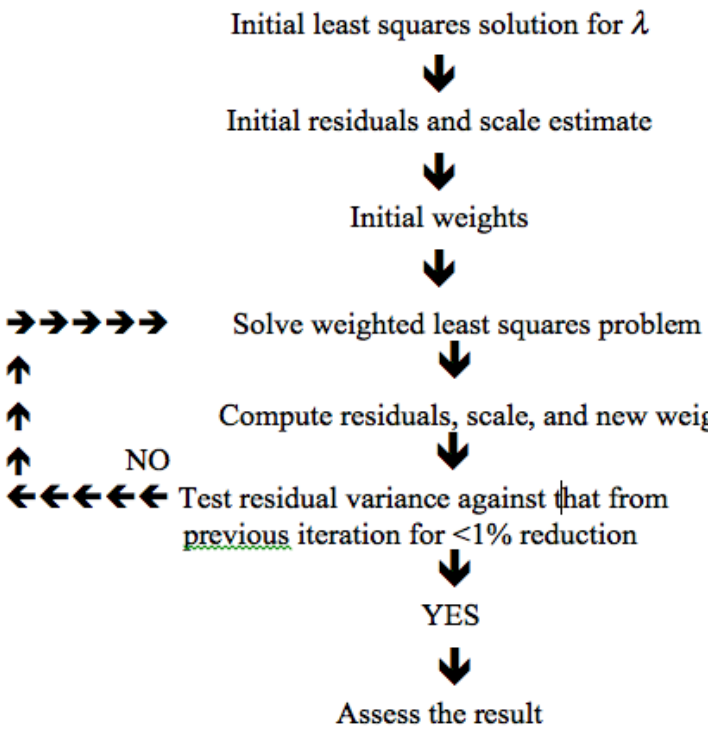

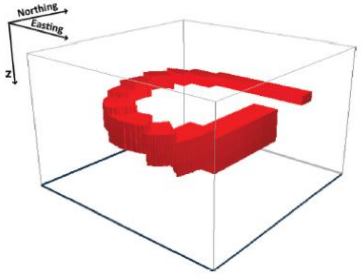

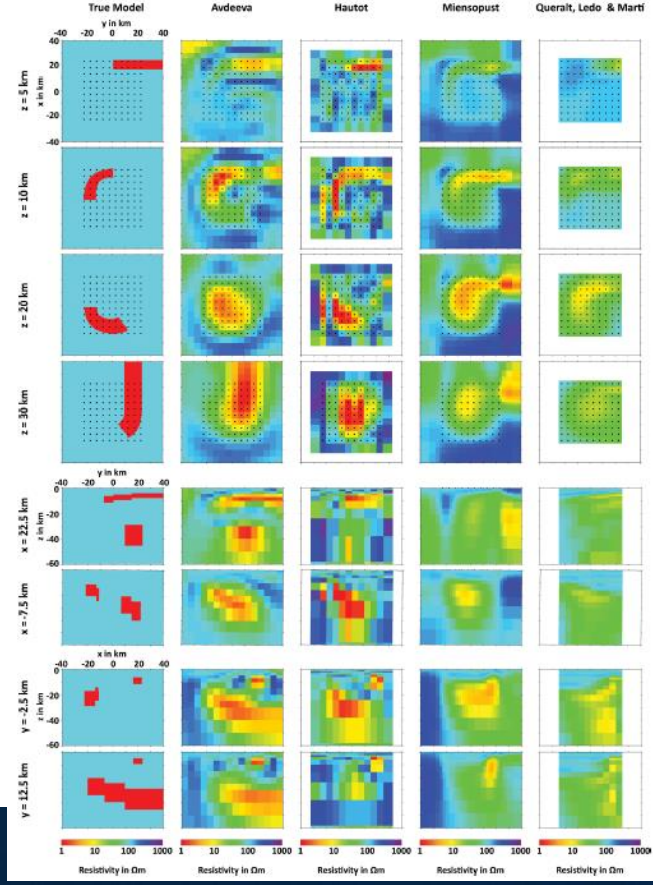

Natural magnetic field spectrum & MT "flavours"

Natural Magnetic Field spectrum

AMT: Audio MT

10+ kHz – 10 Hz

BBMT: Broadband MT

400 Hz – 0.001 Hz

LMT: Low frequency MT

0.1 – 0.0001 Hz

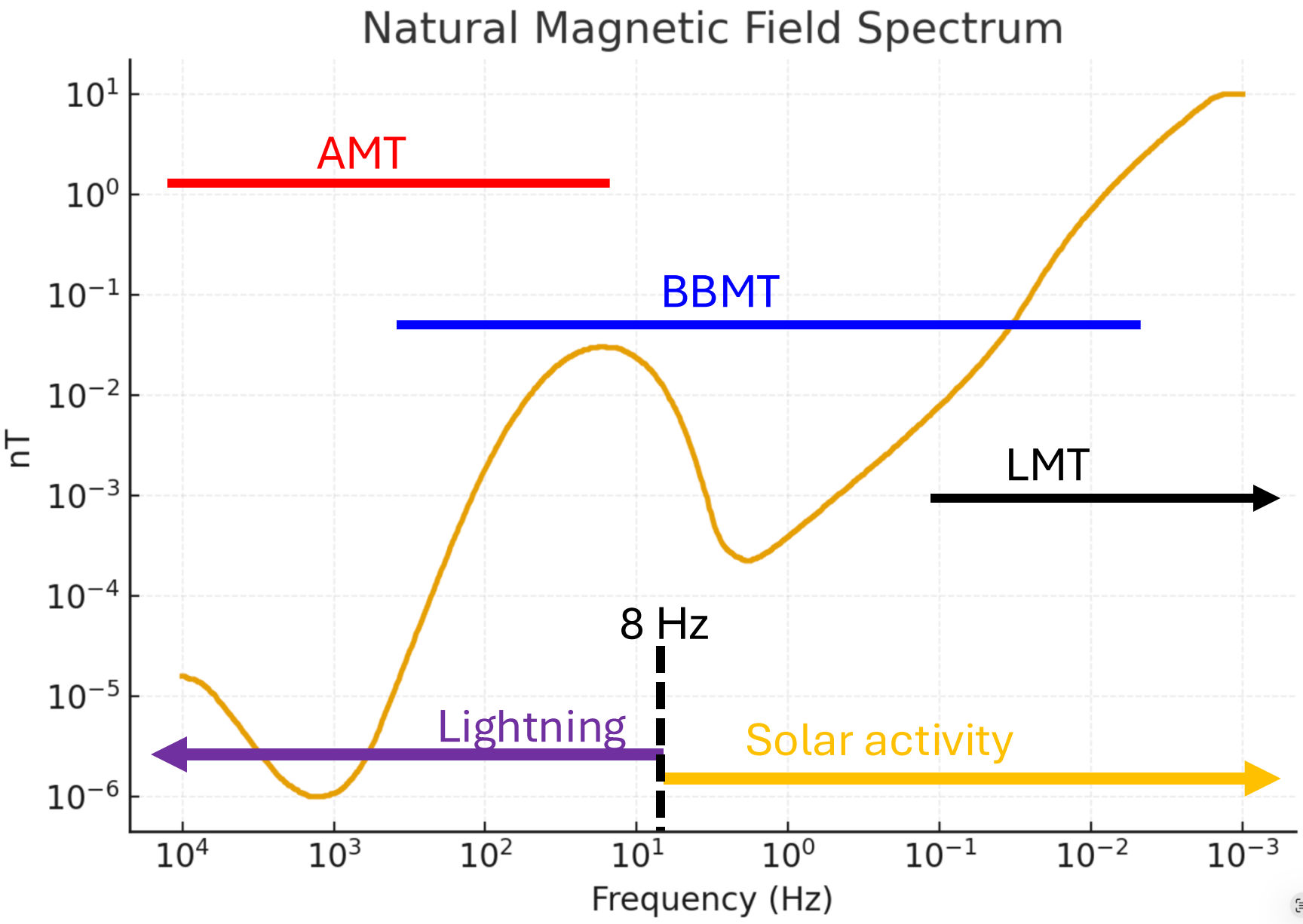

Natural magnetic field spectrum & MT "flavours"

Natural Magnetic Field spectrum

Two signal minima:

AMT deadband: 5 kHz - 800 Hz

(usually beat it with overnight recording)

MT deadband: 0.1 – 10 Hz (also usually beat it with overnight recording)

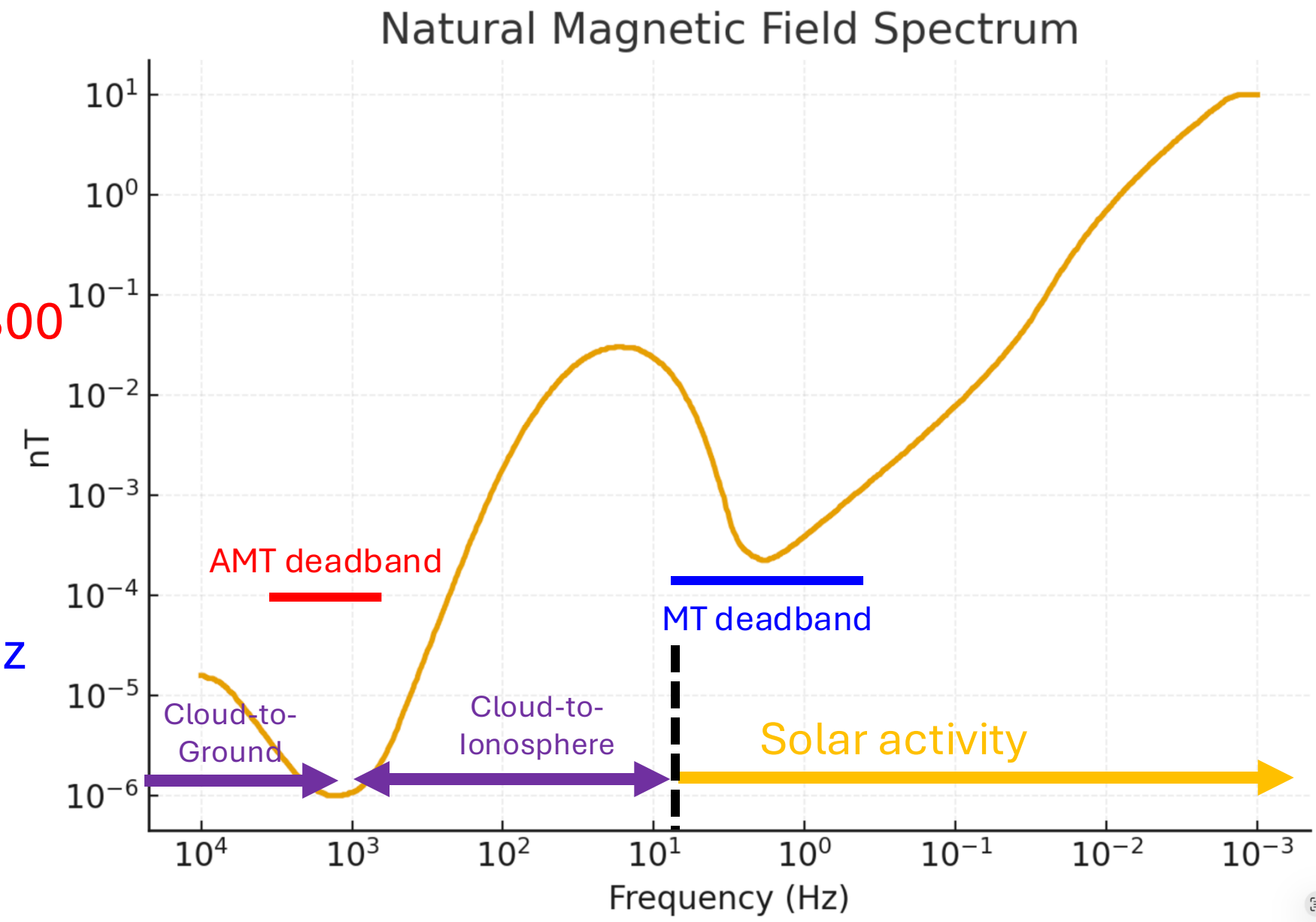

Transfer function basics

Can consider MT and Tipper as causal linear systems with 2 inputs (hx(t), hy(t)) and various outputs (ex(t), ey(t), hz(t)) plus noise on all inputs and outputs.

Impulse responses $h_1(\tau)$ and $h_2(\tau)$ are zero for $\tau<0$, which means in the frequency domain ω:

$$\mathrm{Re}(H_1(\omega)) = H\,(\mathrm{Im}(H_1(\omega))$$

$$\mathrm{Re}(H_2(\omega)) = H\,(\mathrm{Im}(H_2(\omega))$$

(Hilbert transform pairs)

Also known as Dispersion relations, Kramers-Kronig relations, Bode's relation, Kertz operator, Riesz transform

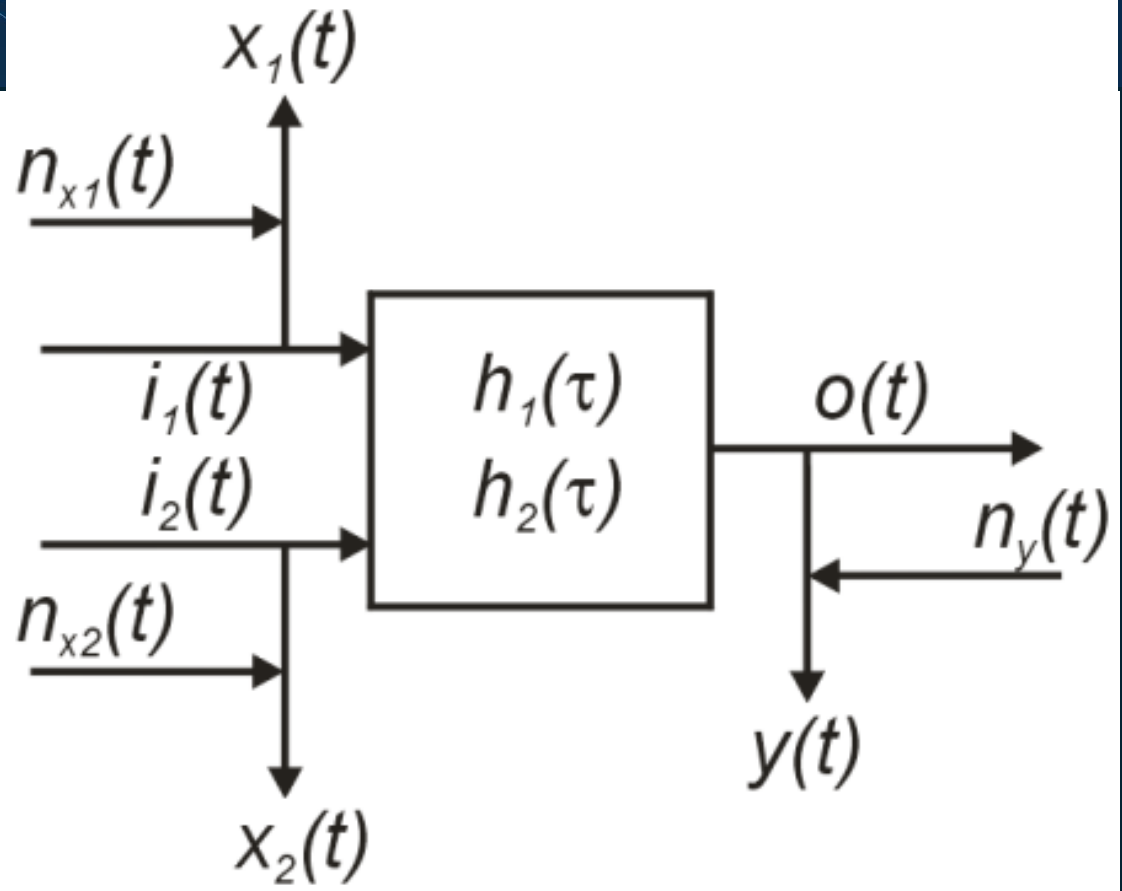

Hilbert transform convolution integral

$$\mathrm{H}(u)(t) = \frac{1}{\pi}\,\mathrm{p.v.}\int_{-\infty}^{+\infty}\frac{u(\tau)}{t-\tau}\,\mathrm{d}\tau,$$

Hilbert transformation

The plot shows the Hilbert transform kernel function (below) being applied to the imaginary part ($\chi_1(\omega)$, blue) of susceptibility to predict the real part ($\chi_2(\omega)$, red)

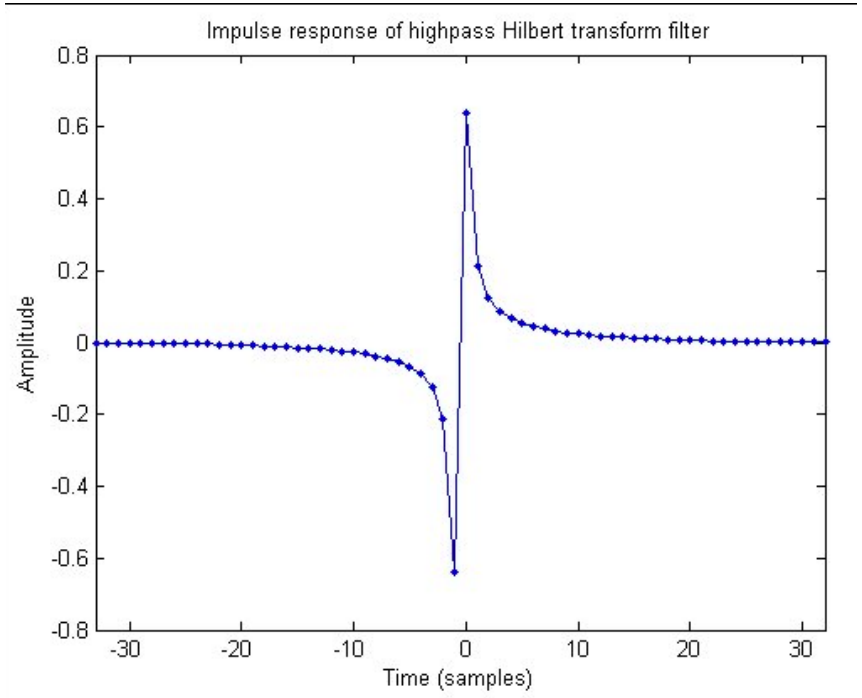

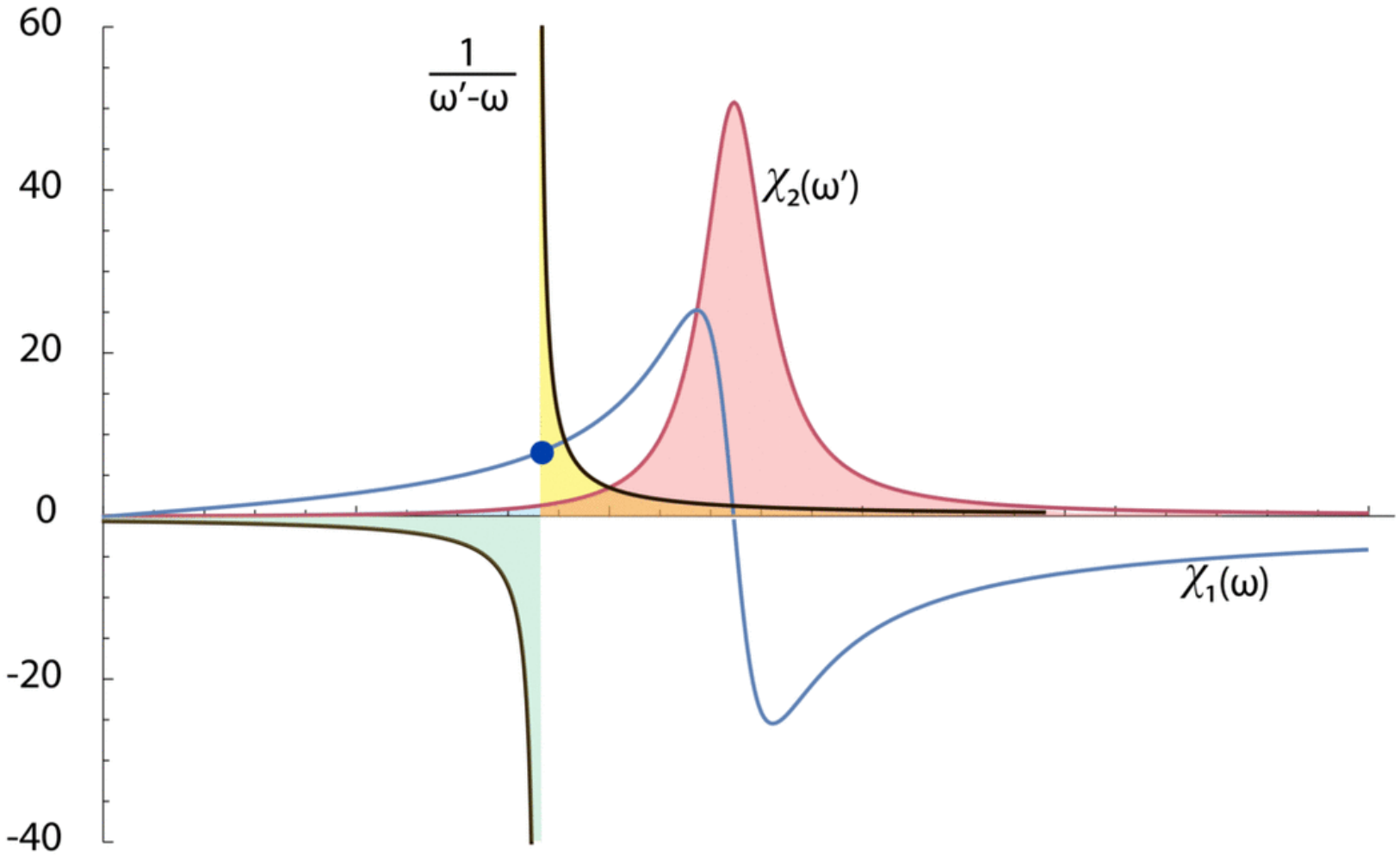

Inequalities that must be obeyed

Expressing impedance in terms of Schmucker's (1970) C-function, and denoting the Real and Imag parts by $g(\omega)$ and $h(\omega)$, Weidelt (1972) showed that a number of inequalities must be obeyed.

$$C(\omega,k)=\frac{1}{i\omega\mu_0}\cdot Z_{xy}(\omega,k)$$

$$C(\omega,k)=g(\omega,k)-ih(\omega,k).$$

$$g\geqq 0 \qquad h\geqq 0,$$

$$Dg\leqq 0,$$

$$0\leqq -D|C|\leqq |C|,$$

$$|DC|\leqq h, \qquad |C+DC|\leqq g,$$

$$|D^2C|\leqq h, \qquad |C+2DC+D^2C|\leqq g.$$

In addition, in the time domain, the derivatives of $c(t)$ must obey the following (Jones, 1980):

$$c'(t)<0, \qquad c''(t)>0, \qquad c'''(t)<0$$

These are very powerful tests of the constraints on the permitted form of the earth's impulse response function $c(t)$.

$$Df=\frac{\omega\,df}{d\omega}=\frac{df}{d\log\omega}=-\frac{df}{d\log T},$$

Implications for MT impedances and RhoA/Pha

For the special case of "minimum phase" response functions, which is true of 1-D MT (Weidelt, 1972) and TM mode in 2-D MT (Weidelt & Kaikkonen, 19940, then as well as:

$$\mathrm{Re}(Zxy(\omega)) = H\,(\mathrm{Im}(Zxy(\omega))$$

(Parker, 1980, D^{+})

we also have:

$$\mathrm{Pha}(H_1(\omega)) = H\,(\mathrm{RhoA}(H_1(\omega))$$

(Parker & Booker, 1996, Rho^{+})

Okak Bay AMT data-set case study: Lessons in dimensionality and scale

Alan G. Jones* and Xavier Garcia‡

The Inverse Problem of Electromagnetic Induction: Existence and Construction of Solutions Based On Incomplete Data

ROBERT L. PARKER

Optimal one-dimensional inversion and bounding of magnetotelluric apparent resistivity and phase measurements

Robert L. Parker [a,*], John R. Booker [b]

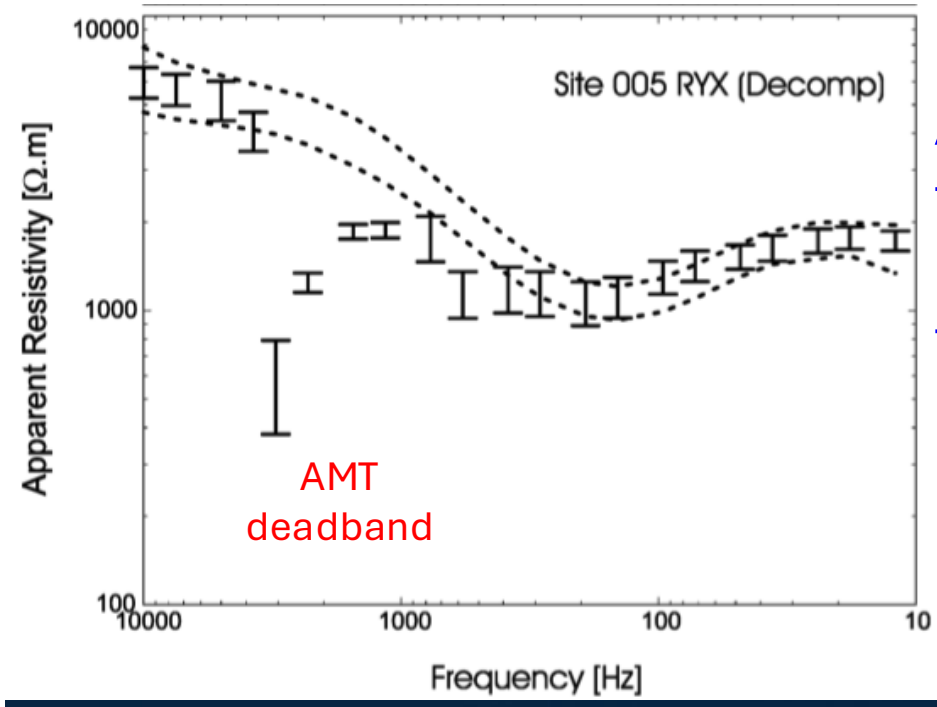

At high frequencies: RhoYX predicted from PhaYX shows "drop-out" in AMT deadband

Implications for MT impedances and RhoA/Pha

For the special case of "minimum phase" response functions, which is true of 1-D MT (Weidelt, 1972) and TM mode in 2-D MT (Weidelt & Kaikkonen, 19940, then as well as:

$$\mathrm{Re}(Zxy(\omega)) = H\,(\mathrm{Im}(Zxy(\omega))$$

(Parker, 1980, D^{+})

we also have:

$$\mathrm{Pha}(H_1(\omega)) = H\,(\mathrm{RhoA}(H_1(\omega))$$

(Parker & Booker, 1996, Rho^{+})

Okak Bay AMT data-set case study: Lessons in dimensionality and scale

Alan G. Jones* and Xavier Garcia‡

The Inverse Problem of Electromagnetic Induction: Existence and Construction of Solutions Based On Incomplete Data

ROBERT L. PARKER

Optimal one-dimensional inversion and bounding of magnetotelluric apparent resistivity and phase measurements

Robert L. Parker [a,*], John R. Booker [b]

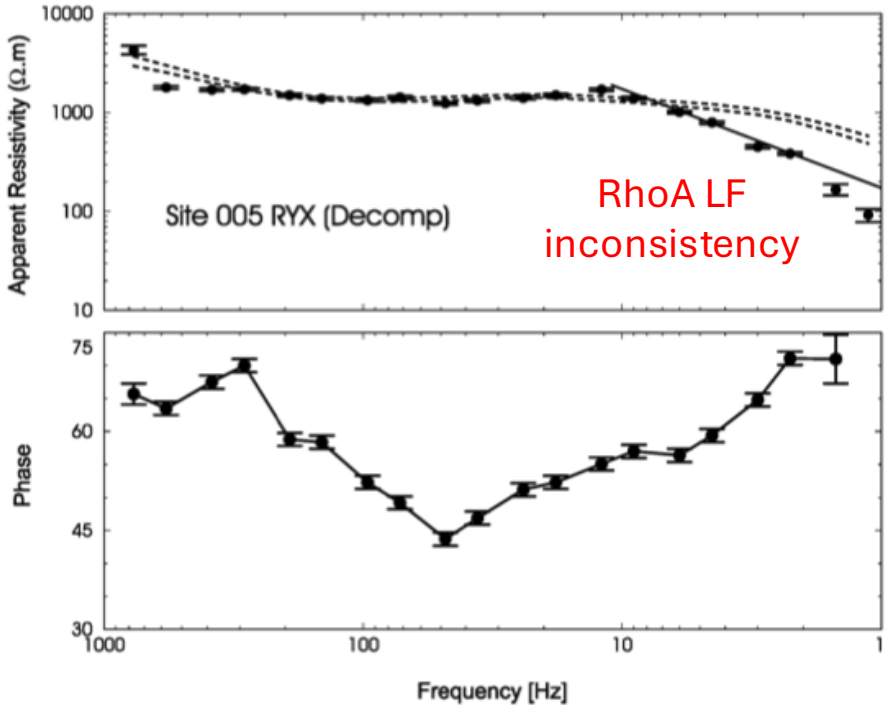

At low frequencies: RhoYX predicted from PhaYX shows inconsistency with "measured" RhoYX

Application of Hilbert Transform to Tippers

We can use the Hilbert Transform relationship on the Tippers to identify non-causal data

The figure shows the Re (solid circles) and Im (open circles) Tzx and Tzy at a site. Error estimates are smaller than the symbols.

To the Im parts I have added error floors of +/- 0.02, which is the error floor reasonable to assume for high quality Tipper data.

The predictions of the Im estimates from the Re estimates are shown by the blue lines

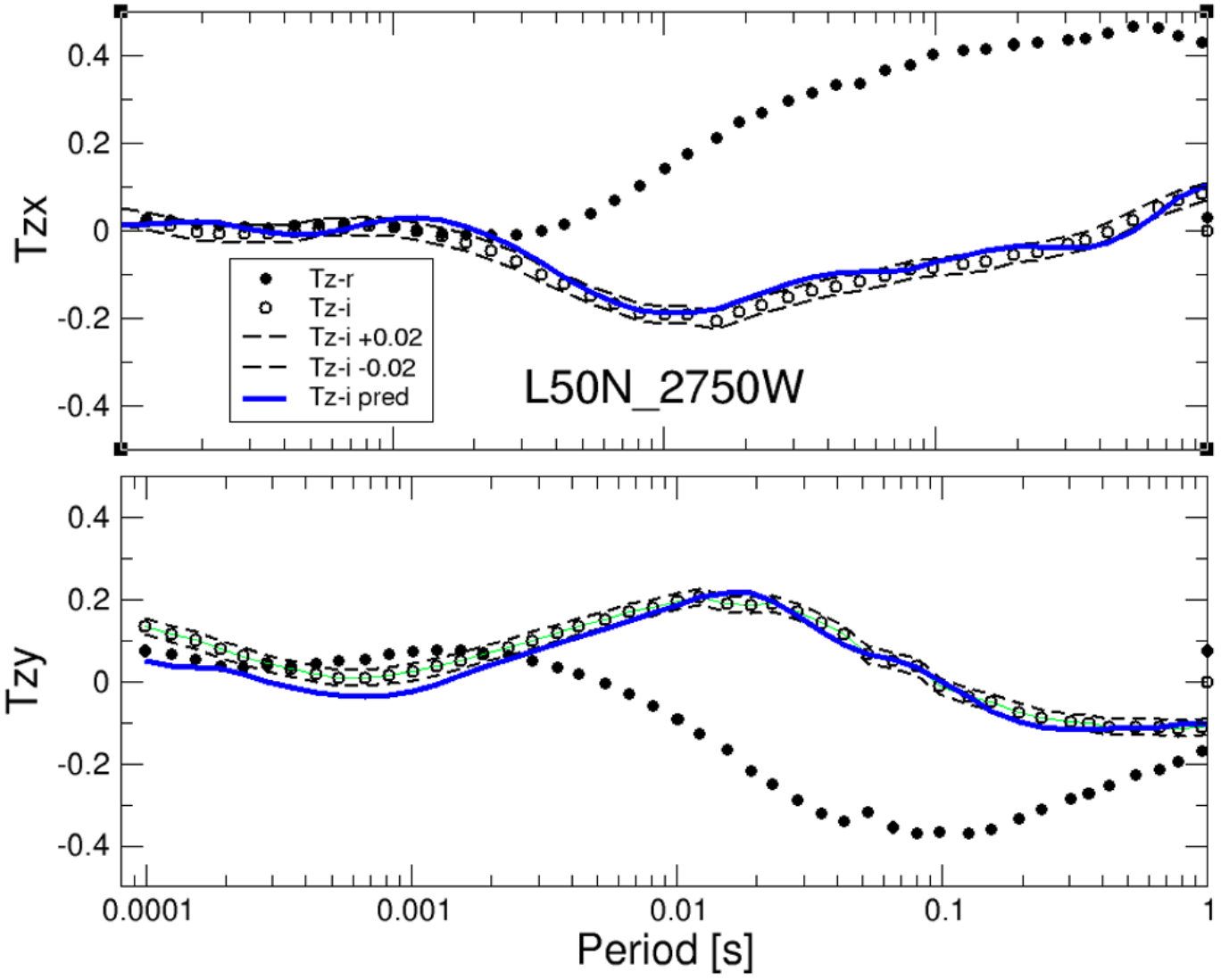

Application of Hilbert Transform to Tippers in the space domain

The Hz component is related to the (Hx,Hy) components through the standard Tipper equation

Hz = Tzx Hx + Tzy Hy

But perhaps less well appreciated is also that the anomalous horizontal fields along a profile are related to the vertical field by Hilbert transformation (Kertz, 1954, discussed in Schmucker, 1980), and is called the Kertz operator.

Example taken from Schmucker (1980):

Z_p = normalized Re(Hz) @ 1cph

h_p = normalized Re(Hx) @ 1 cph

$$h_x(x_0) = -Kh_z(x), \qquad h_z(x_0) = Kh_x(x)$$

$$Kh(x) = -\frac{1}{\pi} \cdot \int_{-\infty}^{\infty} \frac{h(x)}{x - x_0}\, dx$$

$$h_x = \frac{H_{xa}}{H_{x0}}, \qquad h_z = \frac{H_{za}}{H_{x0}}$$

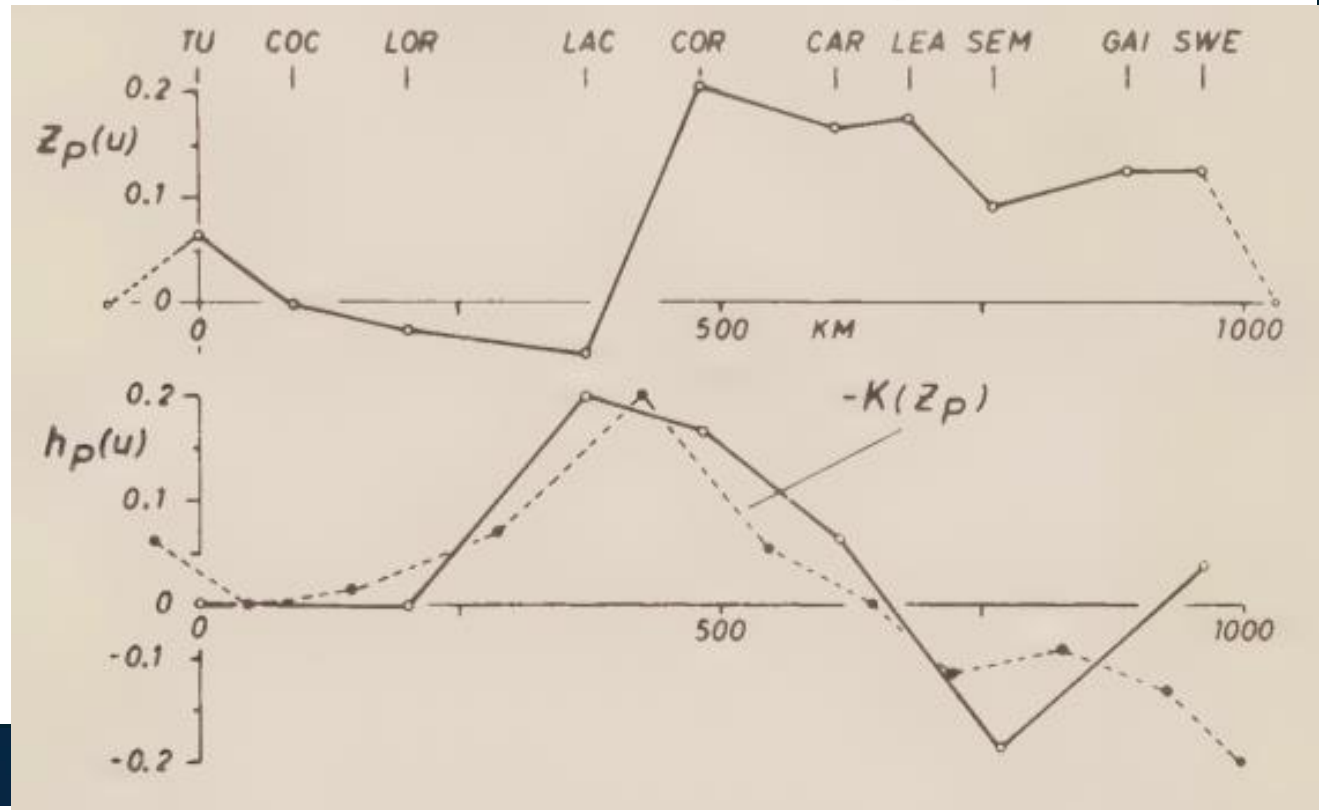

Application of Hilbert Transform to Tippers in the space domain

The Hz component is related to the (Hx,Hy) components through the standard Tipper equation

Hz = Tzx Hx + Tzy Hy

$$h_x(x_0) = -Kh_z(x), \qquad h_z(x_0) = Kh_x(x)$$

$$Kh(x) = -\frac{1}{\pi} \int_{-\infty}^{\infty} \frac{h(x)}{x - x_0}\, dx$$

$$\frac{H_{za}}{H_{x0}}$$

But perhaps less v
that the anomalou
along a profile are
field by Hilbert tra
1954, discussed ir
and is called the Kertz operator.

You can never ignore Hz!
Hz is related to anomalous parts of (Hx,Hy)

Example taken from Schmucker (1980):

Z_p = normalized Re(Hz) @ 1cph

h_p = normalized Re(Hx) @ 1 cph

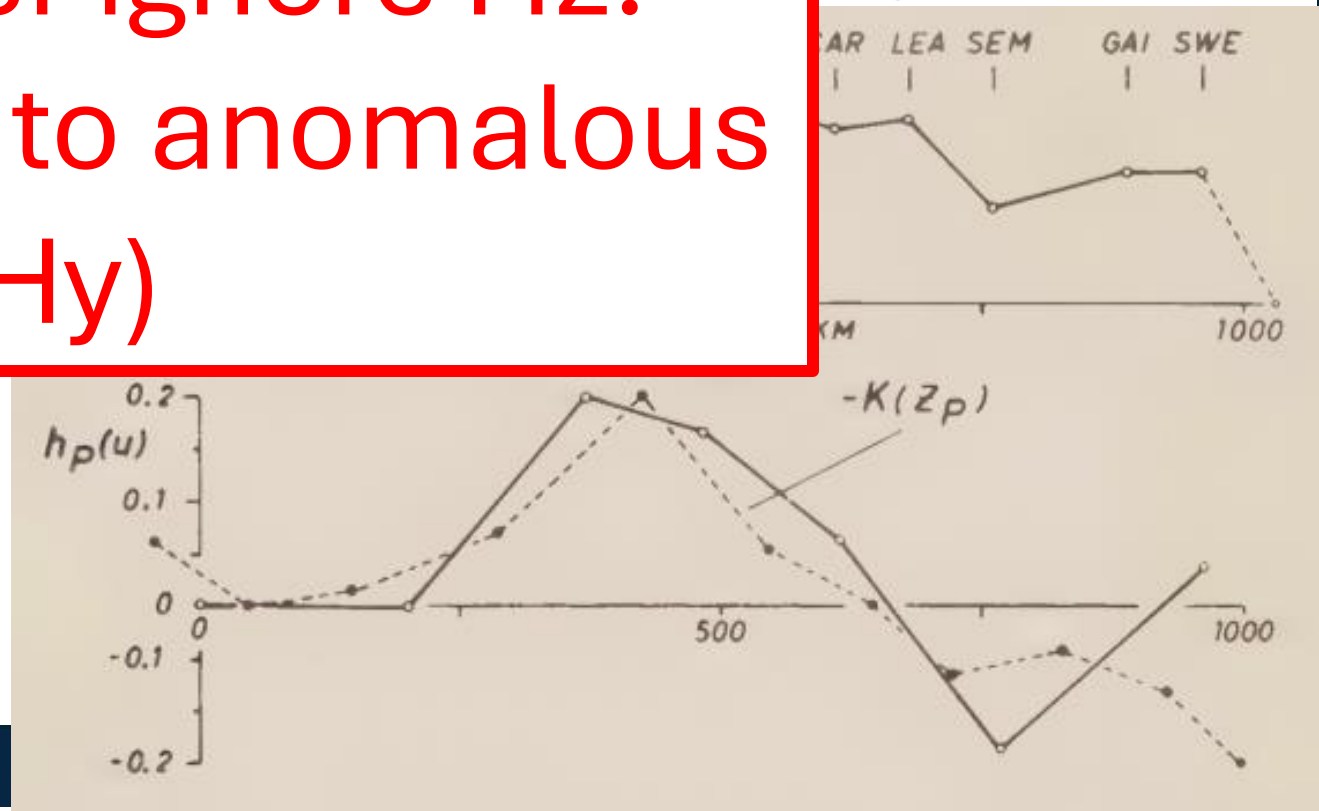

General applicability of Hilbert transform

Zorin et al. (2020a, 2020b) looked at the general applicability of the Hilbert transform for both Re/Im pairs (DR-I) and RhoA/Pha pairs (DR-II)

Showed for some extreme theoretical examples that neither DR-I nor DR-II obeyed.

But an examination of a very large database (>120,000) of onshore MT sites yielded only a handful (<0.1%) of non-causal MT and Tipper tensors

Validity of the dispersion relations in magnetotellurics: Part I—theory

Nikita Zorin[1,2], Elena Aleksanova[1], Hisayoshi Shimizu[2*] and Denis Yakovlev[1]

Validity of the dispersion relations in magnetotellurics. Part II: synthetic and field data

Nikita Zorin[1,2,3], Dmitry Alekseev[4,5,6], Dmitrii Epishkin[1], Hisayoshi Shimizu[2*], Denis Yakovlev[1] and Sergey Zaytsev[1,3,7]

Table 2 The DR violation statistics for the impedance tensors from the onshore MT/BBMT database of Nord-West Ltd

Objects	The amount of impedance tensors examined			
	Total number	Anomalous	Strongly anomalous	Non-causal
Geotraverses 1-SB, 2-DV, 2-DVa, 3-DV, 8-DV, PU (2001–2019, Russia)	7832 (100%)	703 (9.0%)	212 (2.7%)	5 (< 0.1%)
Taymyr Super Object (2005–2019, Russia)	20,484 (100%)	61 (0.3%)	8 (< 0.1%)	0 (< 0.1%)
Other major objects (2004–2019, Argentina, Bolivia, Brazil, Bulgaria, Colombia, India, Iran, Kazakhstan, Russia)	31,910 (100%)	273 (0.9%)	35 (0.1%)	1 (< 0.1%)
All together	60,226 (100%)	1037 (1.7%)	255 (0.4%)	6 (< 0.1%)

Noise auto-spectral bias

The determination of impedance from the fields involves transformation into the frequency domain and construction of auto- and cross-spectra, eg. for a single input with noise ($x(t)=i(t)+n_x(t)$) and single output with noise ($y(t)=o(t)+n_y(t)$), then the estimators are

$$\bar{H}_d(\omega) = \frac{\bar{S}_{xy}(\omega)}{\bar{S}_{xx}(\omega)} = \frac{\bar{S}_{io}(\omega)}{\bar{S}_{ii}(\omega) + \bar{S}_{n_x n_x}(\omega)}$$

$$\bar{H}_u(\omega) = \frac{\bar{S}_{yy}(\omega)}{\bar{S}_{yx}(\omega)} = \frac{\bar{S}_{oo}(\omega) + \bar{S}_{n_y n_y}}{\bar{S}_{oi}(\omega)}$$

H_d underestimates H (so is a downward-based estimator)

H_u overestimates H (so is an upward-biased estimator)

A discussion of bias in magnetotelluric responses

M. Cristina Pomposiello[1], John R. Booker[2], and Alicia Favetto[1]

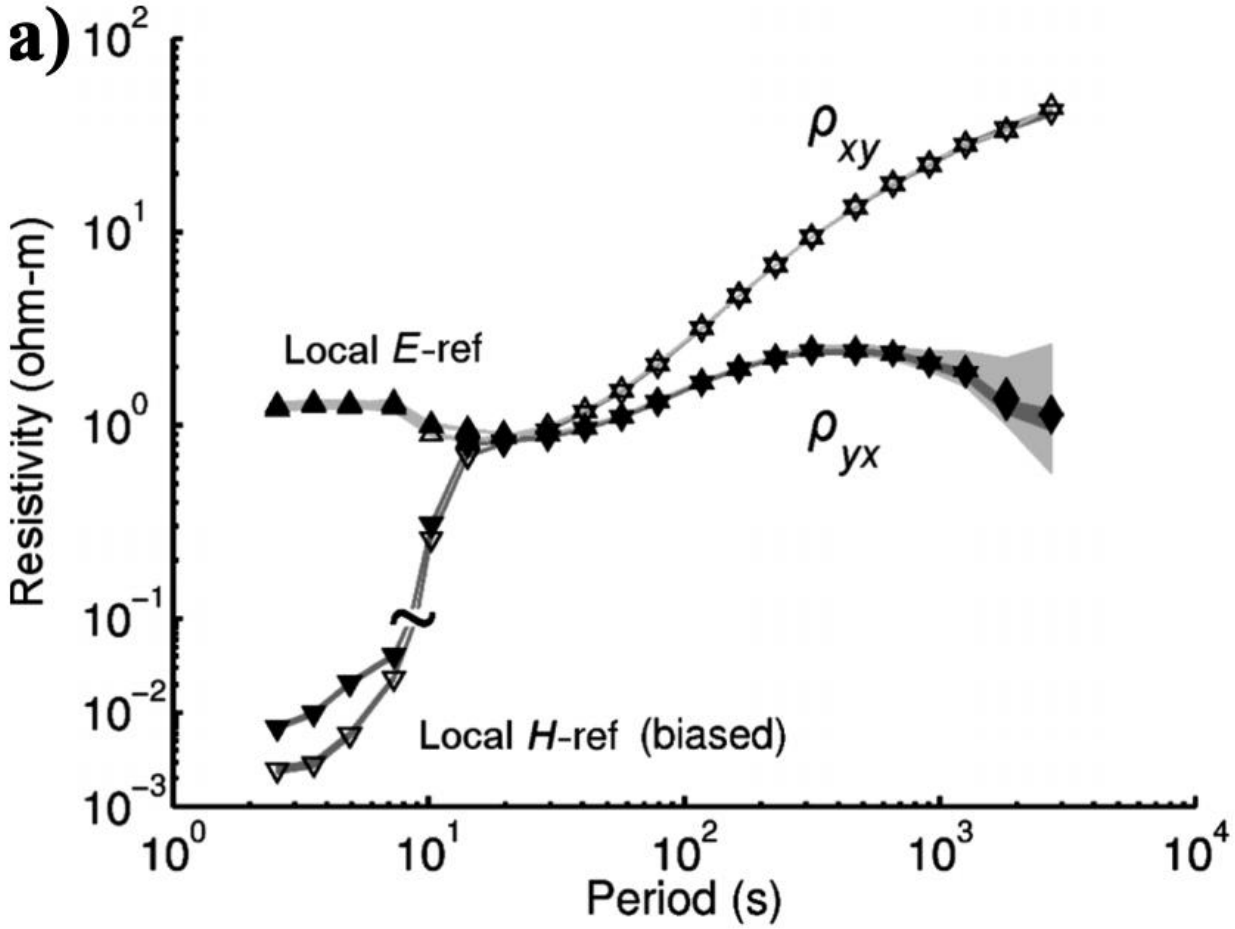

Remote reference to remove auto-spectral bias

Measure a remote reference, which is a "remote" MT site used as a reference, that correlates (does not have to be 100%) with the spectral content of the true input (i) and true output (o)

Economic theory: Reiersøl (1950)

MT: Gamble et al. (1979)

Estimate $H_r(\omega)$ from:

$$\bar{H}_r(\omega) = \frac{\bar{S}_{ry}(\omega)}{\bar{S}_{rx}(\omega)} = \frac{\bar{S}_{ao}(\omega) + \bar{S}_{an_y}(\omega) + \bar{S}_{n_r o}(\omega) + \bar{S}_{n_r n_y}(\omega)}{\bar{S}_{ai}(\omega) + \bar{S}_{an_x}(\omega) + \bar{S}_{n_r i}(\omega) + \bar{S}_{n_r n_x}(\omega)}$$

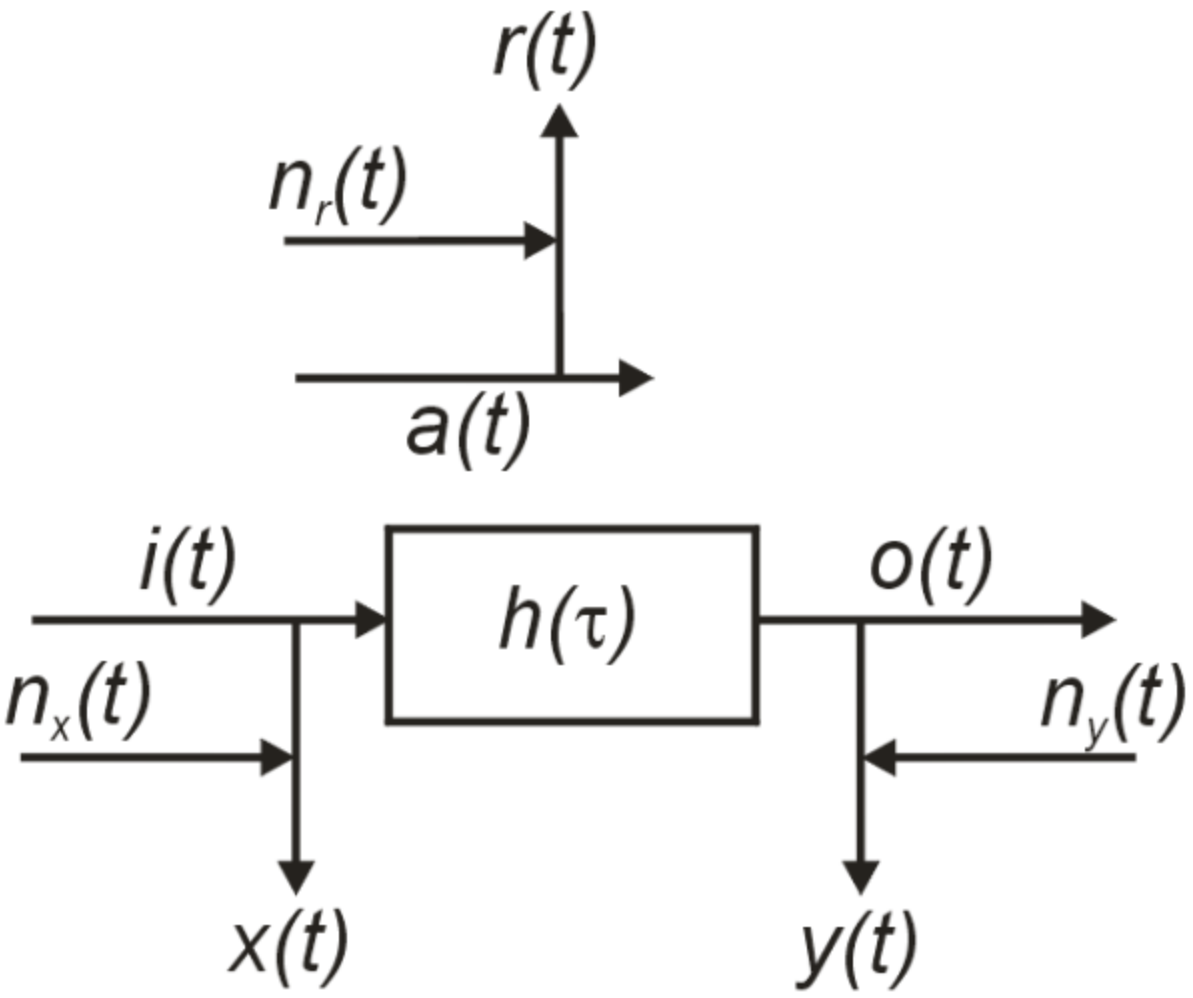

Remote reference to remove auto-spectral bias

Measure a remote reference, which is a "remote" MT site used as a reference, that correlates (does not have to be 100%) with the spectral content of the true input (i) and true output (o)

Economic theory: Reiersøl (1950)

MT: Gamble et al. (1979)

Estimate $H_r(\omega)$ from:

$$\bar{H}_r(\omega) = \frac{\bar{S}_{ry}(\omega)}{\bar{S}_{rx}(\omega)} = \frac{\bar{S}_{ao}(\omega) + \bar{S}_{an_y}(\omega) + \bar{S}_{n_r o}(\omega) + \bar{S}_{n_r n_y}(\omega)}{\bar{S}_{ai}(\omega) + \bar{S}_{an_x}(\omega) + \bar{S}_{n_r i}(\omega) + \bar{S}_{n_r n_x}(\omega)}$$

$$= \frac{\bar{S}_{ao}(\omega)}{\bar{S}_{ai}(\omega)}$$

← True cross spectra of a(t) & i(t)

← True cross spectra of a(t) & o(t)

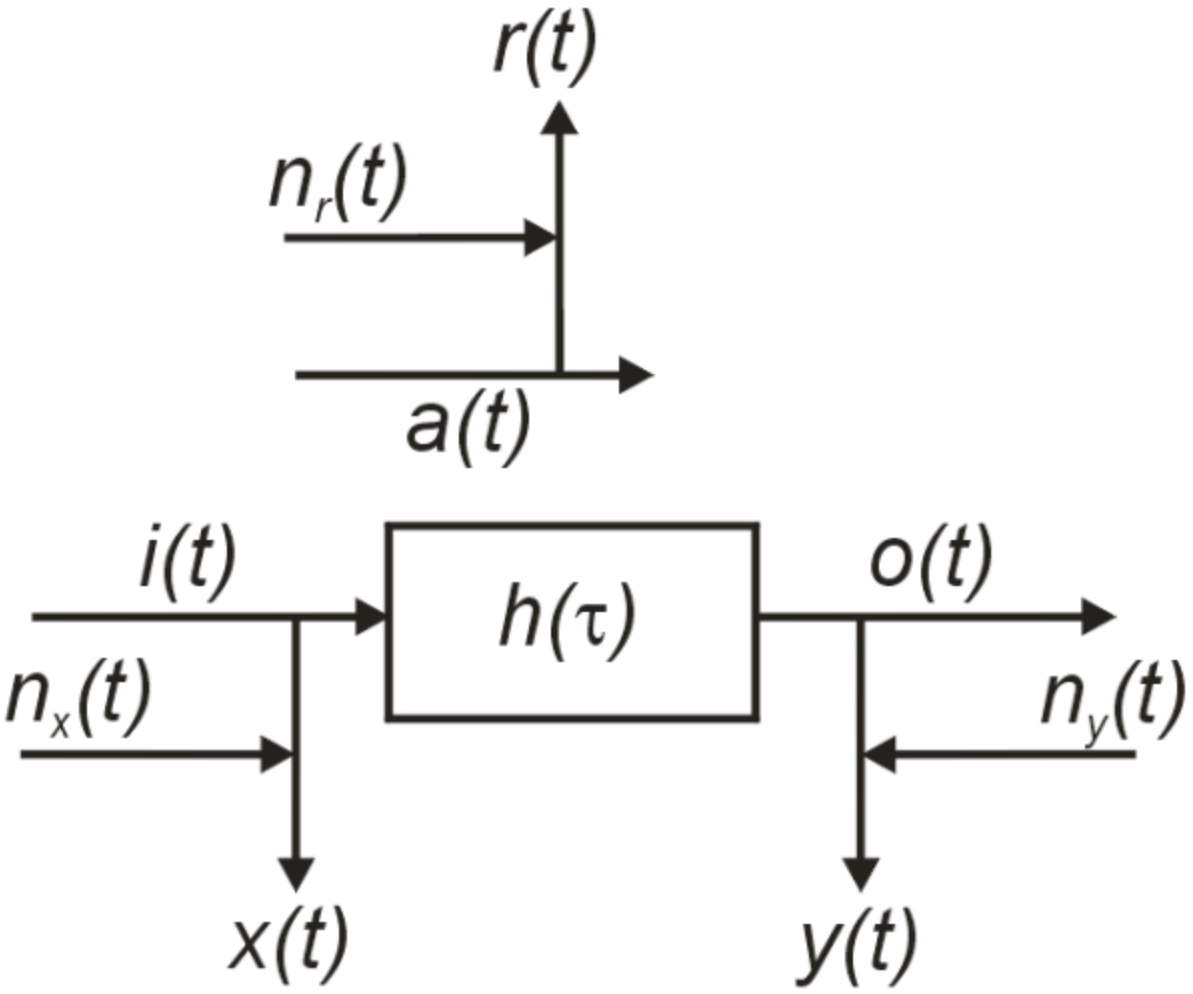

Airborne Natural-Source EM methods (ANSEM)

Airborne natural-source EM methods have been developed in Canada over the last 2 decades:

ZTEM: Z-Axis Tipper EM system of Geotech

- Hz in the air, (Hx,Hy) at the base station

(system copied by the Chinese)

MobileMT of Expert Geophysics

- Unoriented (Hx,Hy, Hz) in the air, (Ex,Ey) at the base station

QAMT: Quantum AMT of Dias Geophysical

- Oriented (Hx,Hy, Hz) in the air, (Hx,Hy) and (Ex,Ey) at the base station

Advantages and limitations of ANSEM methods

All ANSEM methods are measuring the spatial variation of the magnetic field over targets, not the electric field spatial variation (should not be called “MT”).

1 Rapid EM exploration over a large area quickly and for a reasonable cost

2 High ”site” density compared to land-based equivalents – e.g. for ZTEM (Legault et al., 2012), MobileMT (Prikhodko et al., 2024) and QAMT (Larnier et al. 2021) a measurement is computed every 10-20 m on flight lines typically 200 m apart compared to 500 m sites in high density AMT (70x more “sites”)

BUT!!!

1) Most of the anomalous response to a conducting body is in the electric fields!

2) Only useful if the EM response from the deposit is in the frequency range of the airborne systems! (e.g. Olympic Dam isn’t)

3) The anomaly has to have a strong magnetic field response (not true of e.g. conducting spheres, which have the lowest inductive effects of any shape)

Three theoretical systems

Three theoretical systems:

AS1: Airborne system 1: Only Hz measured in the air, and related to horizontal H fields at the base station

AS2: Airborne system 2: Measurement of all 3 components in the air (Hx, Hy, Hz), but without orientation, and related to base station horizontal electric fields

AS3: Airborne system 3: Measurement of all 3 components in the air (Hx, Hy, Hz), with orientation, and related to base station horizontal electric and magnetic fields

Theoretically for perfect data we only need Hz as we can derive the anomalous parts of (Hx,Hy) from the spatial gradient of Hz

Forward calculations: AS1 – Airborne system 1

As an example for AS1, as shown by Holtham and Oldenburg (2010), we can define the two source polarizations as “1” and “2”, then at position “*r*” compared to the base station at position “r_0”,

$$\begin{pmatrix} H_z^{(1)}(r) \\ H_z^{(2)}(r) \end{pmatrix} = \begin{pmatrix} H_x^{(1)}(r_0) & H_y^{(1)}(r_0) \\ H_x^{(2)}(r_0) & H_y^{(2)}(r_0) \end{pmatrix} \begin{pmatrix} T_{zx} \\ T_{zy} \end{pmatrix}$$

Multiplying both sides by the inverse of the (*Hx,Hy*) matrix,

$$\begin{pmatrix} H_x^{(1)}(r_0) & H_y^{(1)}(r_0) \\ H_x^{(2)}(r_0) & H_y^{(2)}(r_0) \end{pmatrix}^{-1} \begin{pmatrix} H_z^{(1)}(r) \\ H_z^{(2)}(r) \end{pmatrix} = \begin{pmatrix} H_x^{(1)}(r_0) & H_y^{(1)}(r_0) \\ H_x^{(2)}(r_0) & H_y^{(2)}(r_0) \end{pmatrix}^{-1} \begin{pmatrix} H_x^{(1)}(r_0) & H_y^{(1)}(r_0) \\ H_x^{(2)}(r_0) & H_y^{(2)}(r_0) \end{pmatrix} \begin{pmatrix} T_{zx} \\ T_{zy} \end{pmatrix}$$

$$\Rightarrow \frac{1}{\left(H_x^{(1)}H_y^{(2)} - H_x^{(2)}H_y^{(1)}\right)} \begin{pmatrix} H_y^{(2)}(r_0) & -H_y^{(1)}(r_0) \\ -H_x^{(2)}(r_0) & H_x^{(1)}(r_0) \end{pmatrix} \begin{pmatrix} H_z^{(1)}(r) \\ H_z^{(2)}(r) \end{pmatrix} = \begin{pmatrix} 1 & 0 \\ 0 & 1 \end{pmatrix} \begin{pmatrix} T_{zx} \\ T_{zy} \end{pmatrix}$$

Forward calculations: AS1 – Airborne system 1

From which we can derive the AS1 tipper transfer functions, viz.,

$$T_{zx} = \frac{H_y^{(2)}(r_0)H_z^{(1)}(r) - H_y^{(1)}(r_0)H_z^{(2)}(r)}{H_x^{(1)}(r_0)H_y^{(2)}(r_0) - H_x^{(2)}(r_0)H_y^{(1)}(r_0)}$$

and

$$T_{zy} = \frac{-H_x^{(2)}(r_0)H_z^{(1)}(r) + H_x^{(1)}(r_0)H_z^{(2)}(r)}{H_x^{(1)}(r_0)H_y^{(2)}(r_0) - H_x^{(2)}(r_0)H_y^{(1)}(r_0)}$$

Forward calculations: AS2 – Airborne system 2

For AS2, airborne system 2, what we would like to do is calculate the admittance tensor, from

$$\begin{bmatrix} Hx \\ Hy \\ Hz \end{bmatrix} = \begin{bmatrix} Axx & Axy \\ Ayx & Ayy \\ Azx & Azy \end{bmatrix} \begin{bmatrix} Ex_b \\ Ey_b \end{bmatrix}$$

However, we do not have orientation of the bird, so cannot derive (Hx, Hy, Hz), but only have their instantaneous directions (Hx', Hy', Hz'). We cannot take the determinant of **A**, as it is not square.

For a bird that is rotating with a yaw, pitch, and roll of angles are α, β and γ, respectively, then the intrinsic 3x3 rotation matrix, **R**, is given by the matrix multiplication of three rotation matrices about axes z, y and x respectively, given by

$$R = R_z(\gamma)\, R_y(\beta)\, R_x(\alpha) = \begin{bmatrix} \cos\gamma & -\sin\gamma & 0 \\ \sin\gamma & \cos\gamma & 0 \\ 0 & 0 & 1 \end{bmatrix} \begin{bmatrix} \cos\beta & 0 & \sin\beta \\ 0 & 1 & 0 \\ -\sin\beta & 0 & \cos\beta \end{bmatrix} \begin{bmatrix} 1 & 0 & 0 \\ 0 & \cos\alpha & -\sin\alpha \\ 0 & \sin\alpha & \cos\alpha \end{bmatrix}$$

$$= \begin{bmatrix} \cos\beta\cos\gamma & \sin\alpha\sin\beta\cos\gamma - \cos\alpha\sin\gamma & \cos\alpha\sin\beta\cos\gamma + \sin\alpha\sin\gamma \\ \cos\beta\sin\gamma & \sin\alpha\sin\beta\sin\gamma + \cos\alpha\cos\gamma & \cos\alpha\sin\beta\sin\gamma - \sin\alpha\cos\gamma \\ -\sin\beta & \sin\alpha\cos\beta & \cos\alpha\cos\beta \end{bmatrix}$$

Sattel: AS2 – Airborne system 2

There are a number of possible ways to calculate the forward problem:

Daniel Sattel (Sattel et al., 2019) does not use the full admittance tensor, but drops the last row and solves for

$$\begin{bmatrix} Hx \\ Hy \end{bmatrix} = \begin{bmatrix} Axx & Axy \\ Ayx & Ayy \end{bmatrix} \begin{bmatrix} Ex_b \\ Ey_b \end{bmatrix}$$

This is fundamentally incorrect as it does not account for the vertical field measurements made in the bird. Sattel derives the apparent conductivity from the determinant of this 2x2 tensor,

$$A_{DET} = A_{xx}A_{yy} - A_{xy}A_{yx}$$

From which an estimate of apparent conductivity, σ_a, can be calculated as above in a manner consistent with calculating apparent resistivity, ρ_a, in MT, viz.,

$$\sigma_a^{(s)} = \mu\omega|A_{DET}|$$

➔ Note that Sattel's approach is rotationally invariant

Cross product: AS2 – Airborne system 2

One can define the cross-product of the two columns, the first column $\mathbf{A}_1$ and the second column $\mathbf{A}_2$, of the admittance tensor. The vector cross product $\mathbf{A}$ is given by $\mathbf{A} = \mathbf{A}_1 \times \mathbf{A}_2$, viz.,

$$\mathbf{A} = \mathbf{A}_1 \times \mathbf{A}_2 = \begin{bmatrix} Axx \\ Ayx \\ Azx \end{bmatrix} \times \begin{bmatrix} Axy \\ Ayy \\ Azy \end{bmatrix} = \begin{bmatrix} det\begin{bmatrix} Ayx & Ayy \\ Azx & Azy \end{bmatrix} \\ -det\begin{bmatrix} Axx & Axy \\ Azx & Azy \end{bmatrix} \\ det\begin{bmatrix} Axx & Axy \\ Ayx & Ayy \end{bmatrix} \end{bmatrix} = \begin{bmatrix} AyxAzy - AzxAyy \\ -AxxAzy + AzxAxy \\ AxxAyy - AyxAxy \end{bmatrix} = \begin{bmatrix} \mathrm{Ax} \\ \mathrm{Ay} \\ \mathrm{Az} \end{bmatrix}$$

Calculating $\|\mathbf{A}\|$, which is the Frobenius norm or Euclidean norm of $\mathbf{A}$,

$$\|\mathbf{A}\| = \sqrt{|\mathrm{Ax}|^2 + |\mathrm{Ay}|^2 + |\mathrm{Az}|^2}$$

From this we can obtain an estimate of apparent conductivity from $\sigma_a^{(c)} = \mu\omega\|\mathbf{A}\|$

➔ Note that the cross-product is rotationally invariant

Radic determinant: AS2 – Airborne system 2

Although only square matrices formally have a determinant, it is possible to define various algebraic relationships that can be used. One of these is from Radic (1969), and expands as follows

$$det_R(\mathbf{A}) = \begin{vmatrix} Axx\ Axy \\ Ayx\ Ayy \\ Azx\ Azy \end{vmatrix} = \begin{vmatrix} Axx & Axy \\ Ayx & Ayy \end{vmatrix} - \begin{vmatrix} Axx & Axy \\ Azx & Azy \end{vmatrix} + \begin{vmatrix} Ayx & Ayy \\ Azx & Azy \end{vmatrix}$$

$$= AxxAyy - AxyAyx - AxxAzy + AxyAzx + AyxAzy - AyyAzx$$

(Note that the first determinant on the RHS is Sattel's approximation.)

From this we can obtain an estimate of apparent conductivity from:

$$\sigma_a^{(r)} = \mu\omega|A_{DET-R}|$$

➔ This estimate is not invariant under rotation.

First order: AS2 – Airborne system 2

Finally for AS2 to First Order we will relate the magnetic fields in the air and the electric fields at the base station simply by their total fields:

$$|E_{horiz}|_{base} = Z_{AS2}\,|H|_{air}$$

Present maps of apparent conductivity, so use admittance formulation:

$$|H|_{air} = A_{AS2}\,|E_{horiz}|_{base} \quad \rightarrow \quad \sigma_a^{(f)} = \omega\mu\, A_{AS2}{}^{\wedge 2}$$

➔ *Note that $\sigma_a^{(f)}$ is a scalar, and is sensitive to source geometry and is not rotationally invariant*

Forward calculations: AS3 – Airborne system 3

AS3, airborne system 3, is the superset in that we can calculate AS1 and AS1 responses, and also the full admittance tensor:

$$\begin{bmatrix} Hx \\ Hy \\ Hz \end{bmatrix} = \begin{bmatrix} Axx\ Axy \\ Ayx\ Ayy \\ Azx\ Azy \end{bmatrix} \begin{bmatrix} Ex_b \\ Ey_b \end{bmatrix}$$

We can also determine the full Tipper matrix:

$$\begin{bmatrix} Hx \\ Hy \\ Hz \end{bmatrix} = \begin{bmatrix} Txx\ Txy \\ Tyx\ Tyy \\ Tzx\ Tzy \end{bmatrix} \begin{bmatrix} Hx_b \\ Hy_b \end{bmatrix}$$

← ZTEM gives (Tzx,Tzy)

And the horizontal inter-station transfer functions (see Campanya et al., 2016):

$$\begin{bmatrix} Hx_1 \\ Hy_1 \end{bmatrix} = \begin{bmatrix} Hxx & Hxy \\ Hyx & Hyy \end{bmatrix} \begin{bmatrix} Hx_2 \\ Hy_2 \end{bmatrix}$$

The advantages of complementing MT profiles in 3-D environments with geomagnetic transfer function and interstation horizontal magnetic transfer function data: results from a synthetic case study

Joan Campanyà,[1] Xènia Ogaya,[1] Alan G. Jones,[1,*] Volker Rath,[1] Jan Vozar[1,†] and Naser Meqbel[2]

End-member models

To understand the ANOMALOUS EM FIELDS associated with resistivity models of the subsurface, it is useful to study the two end-member models:

2-D Contact: Has the greatest inductive and galvanic effects

Sphere: Has the smallest inductive and galvanic effects

2-D contact model analytical response

A contact is the most extreme model in terms of inductive and galvanic effects

Two modes:
TE mode: Electric inducing field along strike: Ex,Hy, Hz

TM mode: Magnetic inducing field along strike : Hx,Ex,Ex

Fields of a 2-D contact derived analytically using the approaches of Weaver et al. (1984, 1986)

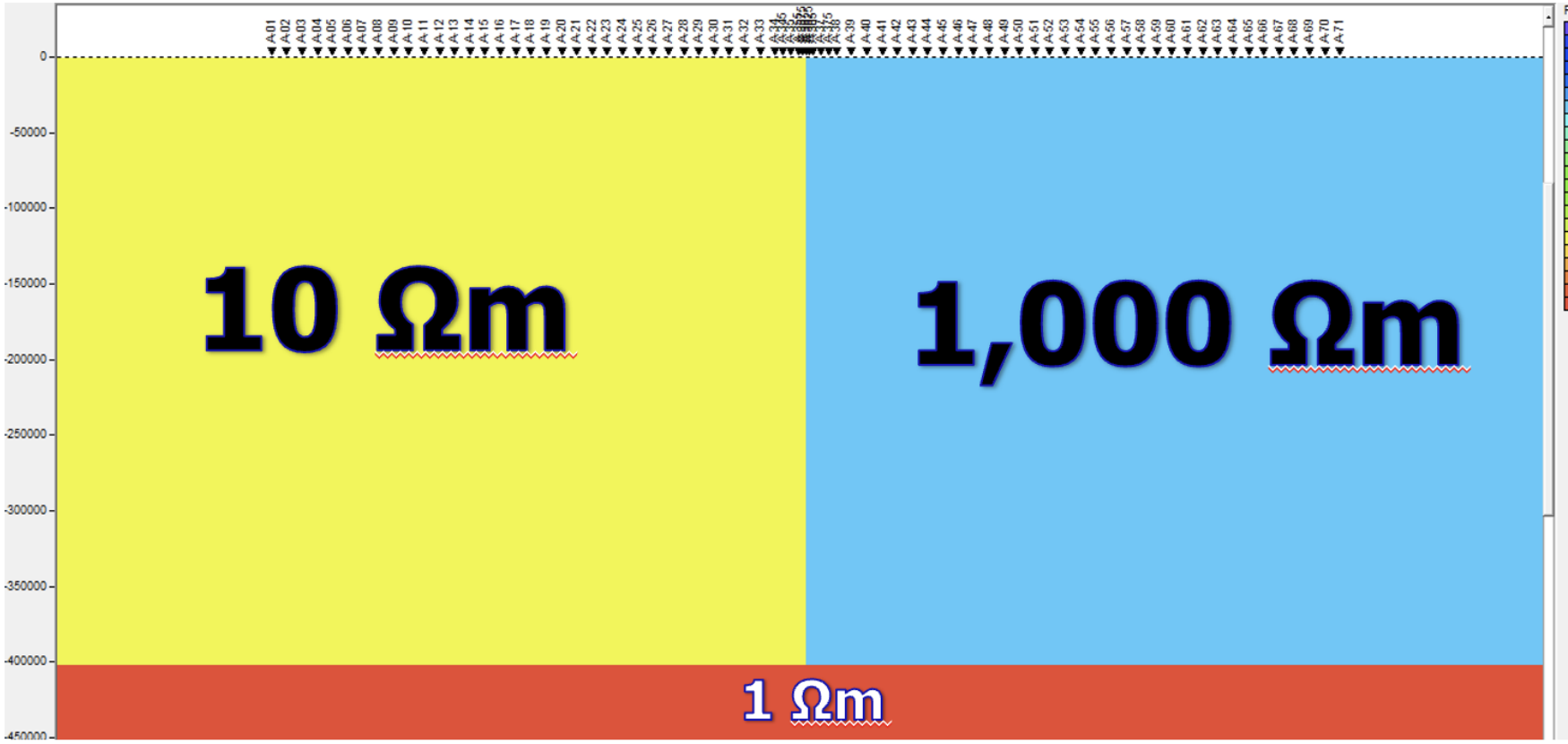

TE Fields of a 2-D contact @ 1 Hz

TE Ex electric fields shows a factor of 5 increase, but poor localization of contact location

TE Hy shows 65% anomaly on the conductive site, 20% on the resistive side, good localization

TE mode

Ex

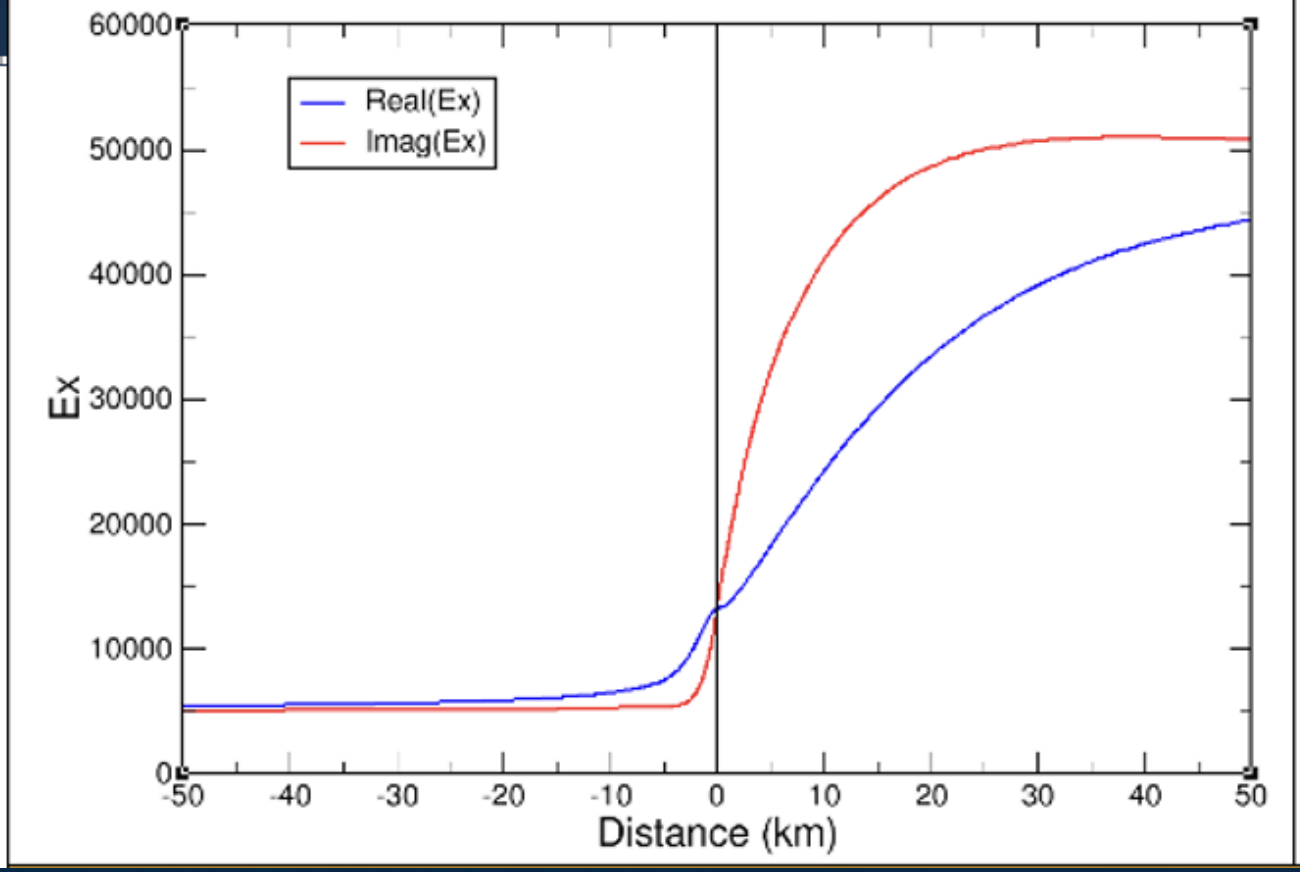

Hy

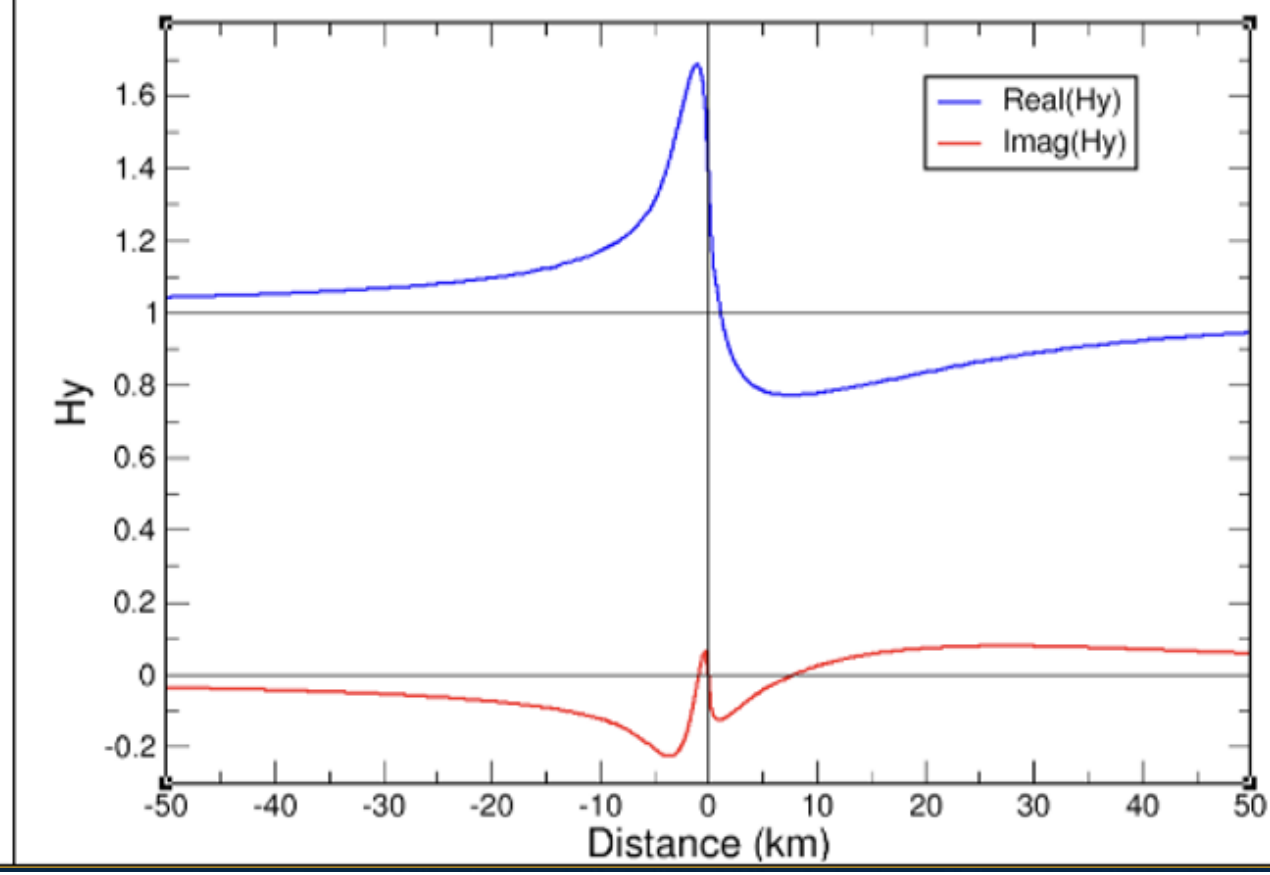

TM Fields of a 2-D contact @ 1 Hz

TM: Ey electric field an order of magnitude increase (Ohm's Law), excellent localization

TM: **No magnetic field response to the contact in TM mode in 2-D**

TM mode

Ey

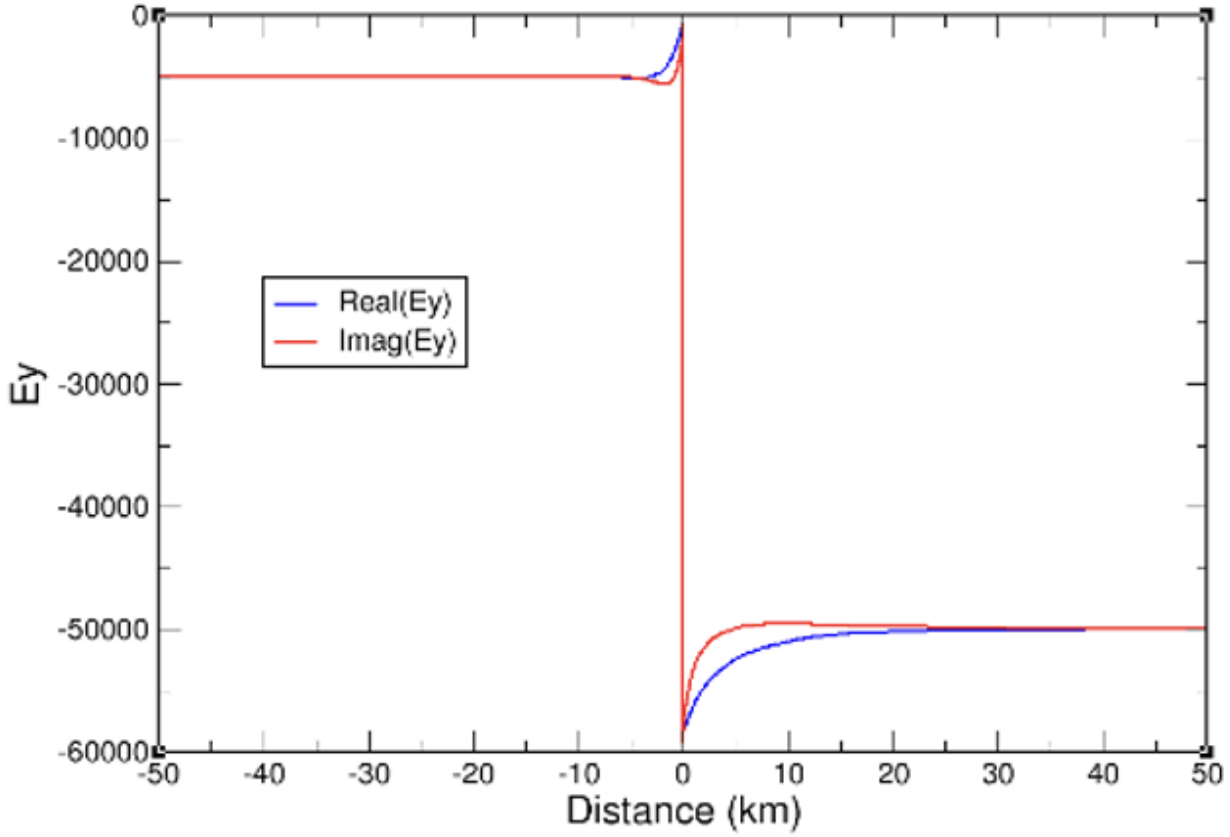

Hx

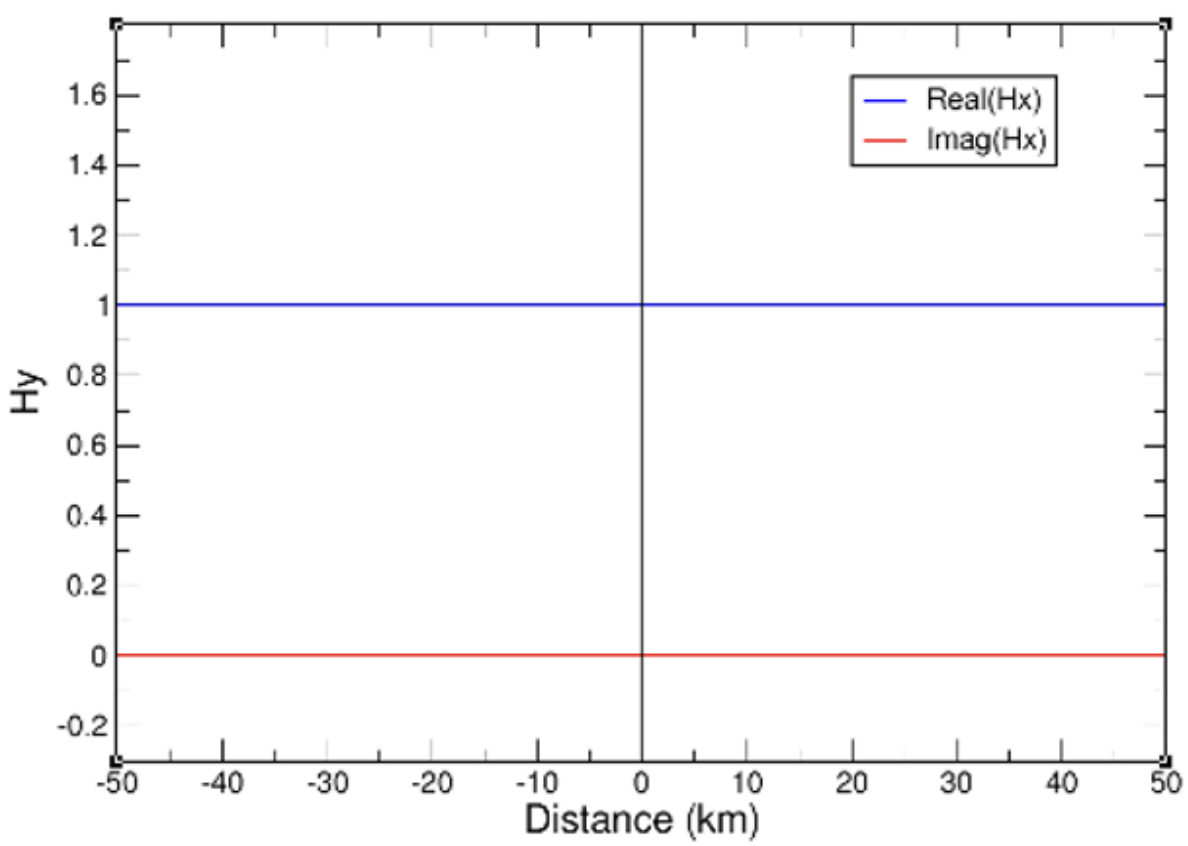

MT and Titan24 responses at 1 Hz

The MT responses (TE=blue; TM=red) and Titan24 TE (green) responses at 1 Hz across the fault.

Titan24 TM = MT TM

Greatest sensitivity is the TM RhoA in MT & Titan24 due to discontinuity in the Ey field

Titan24 TE response to the contact is muted as it only acquires Ex and not the spatially-varying Hy

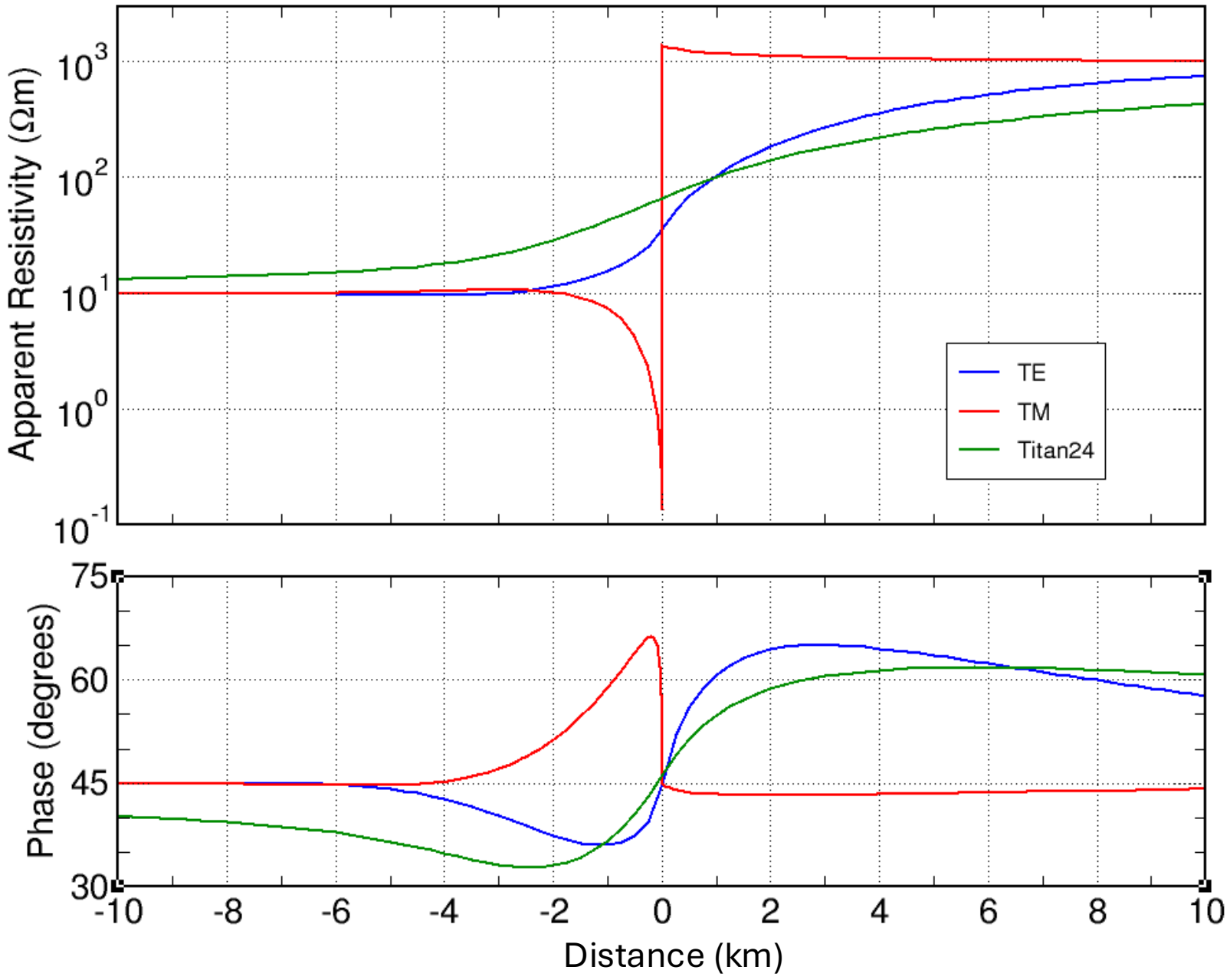

MT and AS2 ("MobileMT") responses at 1 Hz

The MT responses (TE=blue; TM=red) and AS2 First Order (green) responses at 1 Hz across the fault.

Greatest sensitivity is the TM RhoA in MT due to discontinuity in the Ey field

Keep in mind that AMT may be spatially sampling every 250 m or 500 m, whereas ANSEM methods are sampling every 20 m.

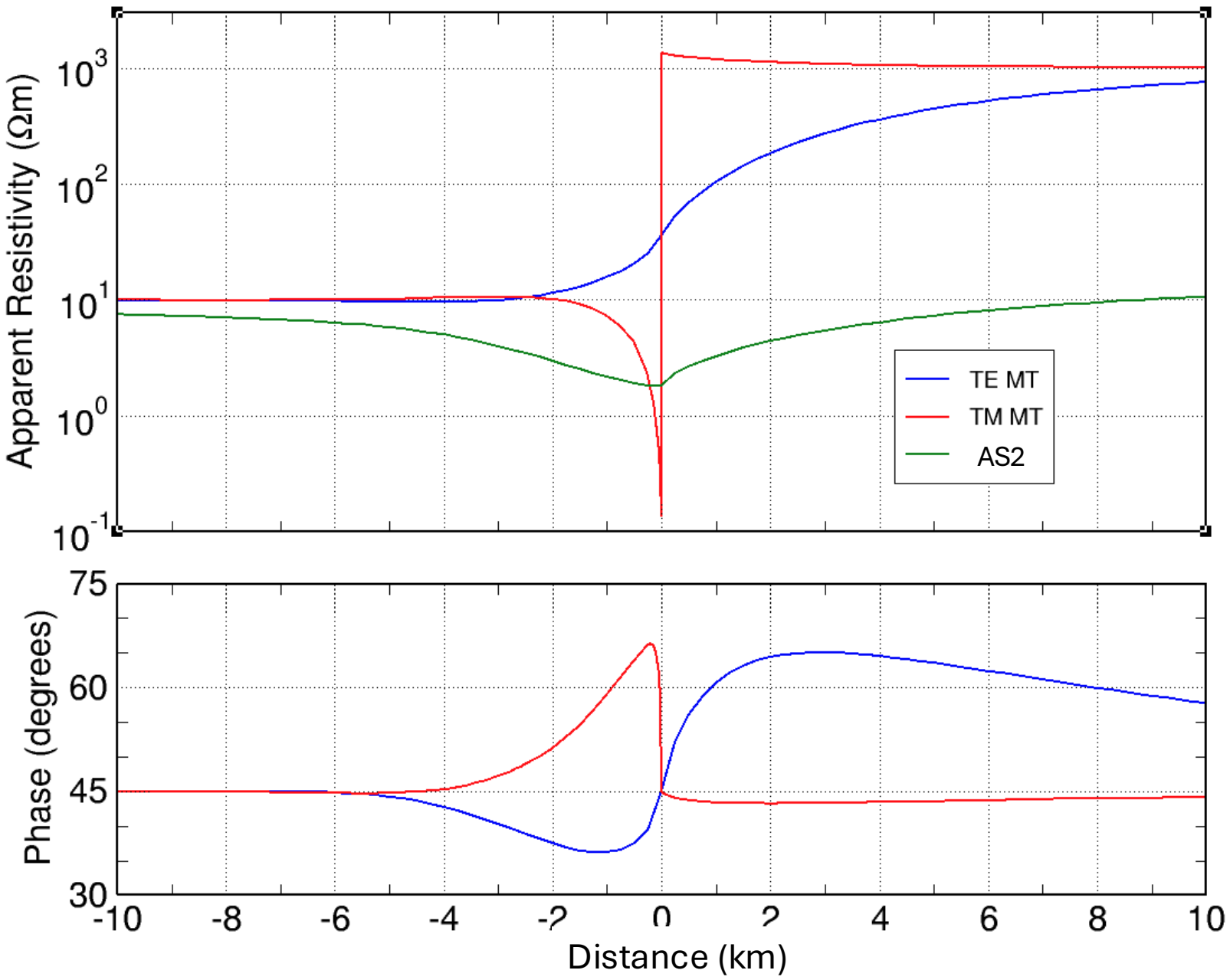

Tipper and AS1 (“ZTEM”) responses at 1 Hz

The Tipper responses and AS1 responses at 1 Hz across the contact.

Greatest locational sensitivity is the AS1 responses as for Tippers the local Hz is reduced by local (Hx,Hy)

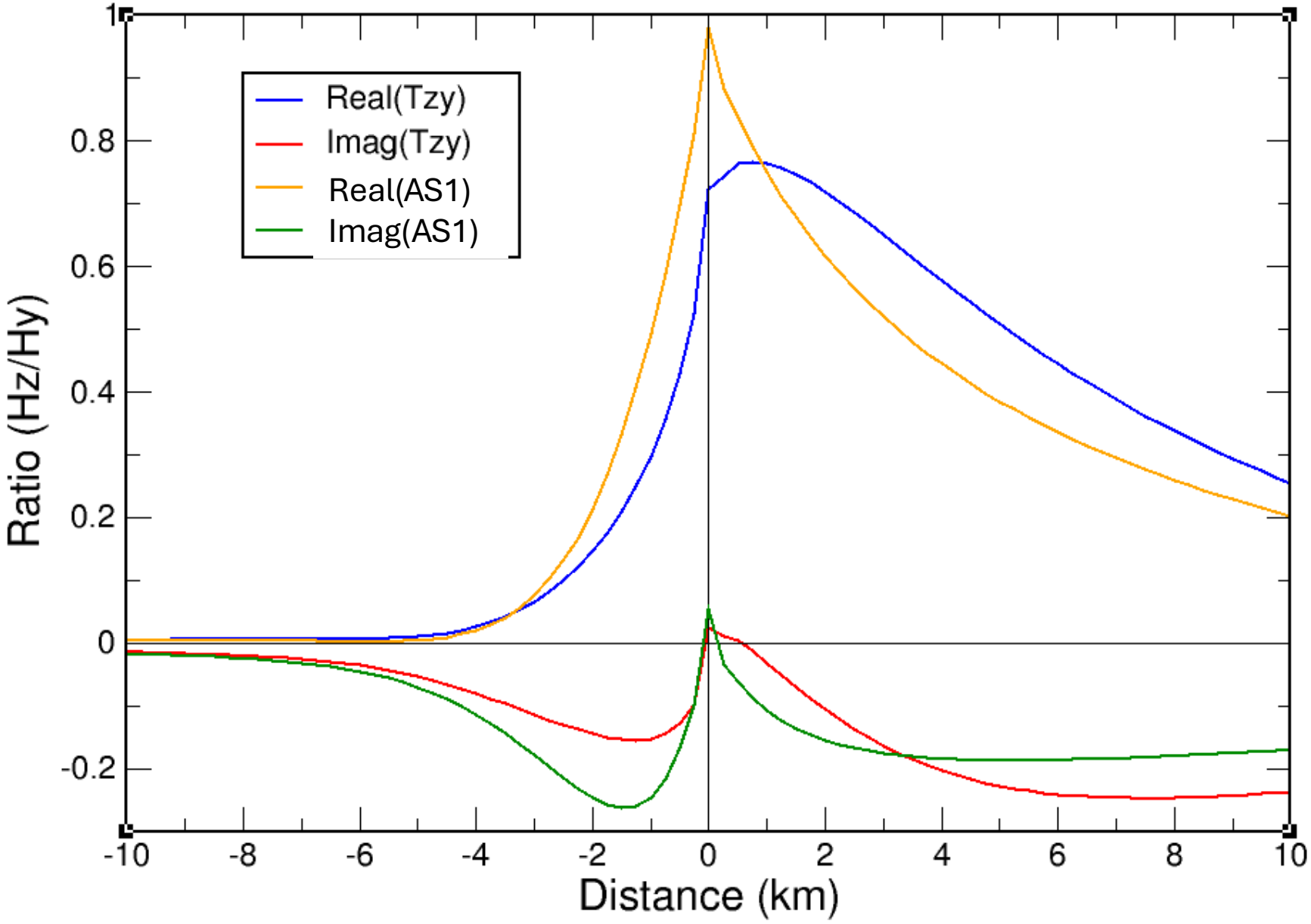

EM fields and responses over a conducting sphere

A conducting sphere of 500 m radius and resistivity 0.1 Ωm at a depth of 750 m in a host of 1,000 Ωm

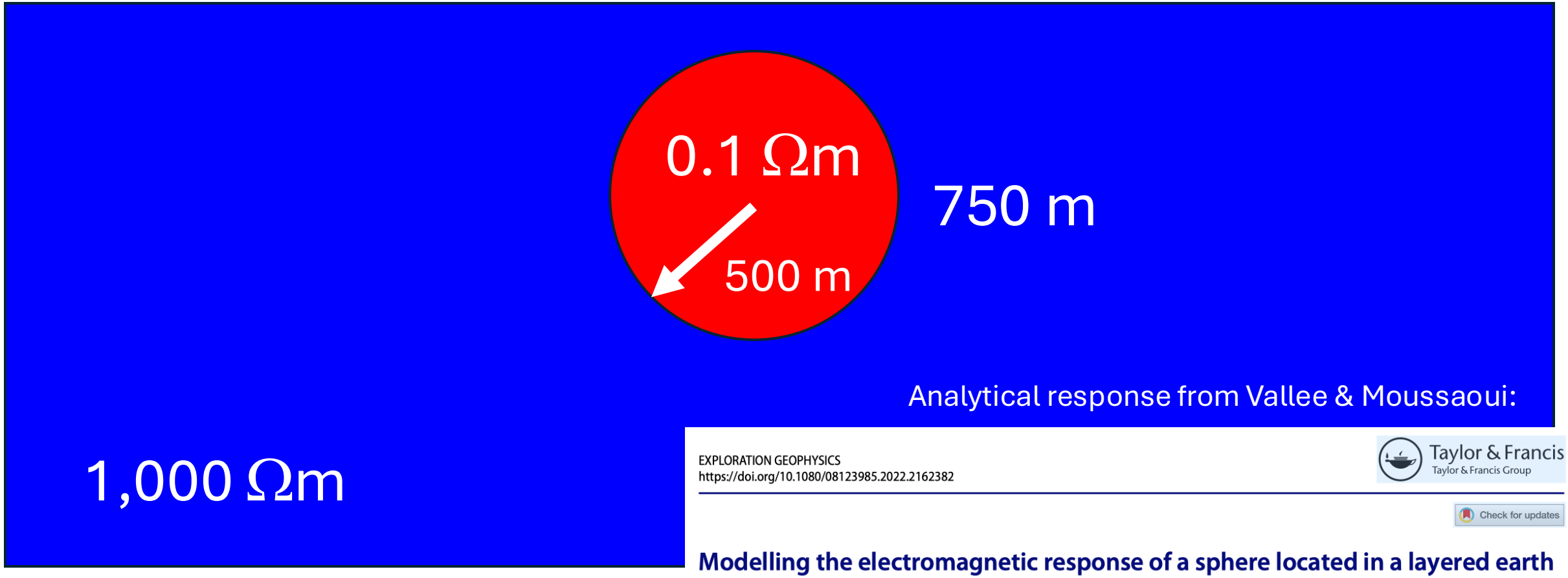

Analytical response from Vallee & Moussaoui:

EXPLORATION GEOPHYSICS
https://doi.org/10.1080/08123985.2022.2162382
Taylor & Francis
Taylor & Francis Group
Check for updates

Modelling the electromagnetic response of a sphere located in a layered earth

Marc A. Vallée and Mouhamed Moussaoui

MT responses at centre site

MT responses at the site directly over the centre of the sphere

Maximum anomalous Pha response at 500 Hz (maximum induction)

Maximum anomalous Rho response at 10 Hz (galvanic effects)

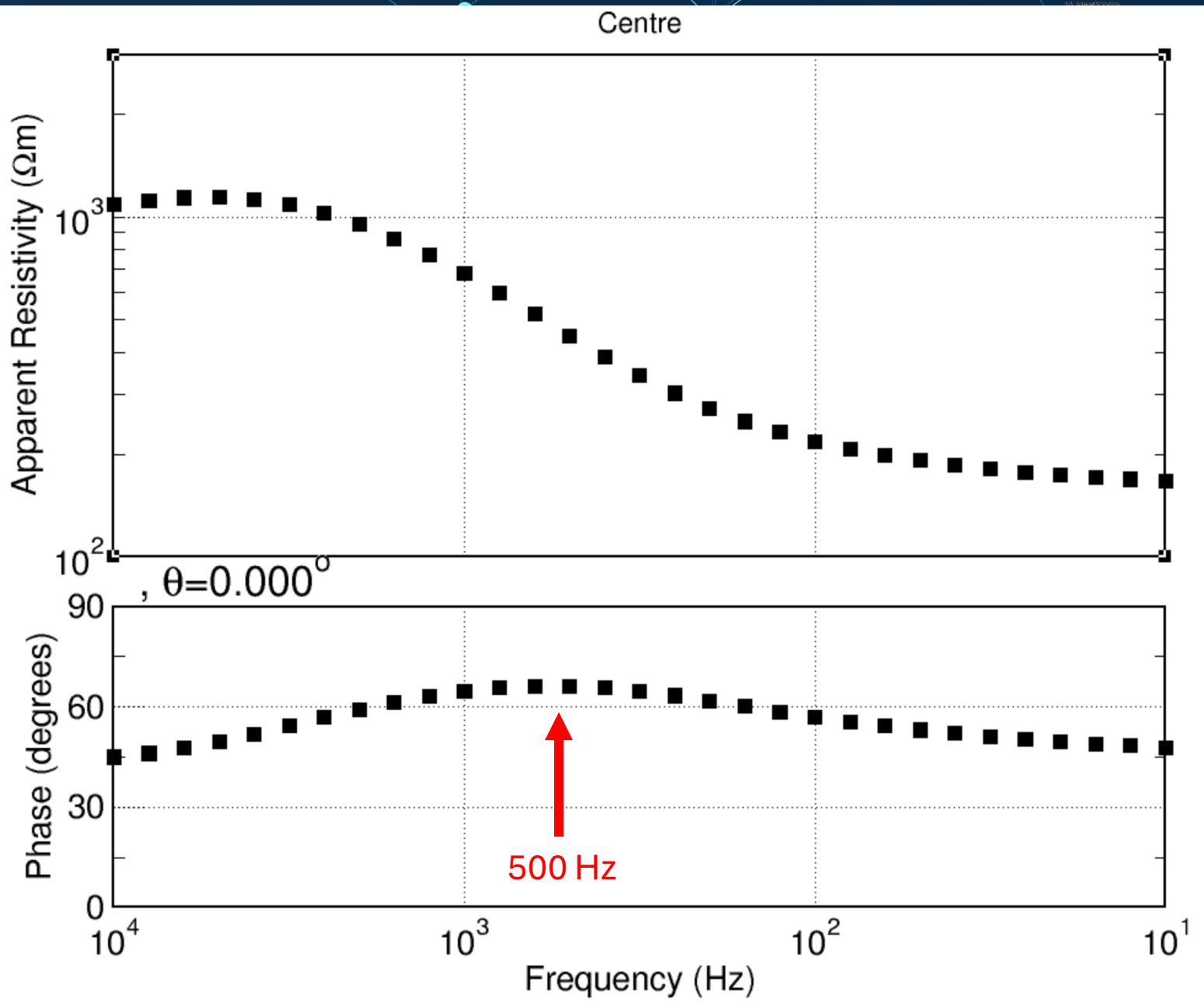

EM fields – Re(Ex)

Greatest induction at 500 Hz

Re(Ex) for N-S e-field source

Anomaly is 2x (100%) greater than background

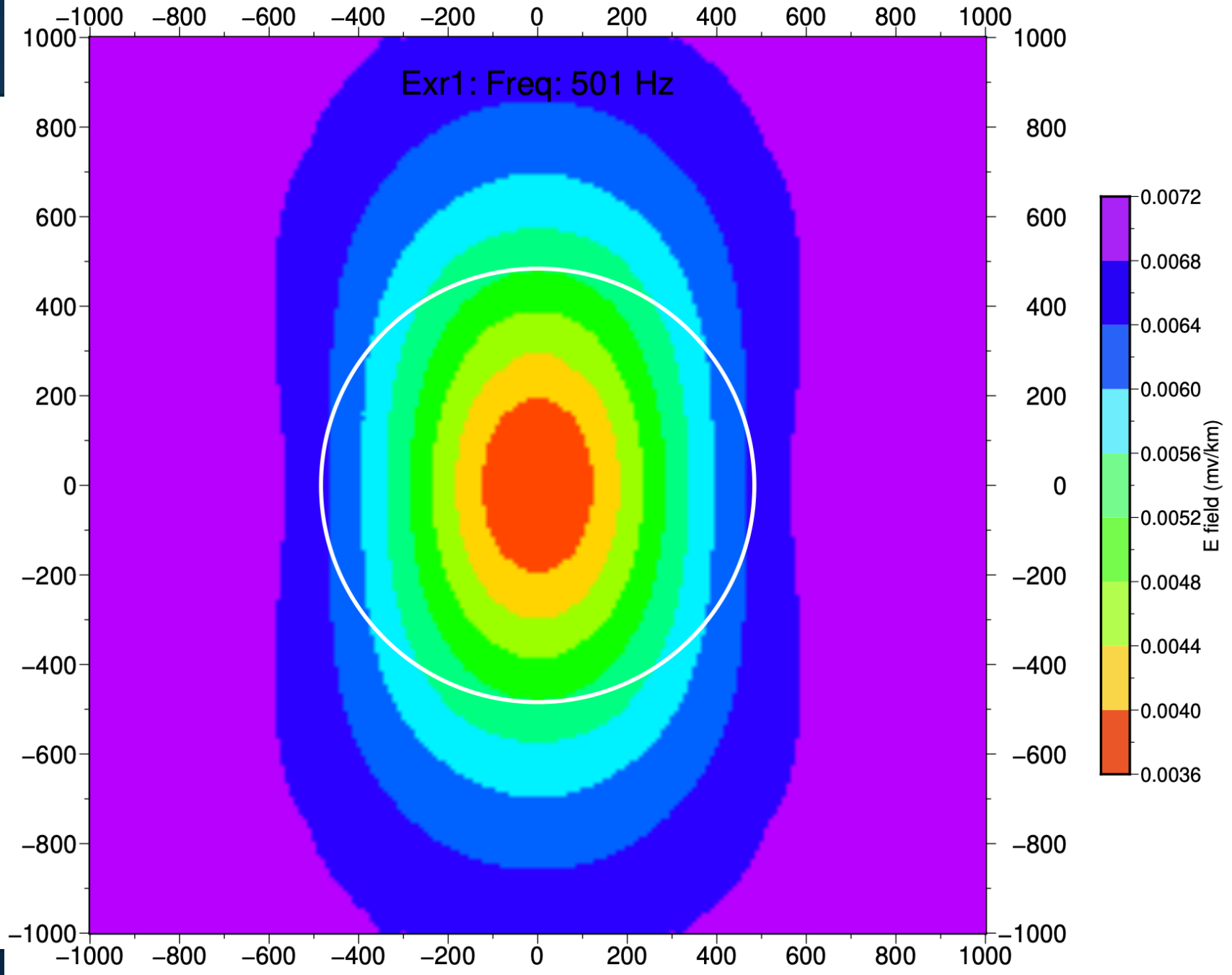

EM fields – Re(Hy)

Greatest induction at 500 Hz

Re(Hy) for N-S e-field source

Anomaly is 1.11 (11%) greater than background

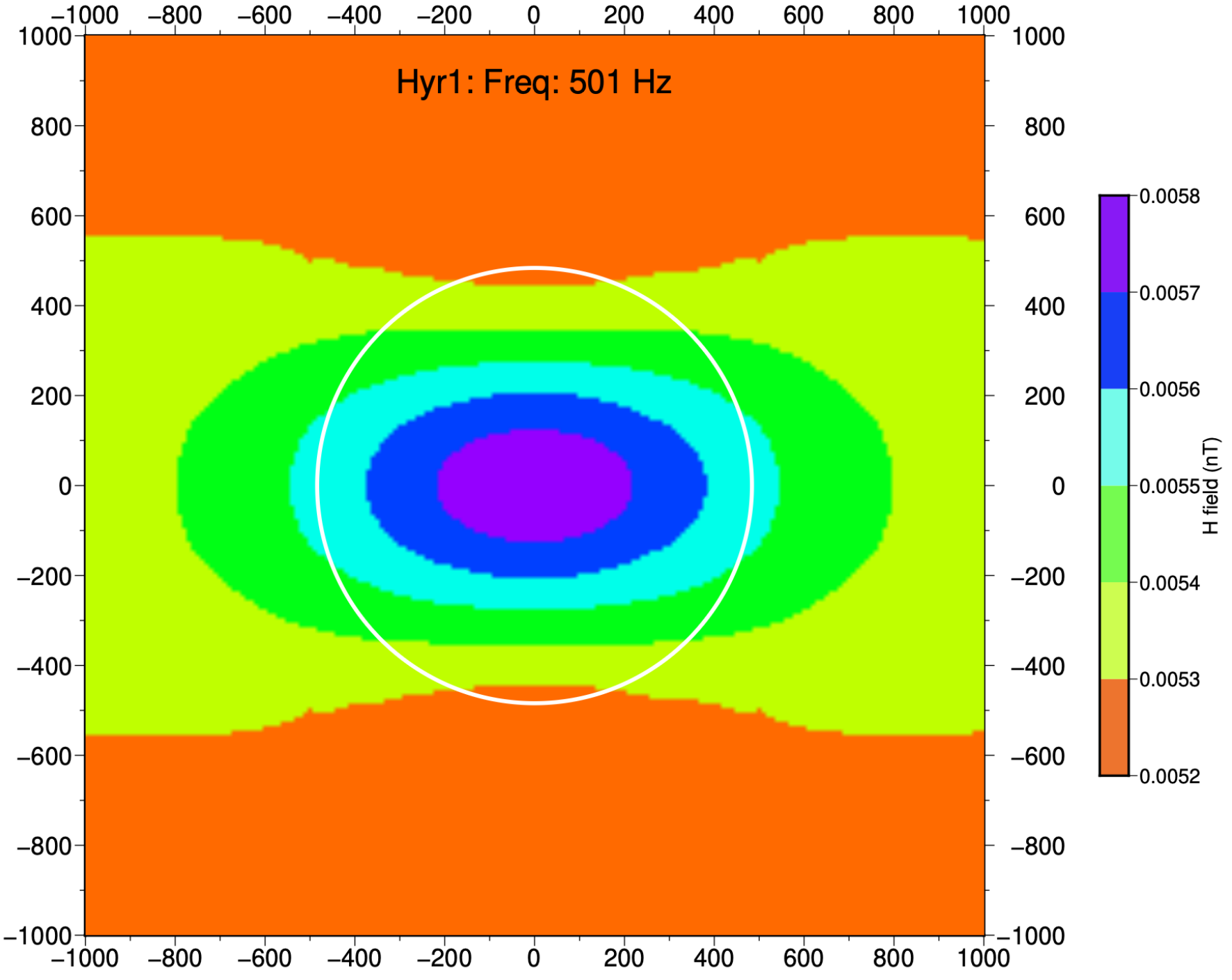

MT RhoXY response at 10 Hz & PhaXY response at 500 Hz

Rho min: 47.8 Ωm (1.4 decades)

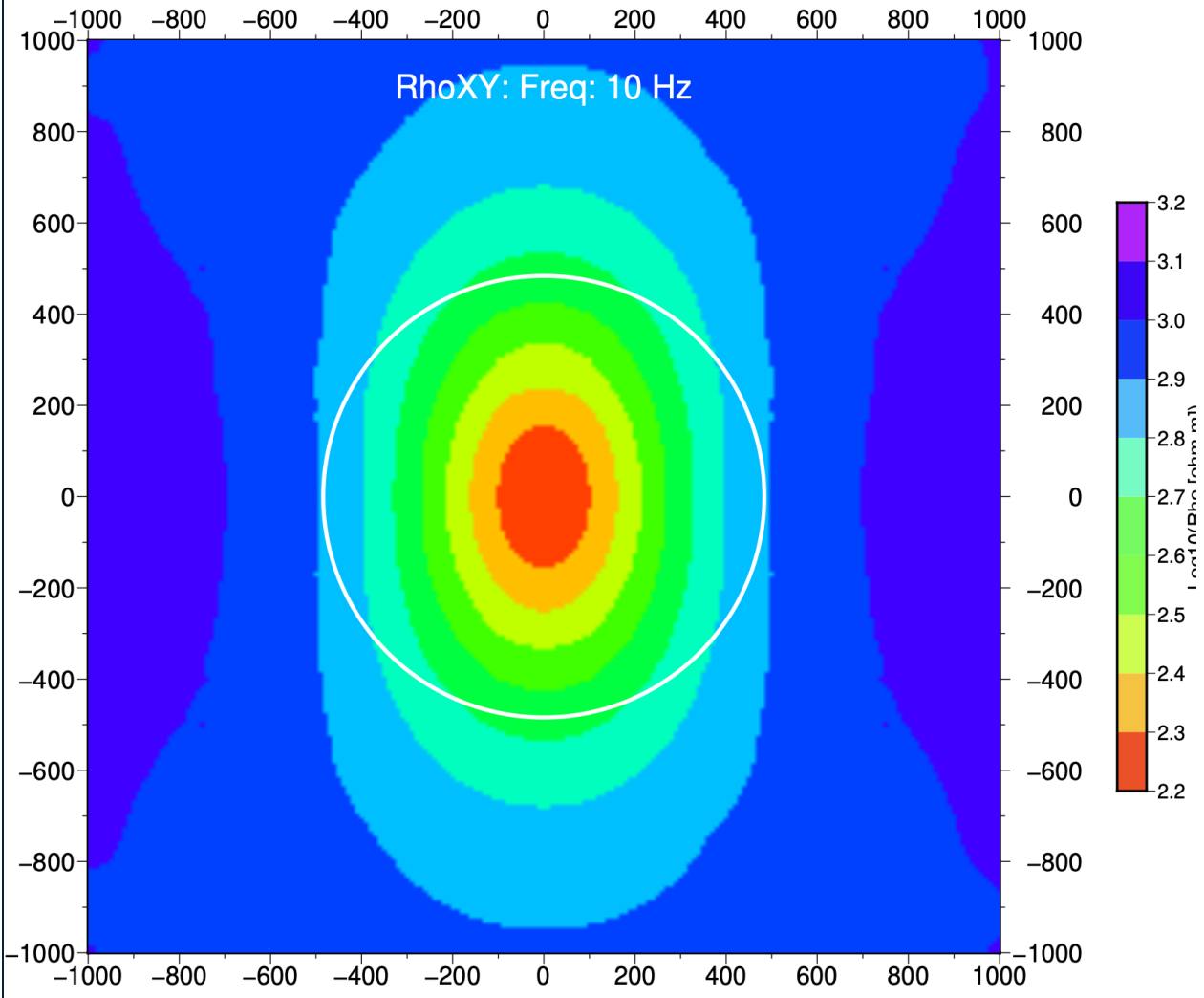

Pha max: 66.2° (21.1°)

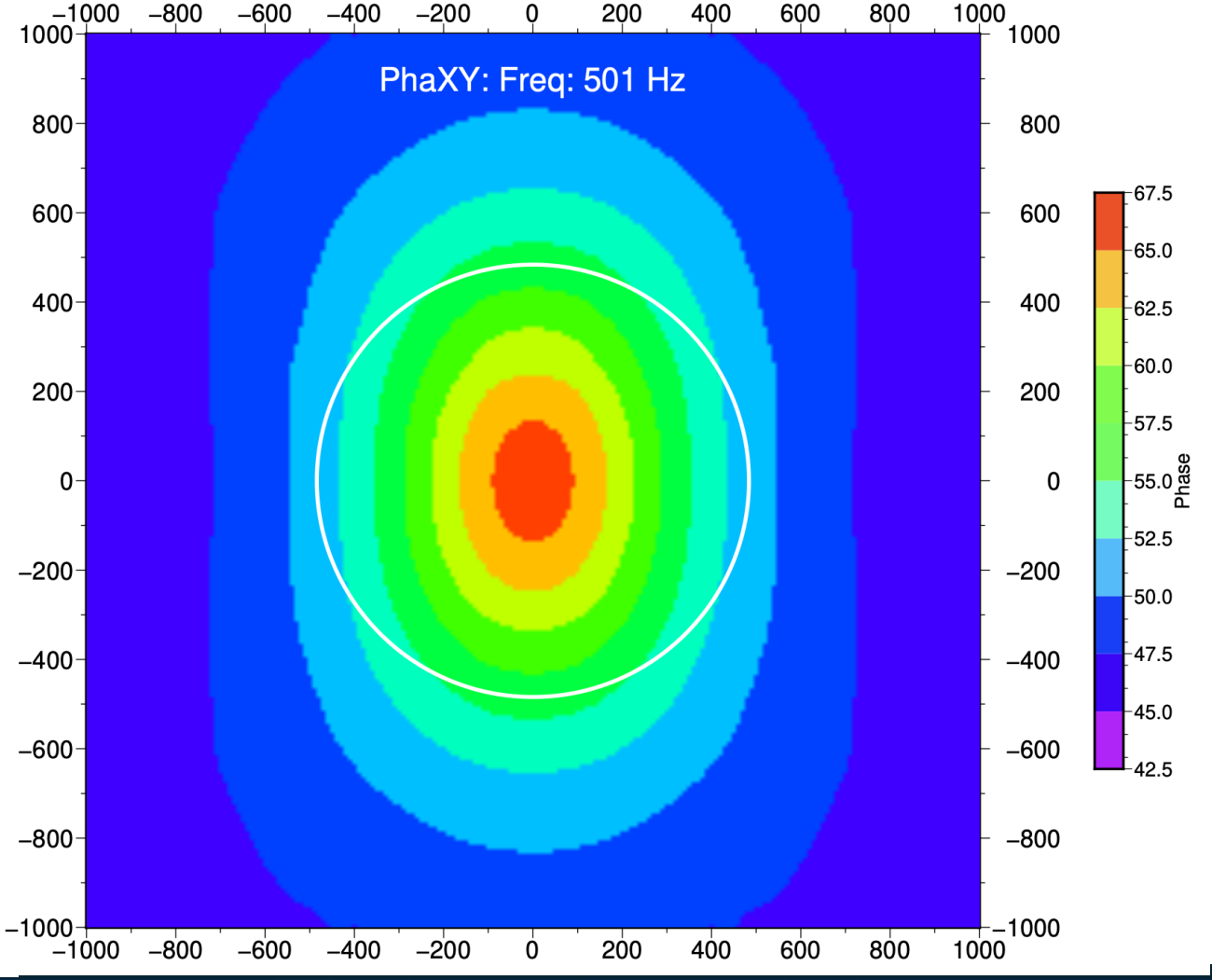

Airborne responses at 79 Hz (greatest anom. H fields)

AS1 max @ 79 Hz: 0.063

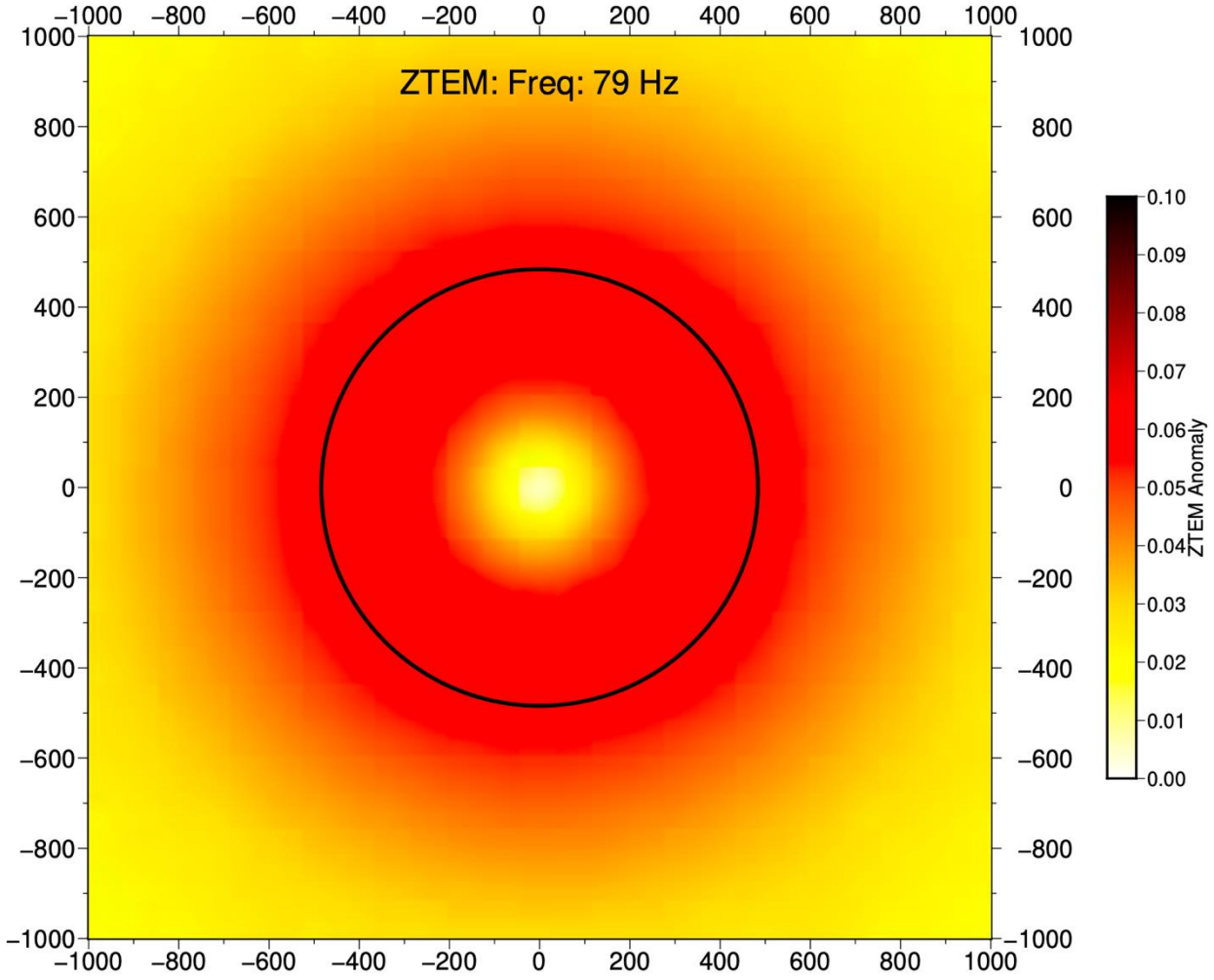

AS2 min @ 79 Hz: 0.142 (4.7%)

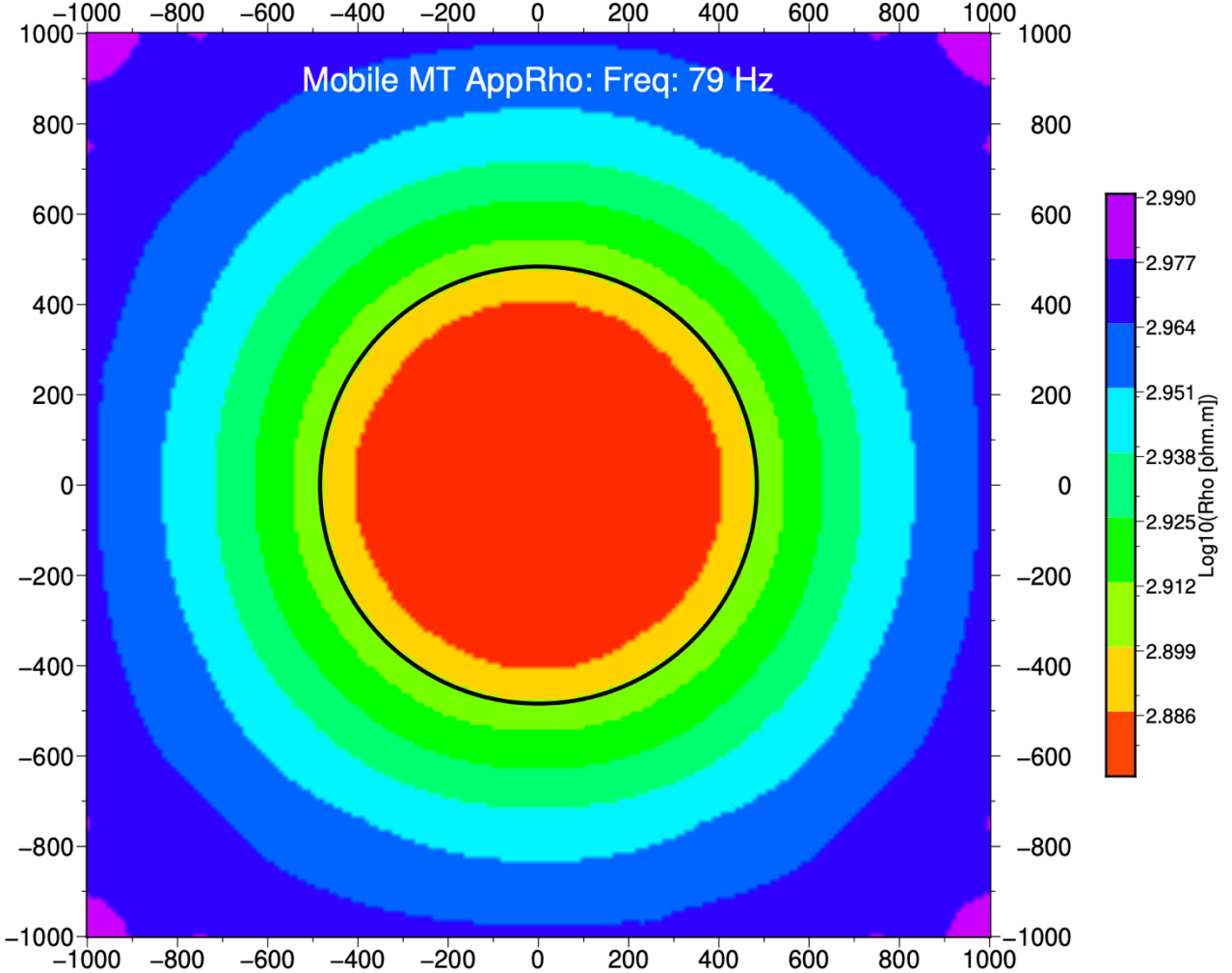

Comparing MT and MobileMT responses @ 79 Hz

Plot of MT RhoXY and AS2 Rho at 79 Hz on same colour scale

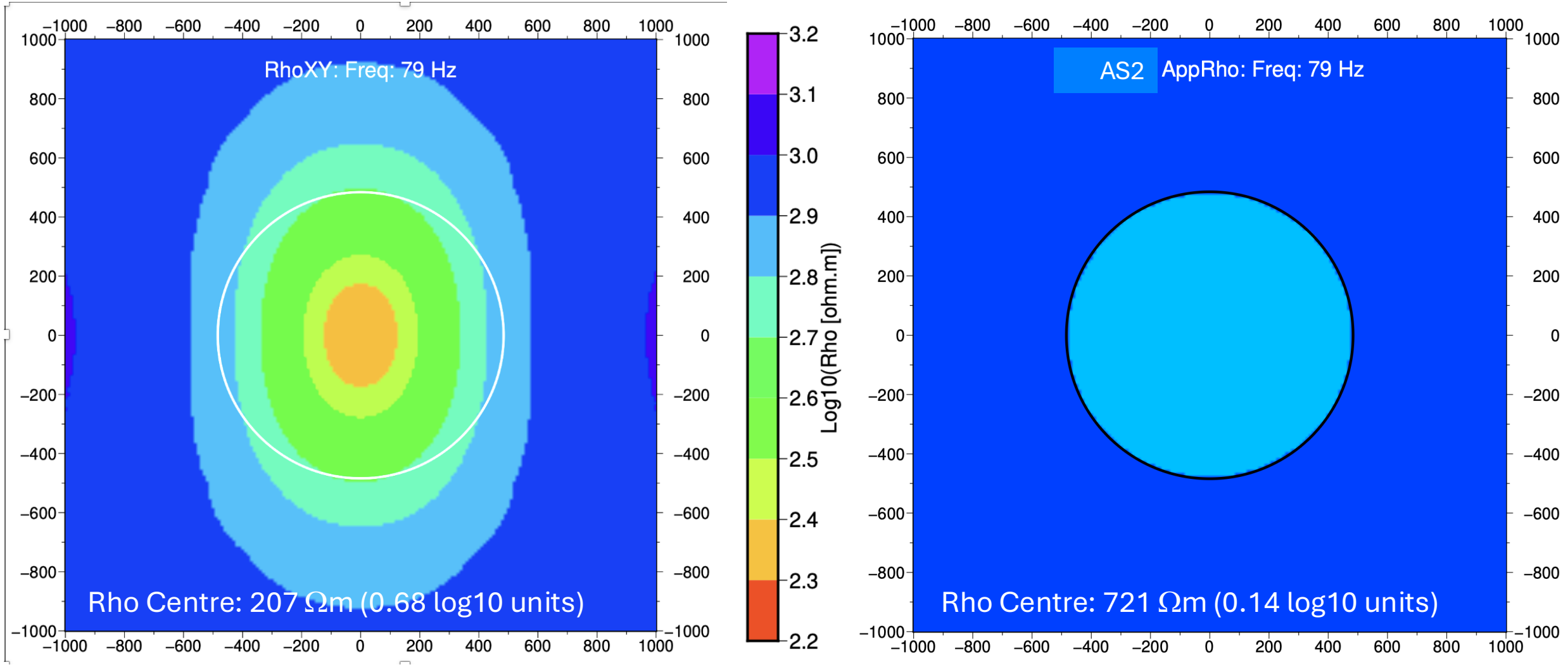

Mineral systems mapping

Regional → Deposit → Camp

Mineral System concept emerged from Australia in the mid-1990s (Wyborn, Heinrich & Jaques, 1994).

Australian National University

Home Profiles **Research output** Projects Research units

Australian Proterozoic Mineral Systems: Essential Ingredients and Mappable Criteria

L.A.I. Wyborn*, C.A. Heinrich, A.L. Jaques

Mineral System concept

The **mineral system concept** views ore deposits not as isolated anomalies but as the local manifestation of large-scale, dynamic geological systems, in which source reservoirs, energy/transport processes, pathways, depositional traps, and preservation conditions interact across multiple spatial and temporal scales to concentrate minerals into economically recoverable accumulations.

McCuaig & Hronsky (2014) synthesized a universal, process-based framework for mineral systems and translated it into practical targeting workflows

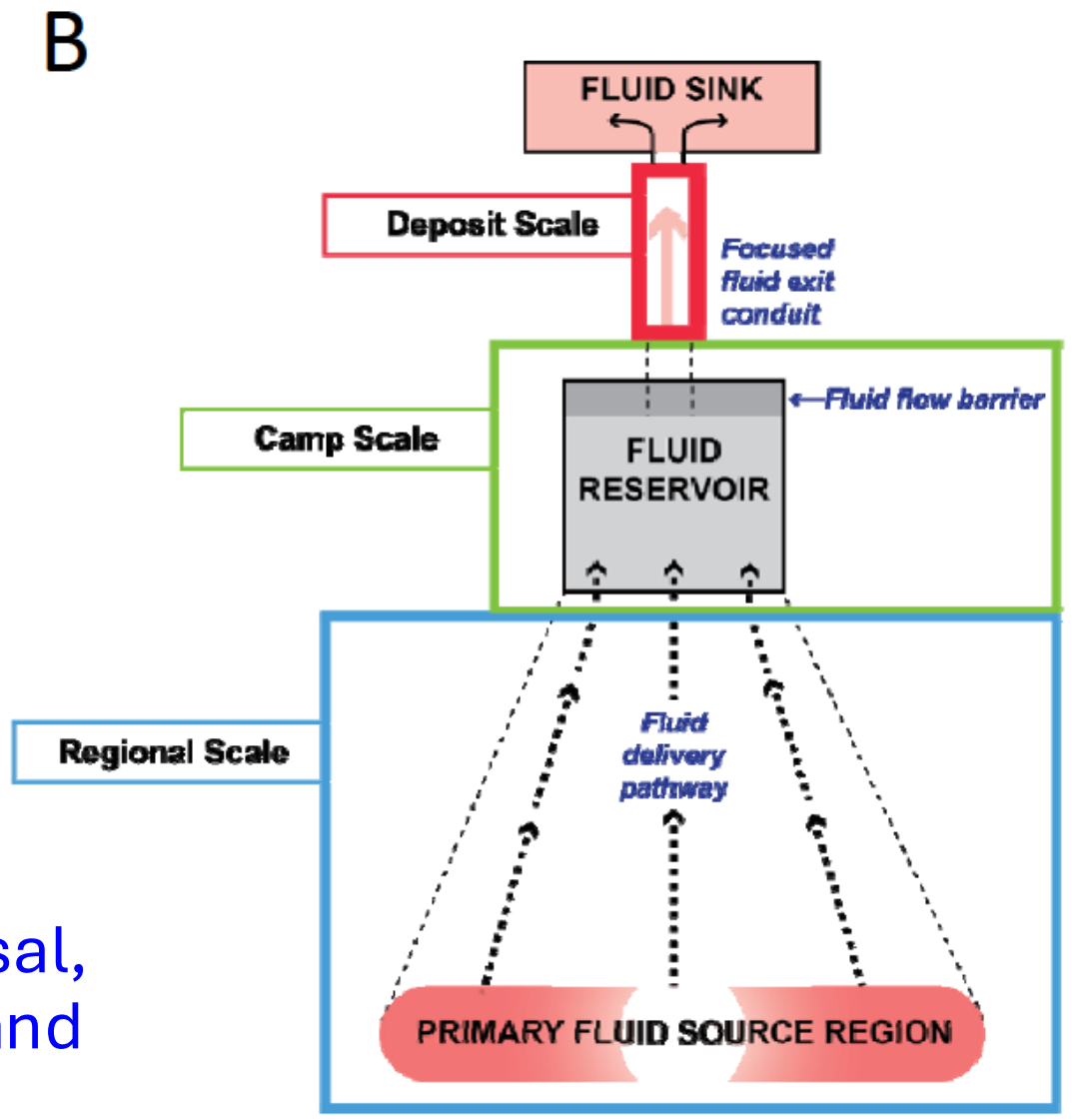

Mineral System concept

Contemporaneously, Begg (2015) listed the geophysical techniques for Architecture mapping and Deposit Detection

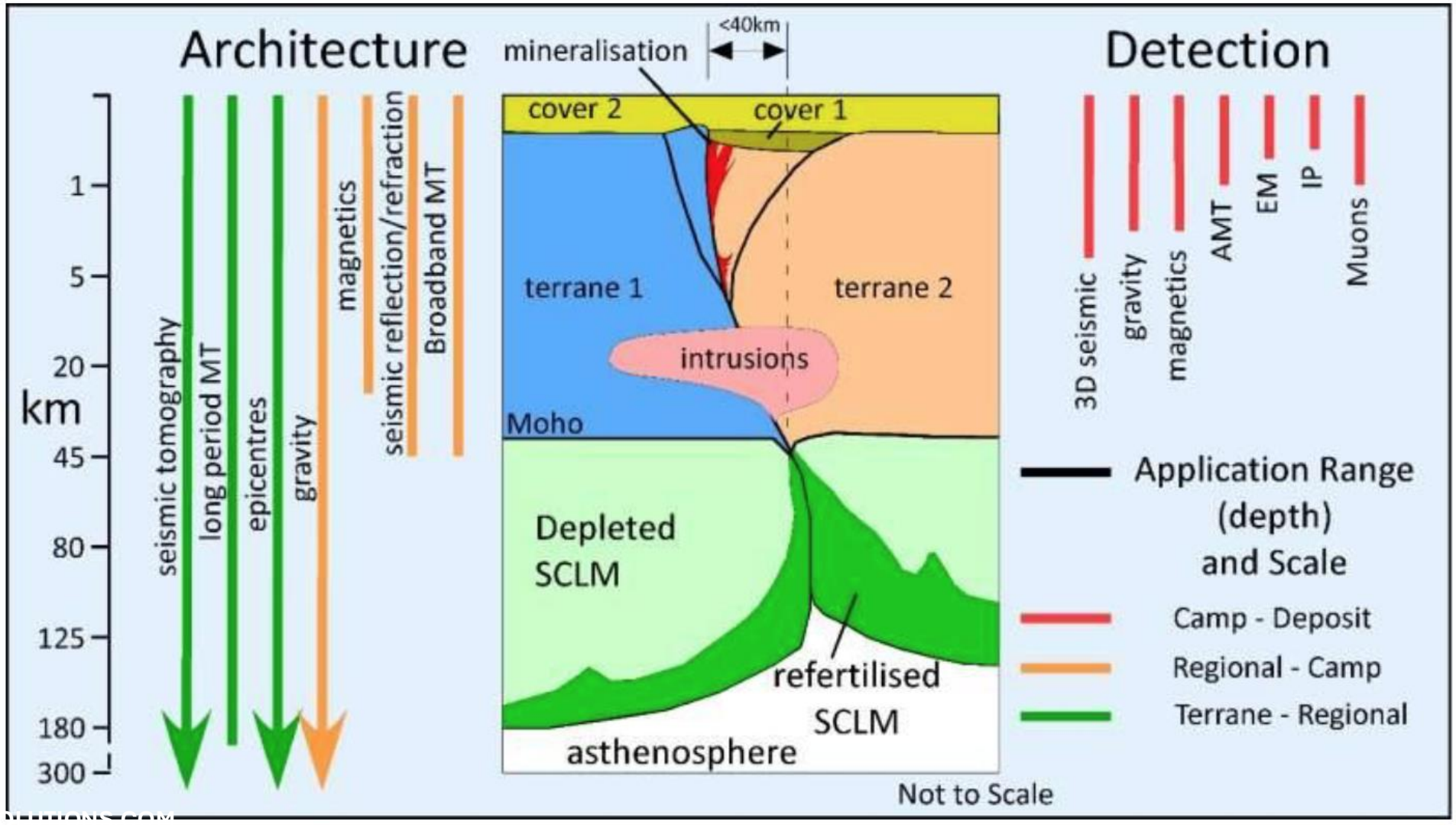

Loe frequency MT (LMT) for Regional Scale mapping

Map at lithospheric scale first – 100s km = Long Period MT

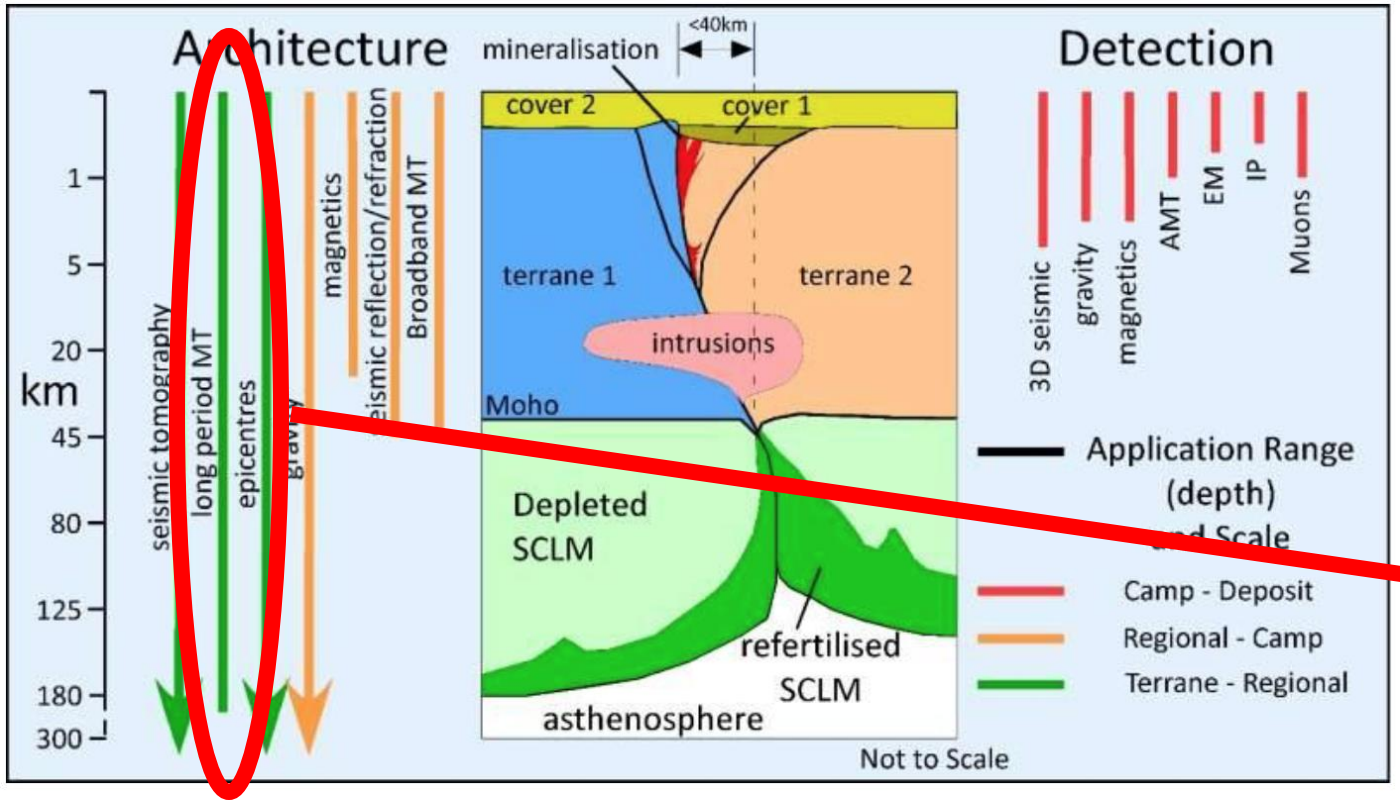

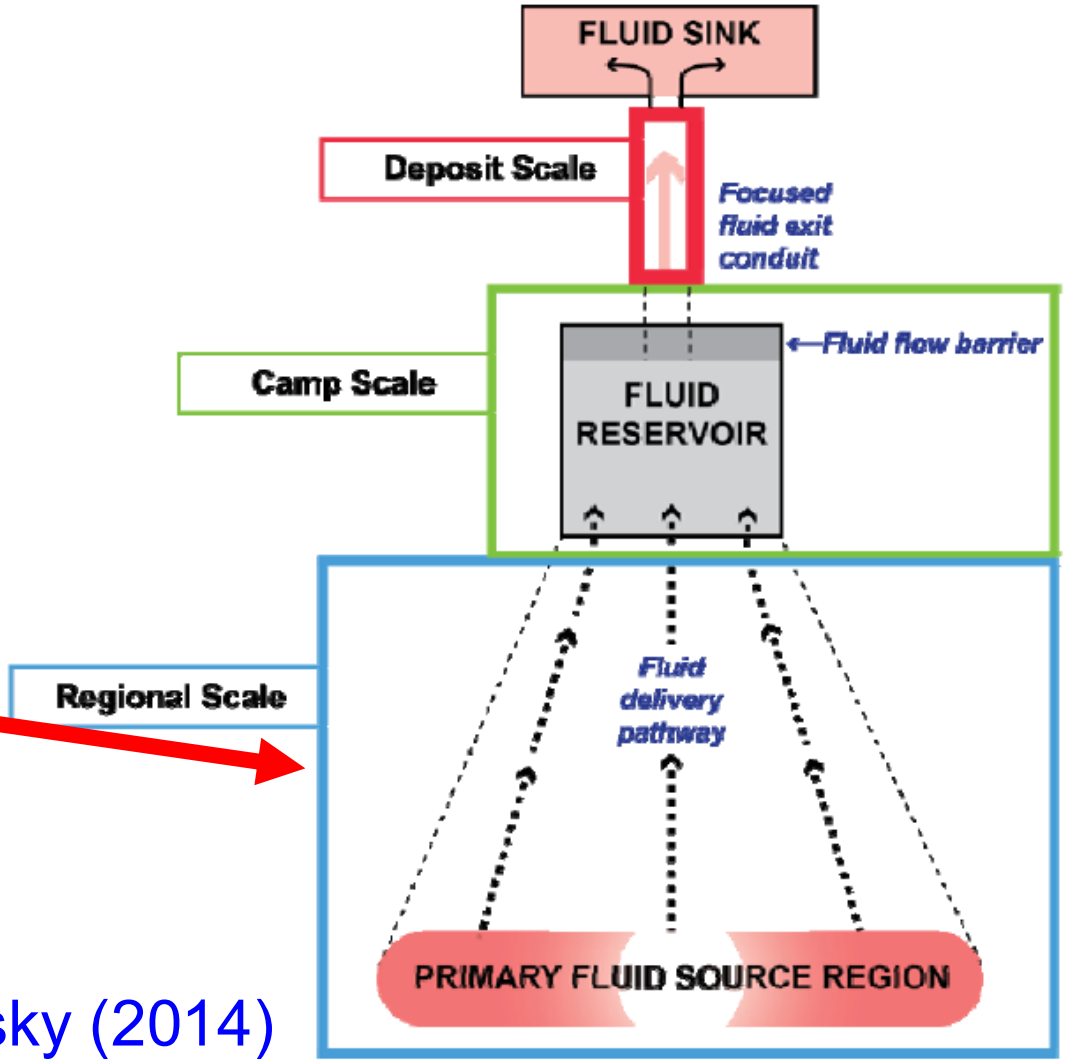

Begg (2015)

McCuaig & Hronsky (2014)

Broadband MT (BBMT) for Camp Scale mapping

Map at crustal scale next – 10s km = Broadband MT

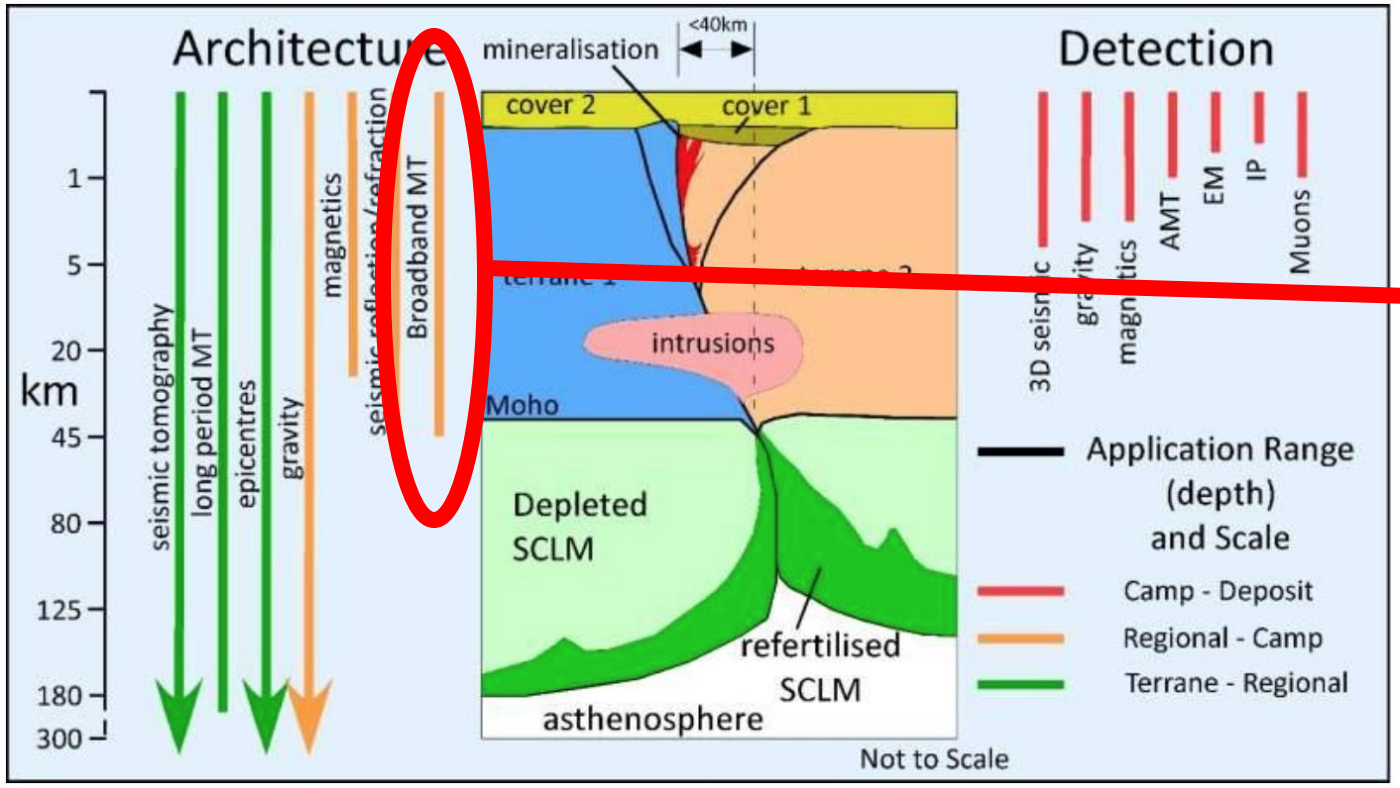

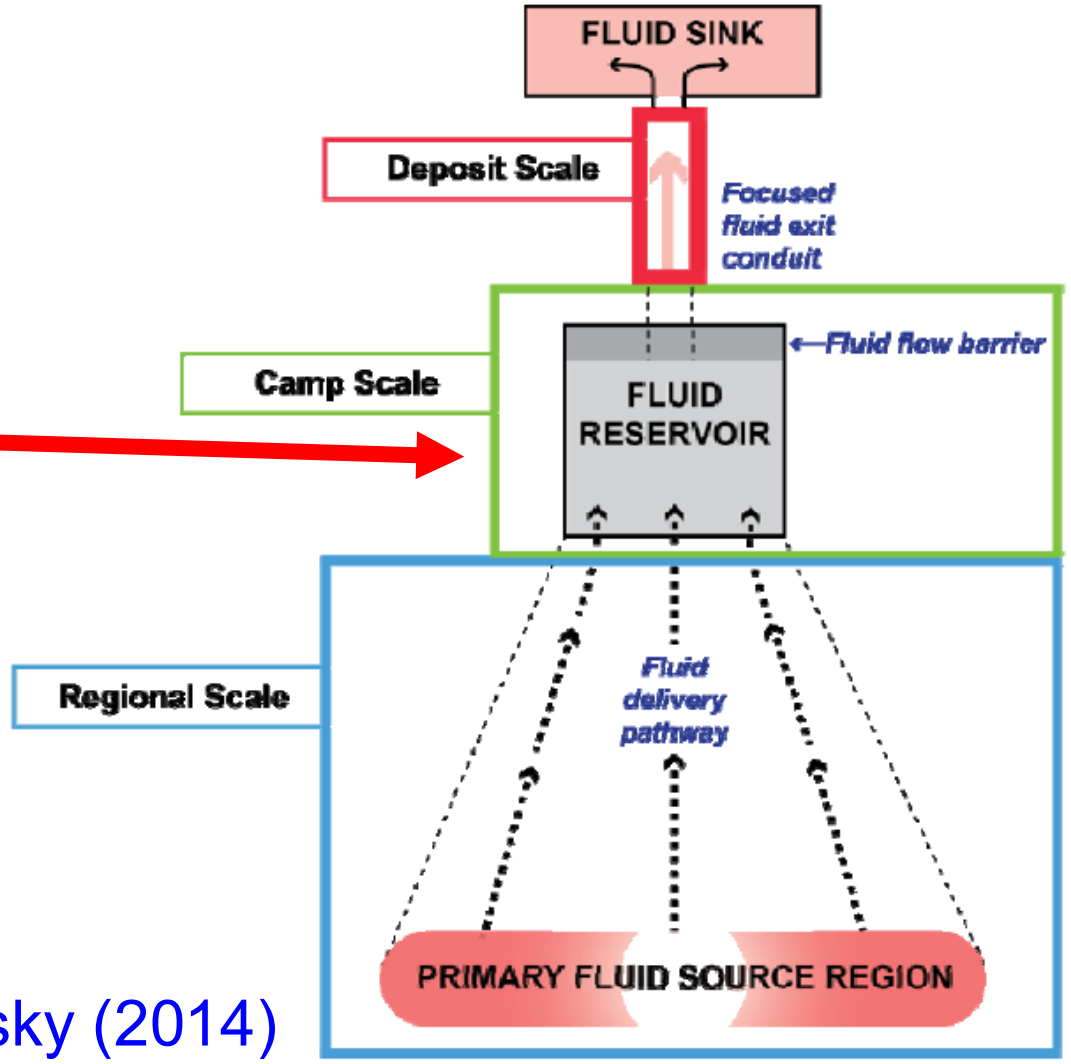

Begg (2015)

McCuaig & Hronsky (2014)

Audio MT (AMT) for Deposit Scale mapping

Finally at target scale – 100s m = Audio MT (and possibly airborne methods)

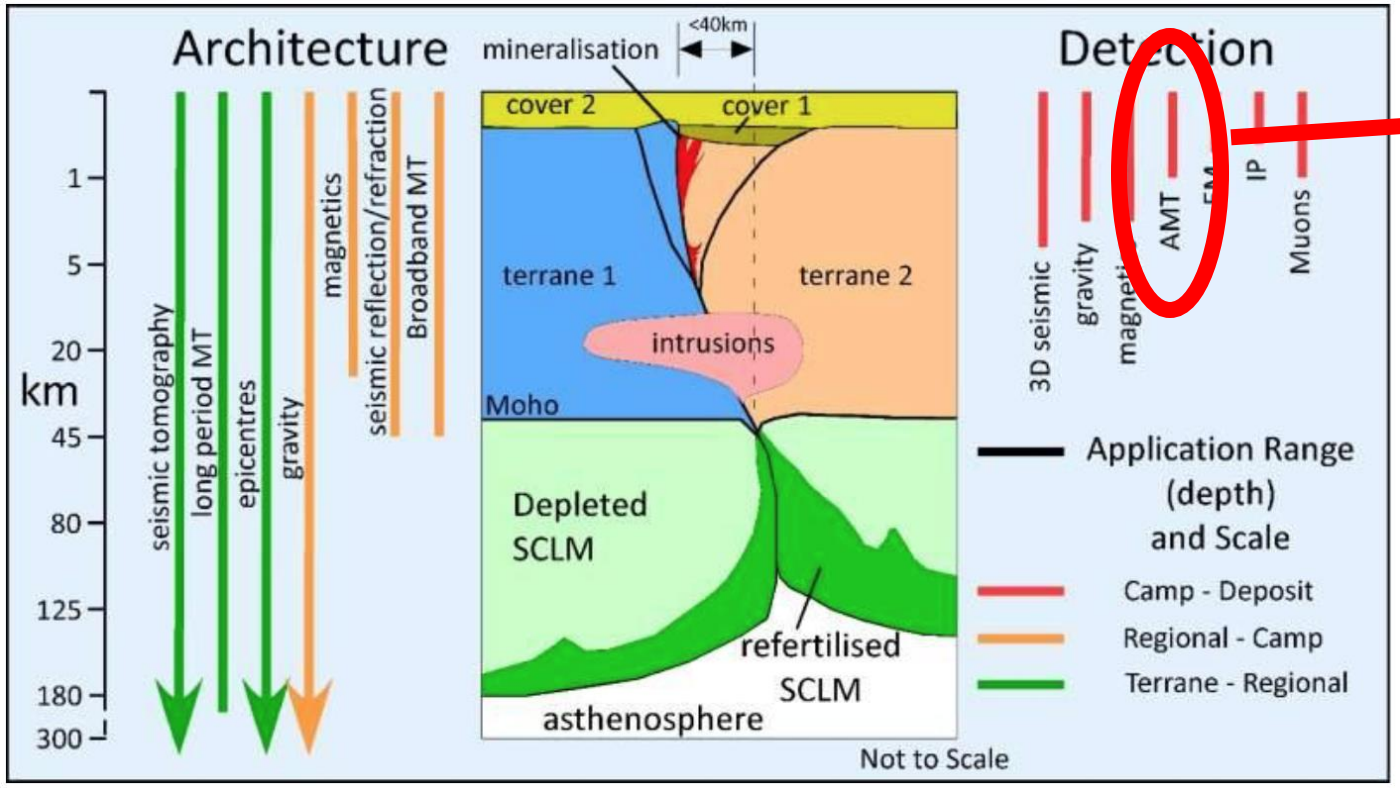

Begg (2015)

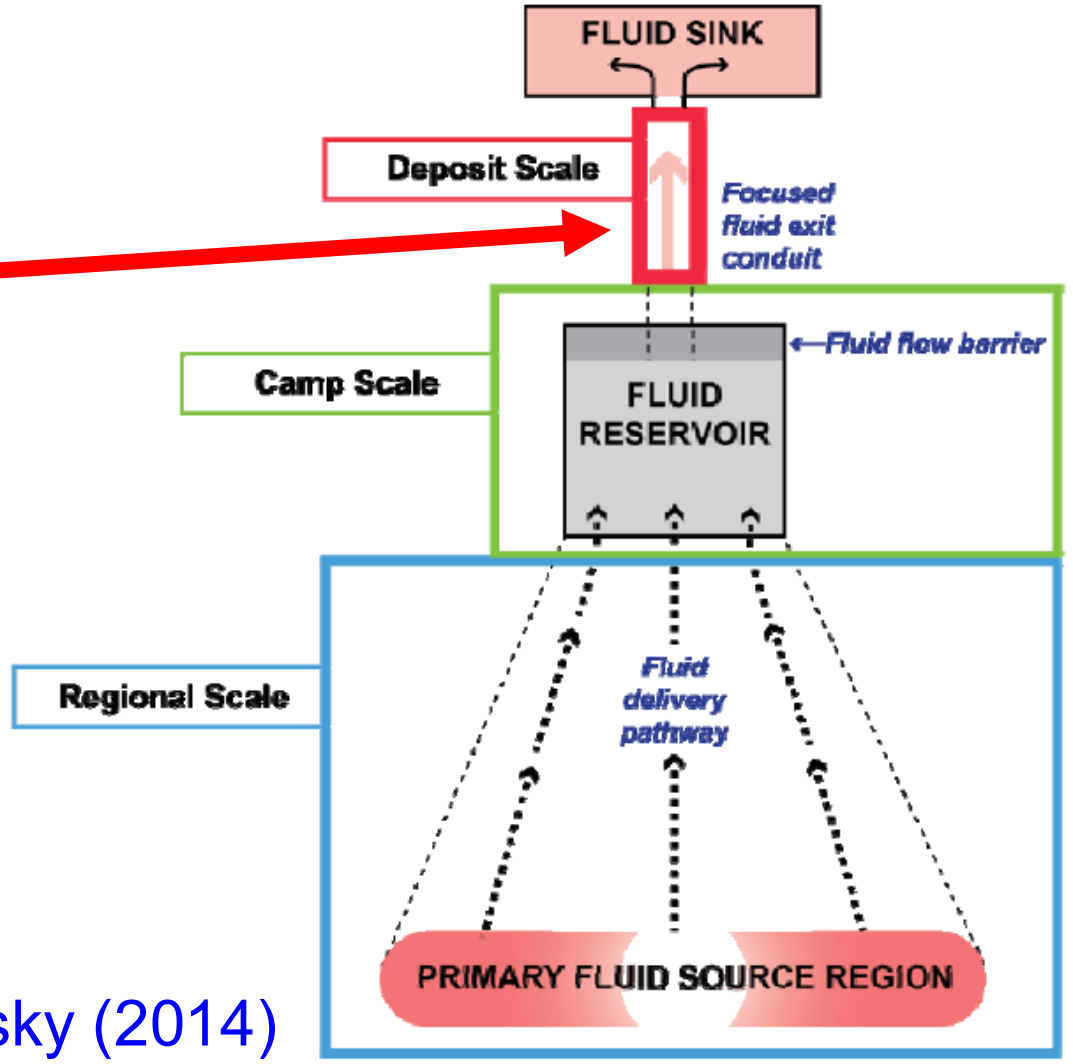

McCuaig & Hronsky (2014)

LMT survey example

Low frequency regional scale MT survey

Data from 0.06 – 0.0002 Hz (18 – 5,000 s)

Site spacing averaging 10 km

2-D inversion modelling of the sites along the marked profile

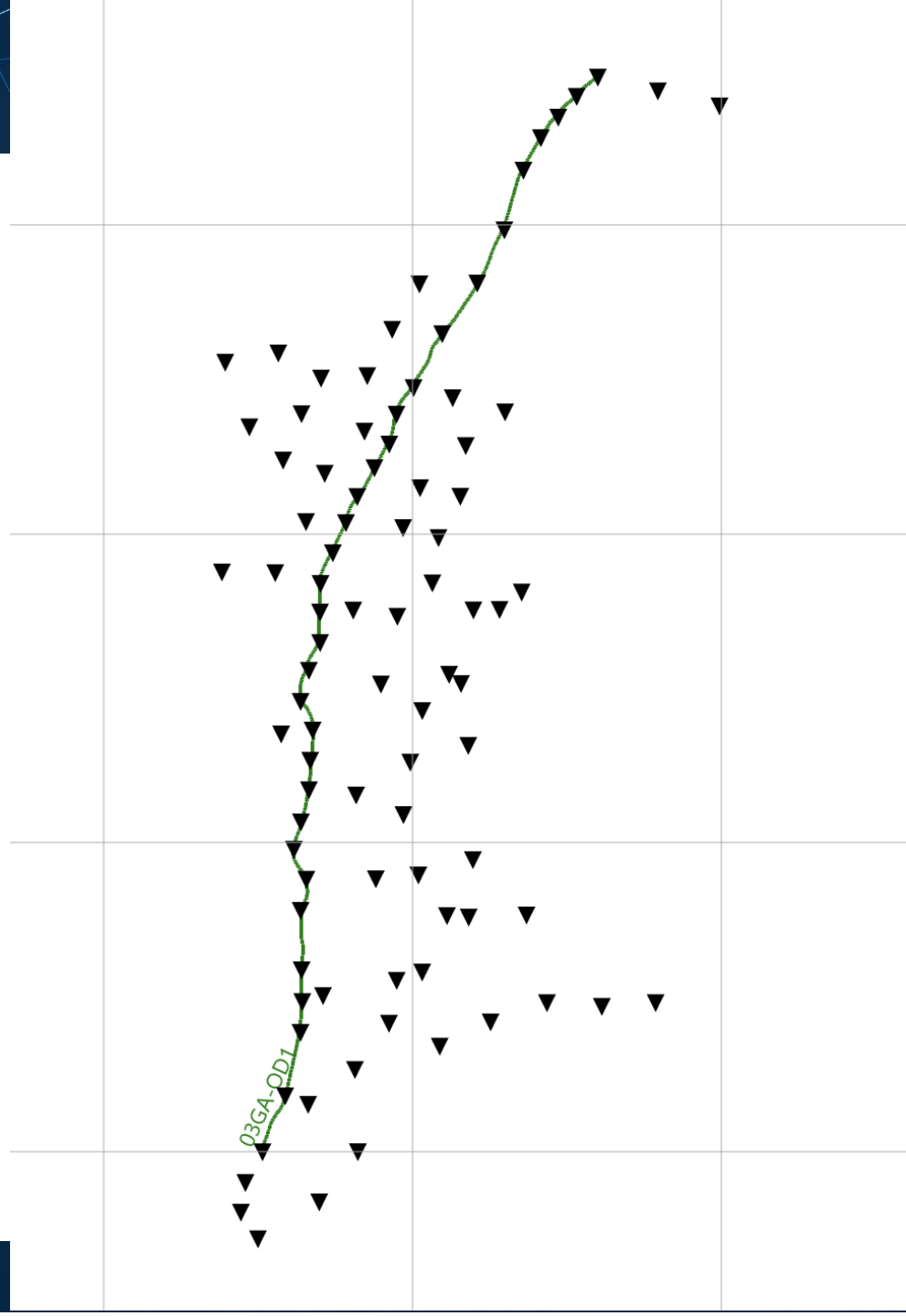

Regional model from LMT profile

2-D Model from LMT survey

2D Model of a segment of an extensive profile with sites approx. 10 km apart

LMT Data from 0.06 – 0.0002 Hz (18 – 5,000 s)

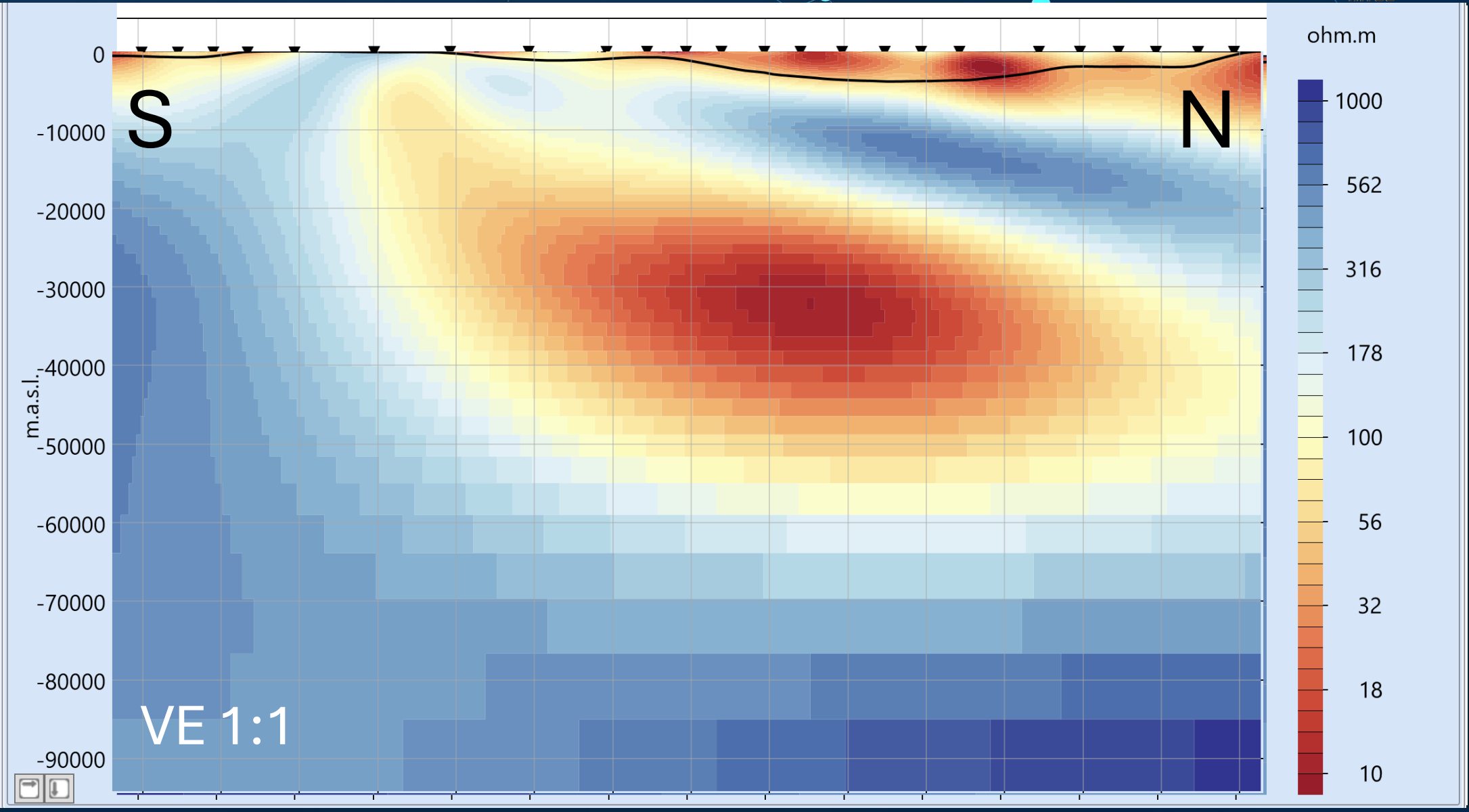

Regional model – site over top of conductor

Beautiful quality LMT data!

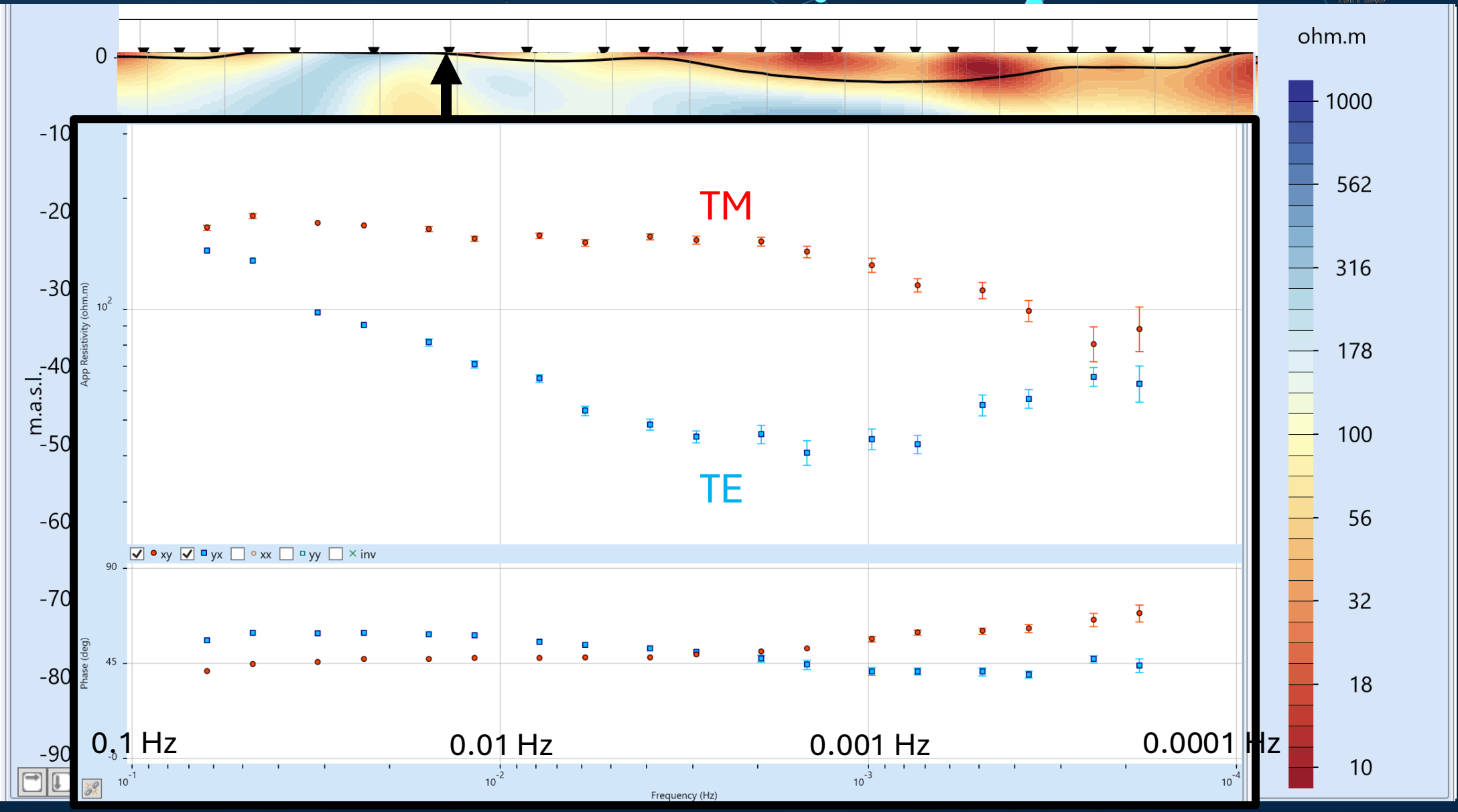

BBMT infill

Broadband MT infill (red sites)

Data from 460 Hz – 0.01 Hz

Site spacing averaging 2 km

New 2-D inversion modelling of the sites along the marked profile

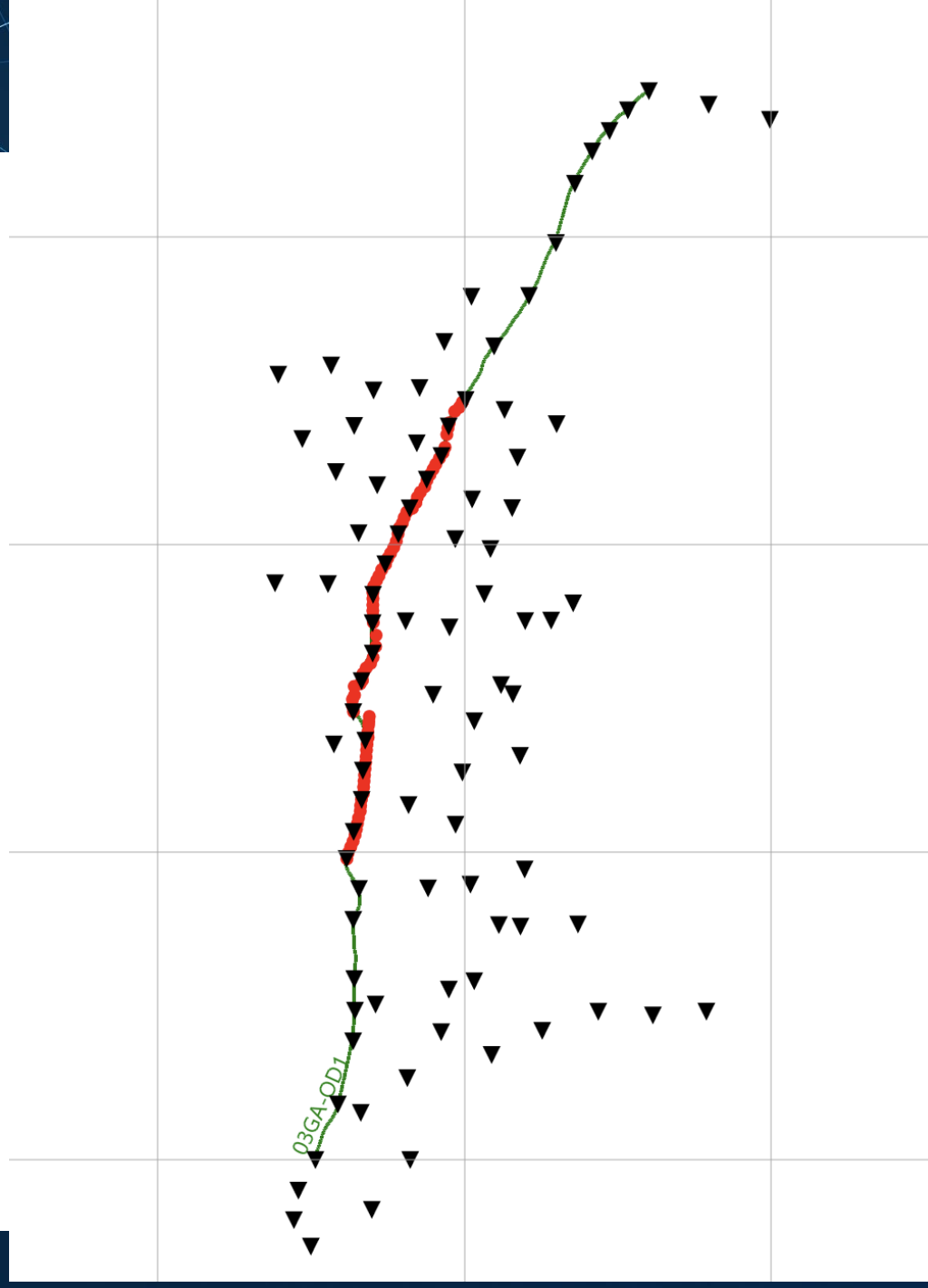

Camp scale model with BBMT infill

2-D model from BBMT infill every 2 km

BBMT Data from 460 Hz – 0.01 Hz

LMT Data from 0.06 – 0.0002 Hz

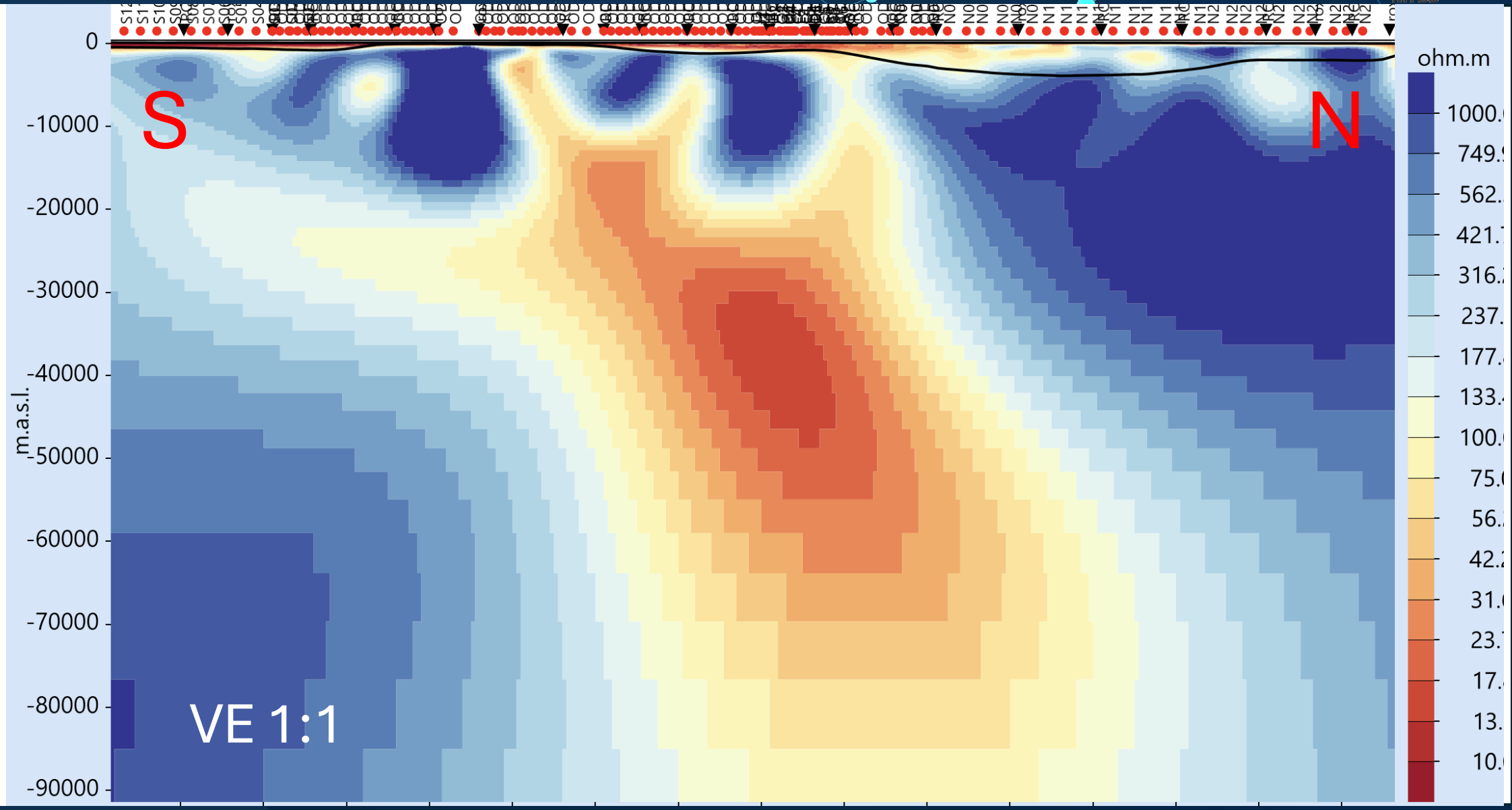

LMT+BBMT model – site on top of middle conductor

2-D model from BBMT infill every 2 km

Data from 460 Hz – 0.01 Hz

LMT Data from 0.06 – 0.0002 Hz

No AMT response due to cover!

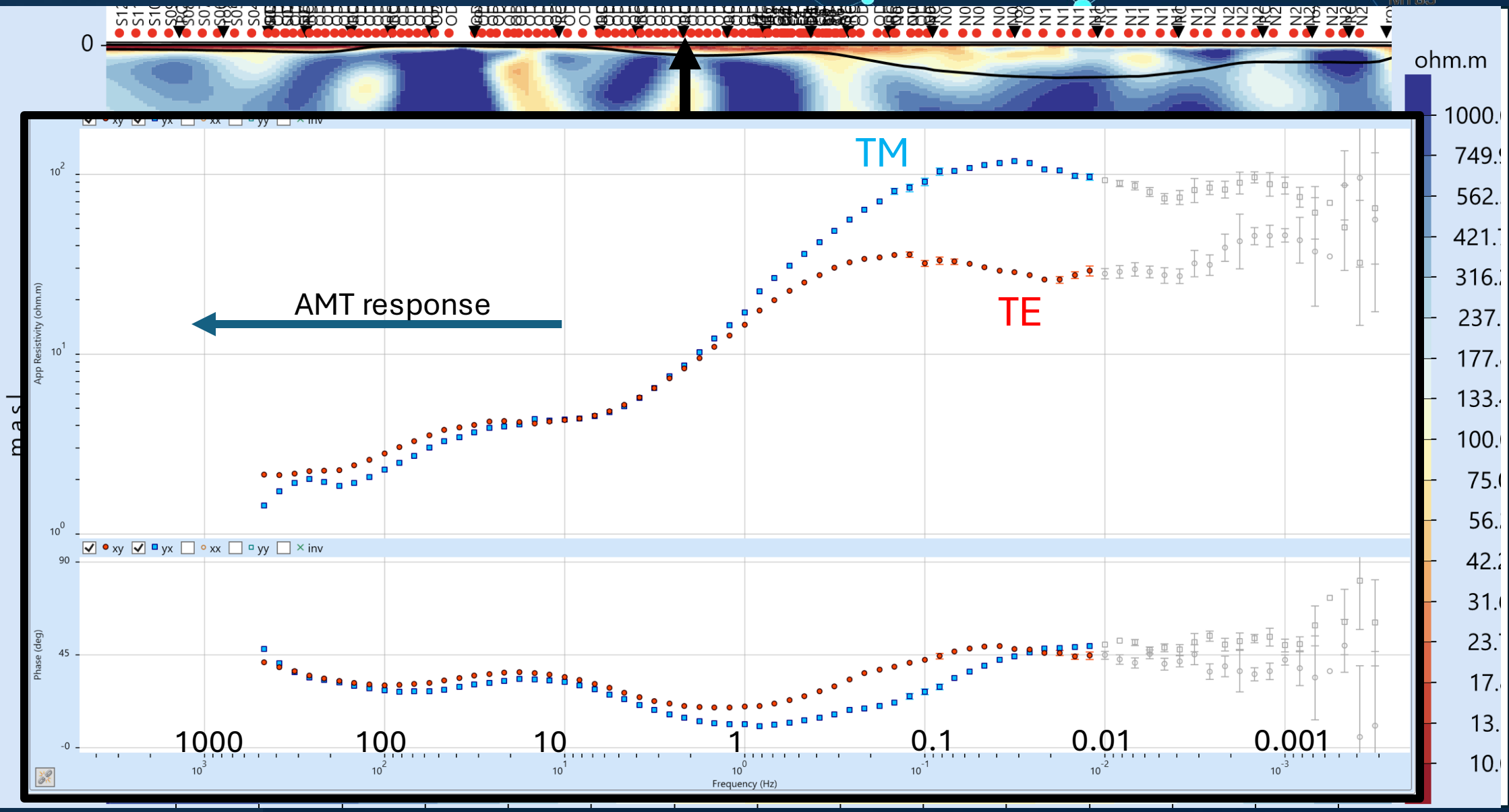

Olympic Dam and other IOCG deposits

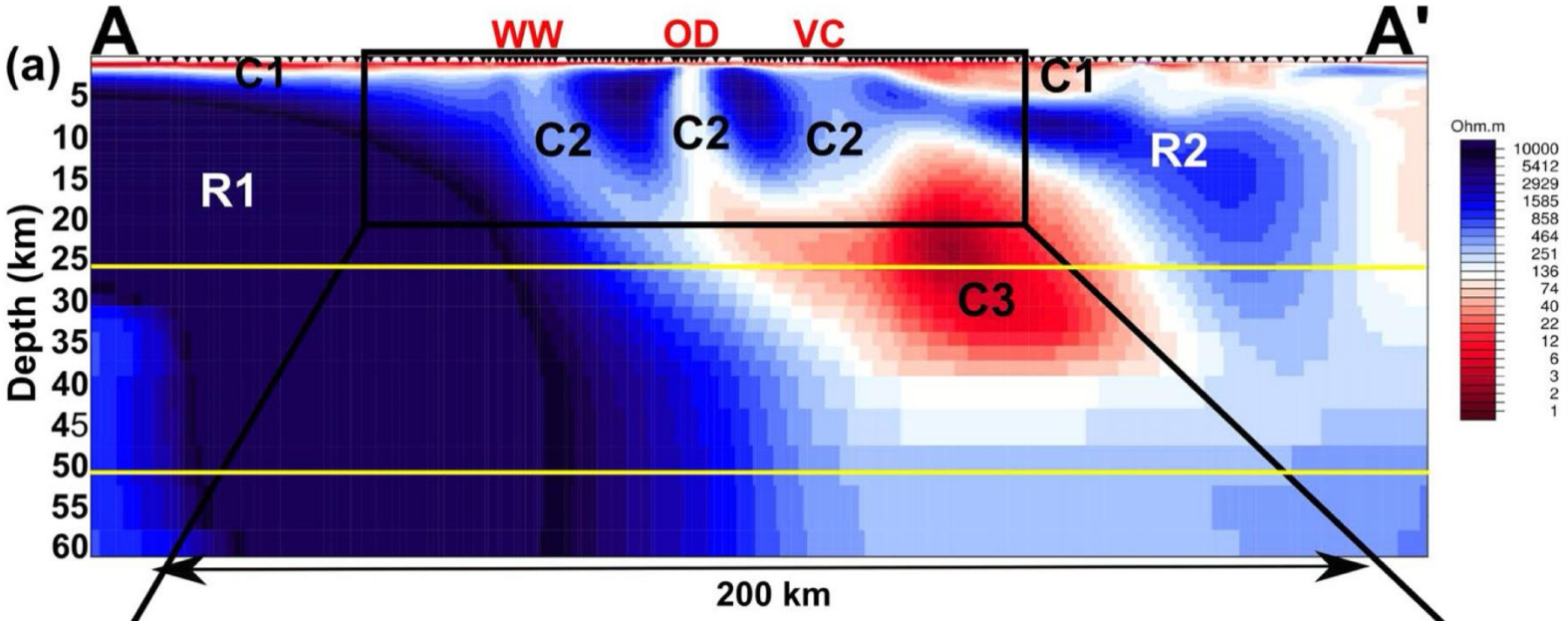

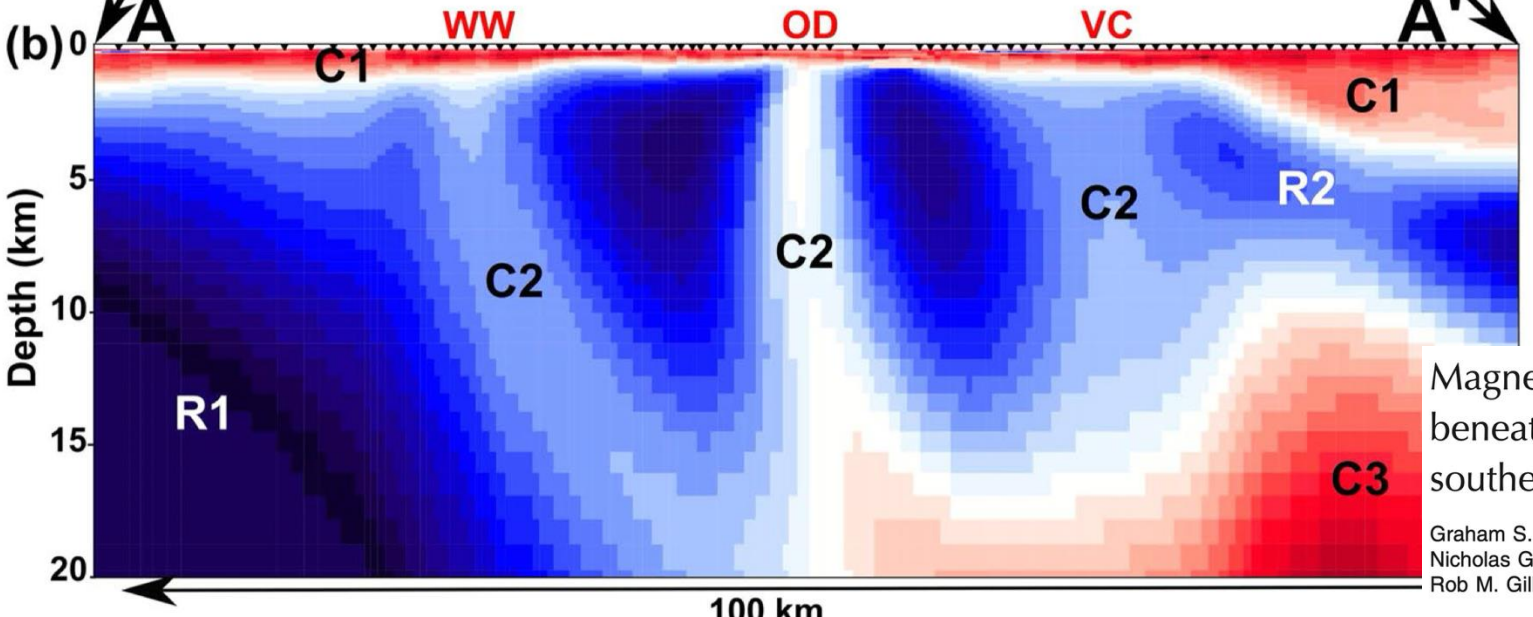

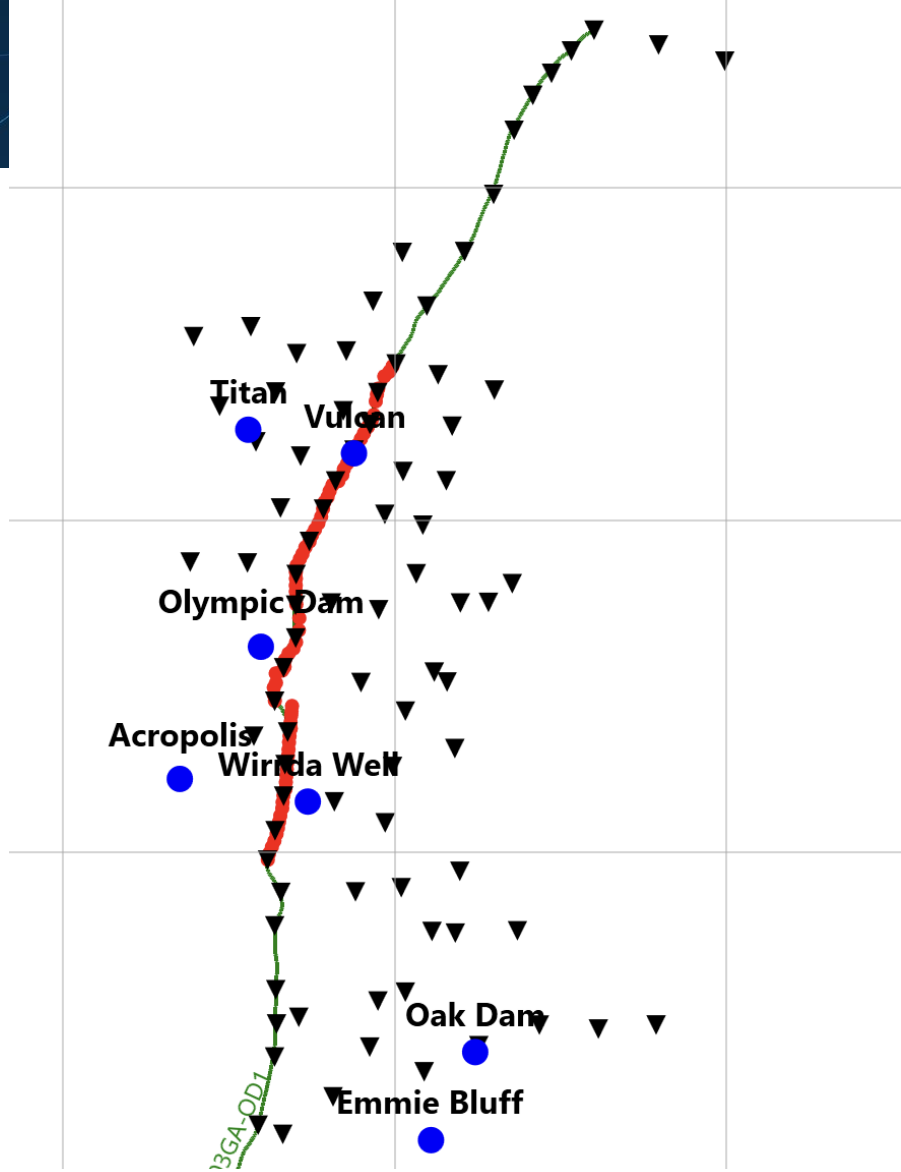

Magnetotelluric evidence for a deep-crustal mineralizing system beneath the Olympic Dam iron oxide copper-gold deposit, southern Australia

Graham S. Heinson*
Nicholas G. Direen
Rob M. Gill

Continental Evolution Research Group, University of Adelaide, DP 313, Adelaide, South Australia, 5005, Australia

Olympic Dam and other IOCG deposits

Olympic Dam is the world's type-example iron oxide-copper-gold (IOCG) deposit in the Mesoproterozoic Gawler Craton (~1.59 Ga), concealed beneath ~300–350 m of conducting cover.

Olympic Dam was discovered in 1974-75 by Western Mining Corporation (WMC) using gravity and magnetic surveys while searching for copper in buried sedimentary rocks in South Australia.

Valuation of over US$1T.

➔ **How many more Olympic Dams are out there waiting to be found???**

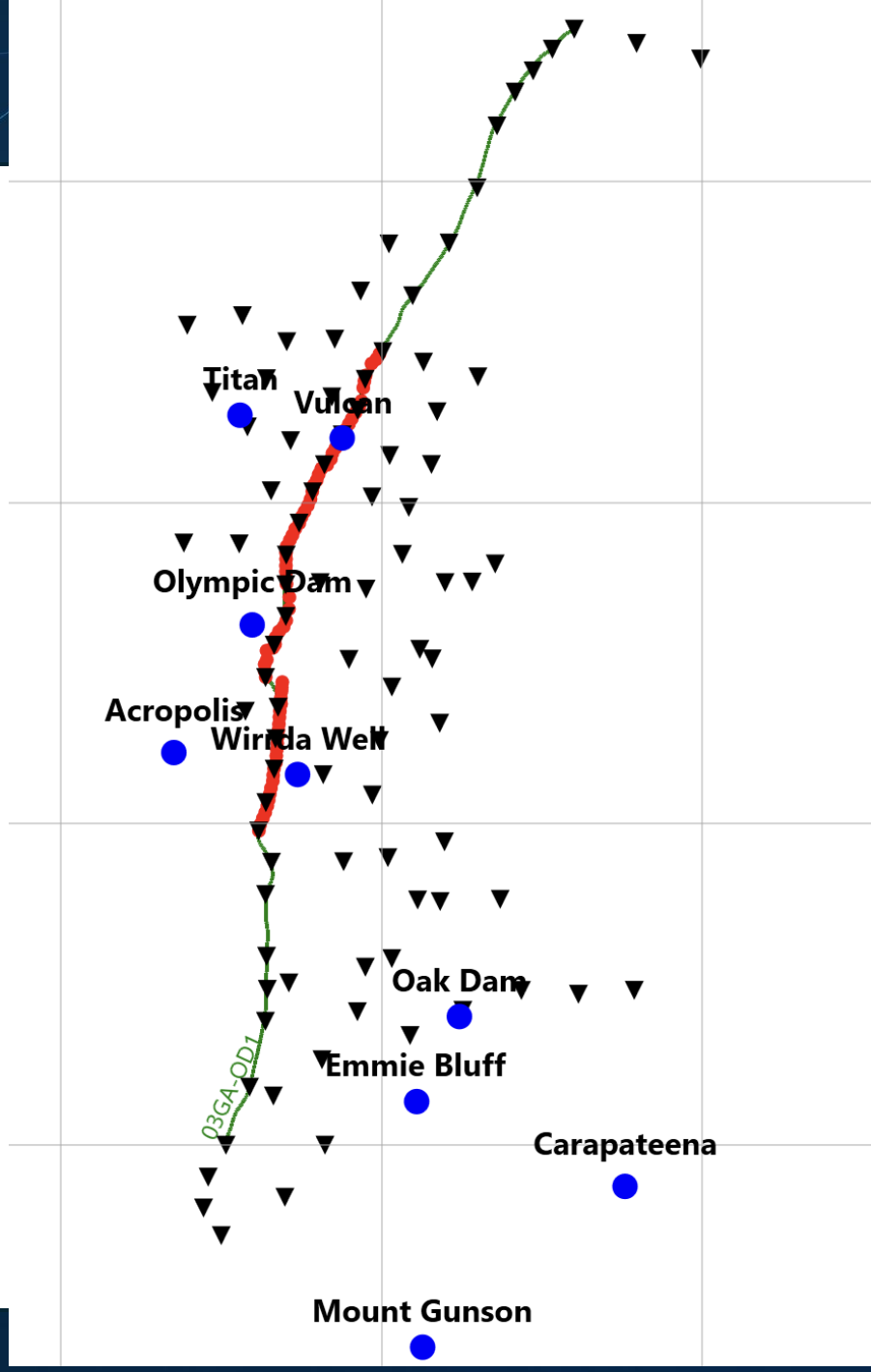

AusLAMP

The 2008 Olympic Dam (OD) MT model of Heinson et al. was one of the main driving forces behind the justification for the creation of the Australian Lithospheric Architecture Magnetotelluric Project (AusLAMP) that is acquiring low-frequency magnetotelluric (LMT) data at approximately 3,000 sites across the Australian continent on a half-degree grid spacing (approximately 55 km) during deployments of 4-6 weeks.

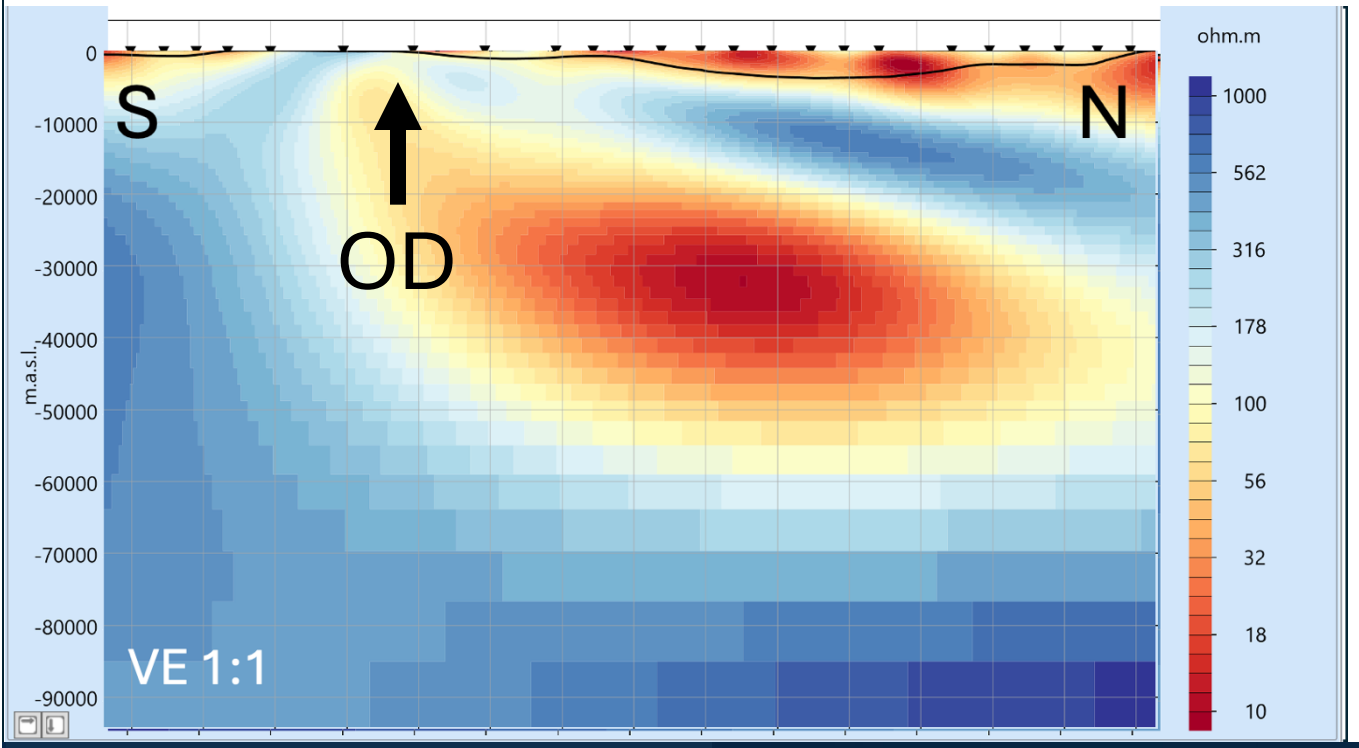

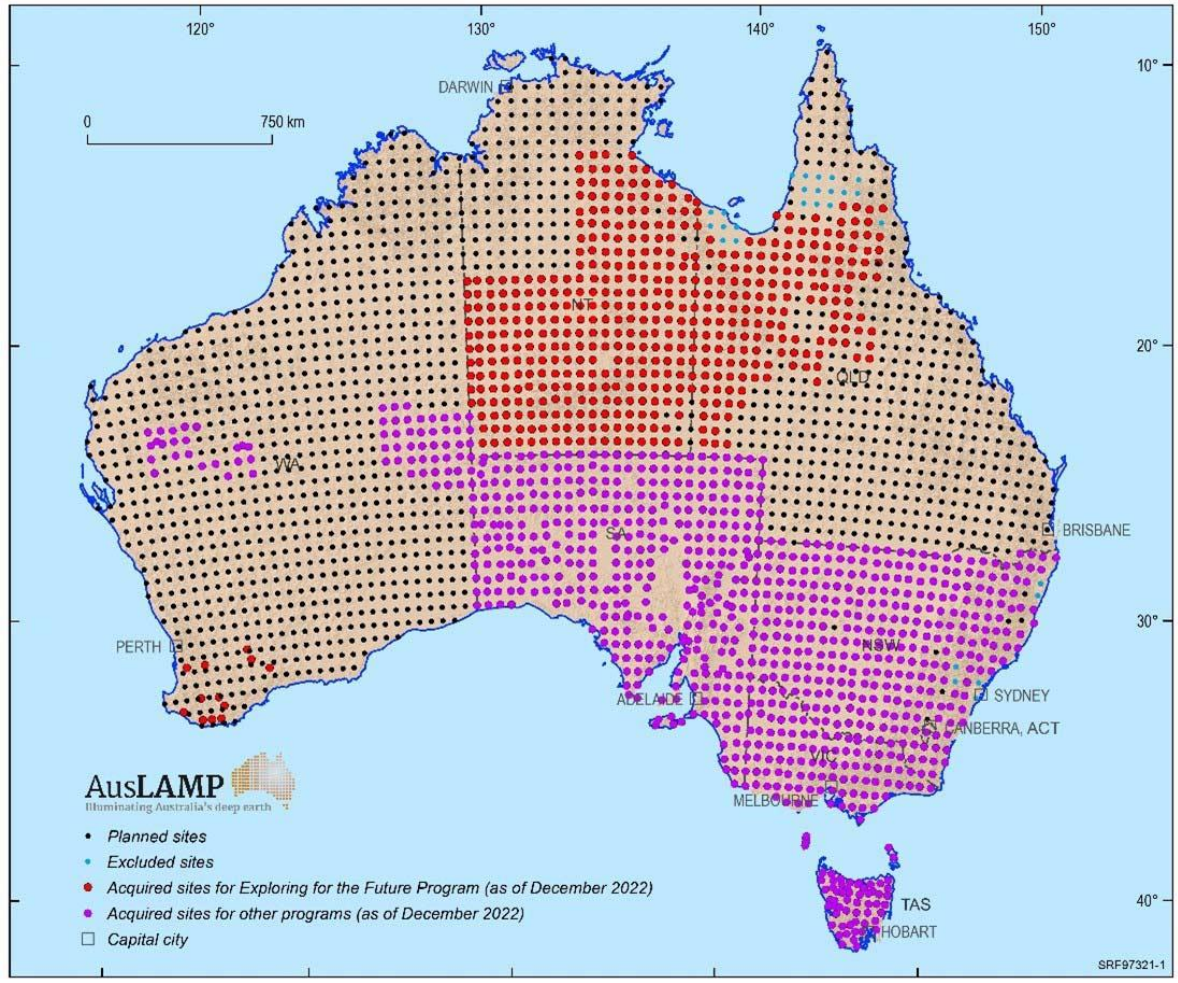

BBMT follow-up: Vulcan

Following the Olympic Dam profiling, a 3-D array was conducted over the Vulcan IOCG deposit.

100-site 3D broadband MT (100 – 0.01 Hz) square array with sites separated 1 km.

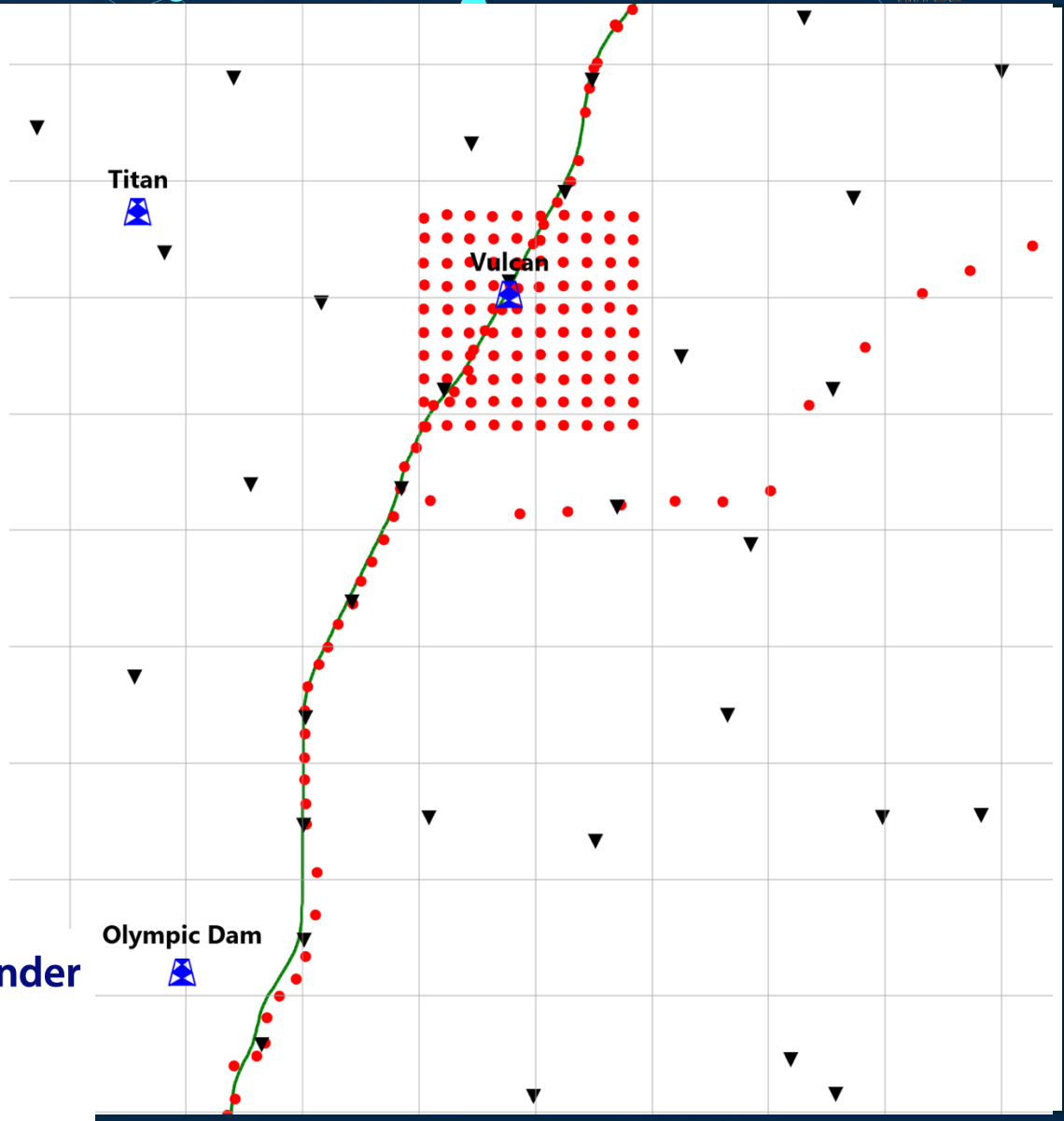

Magnetotelluric imaging of an iron-oxide copper gold (IOCG) deposit under thick cover

Ben Kay [a], Graham Heinson [a], Goran Boren [a], Ying Liu [a,b], Simon Carter [a,c], Gerrit Olivier [d,e], Tim Jones [e], Rebecca Abel [f], Lisa Vella [f] and Louise McAllister [f]

BBMT follow-up: Vulcan

Most remarkable finding is detection of anomalously low-resistivity (< 30 Ωm) zone to NE.

Appears as a vertical conductor to at least 5 km.

It is argued this feature represents the pathway of metal-rich fluids generated from pro-grade metamorphic reactions associated with 1590 Ma widespread magmatic event, and that the reduction in resistivity is due to the precipitation of graphite in reducing conditions from CO2 rich fluids.

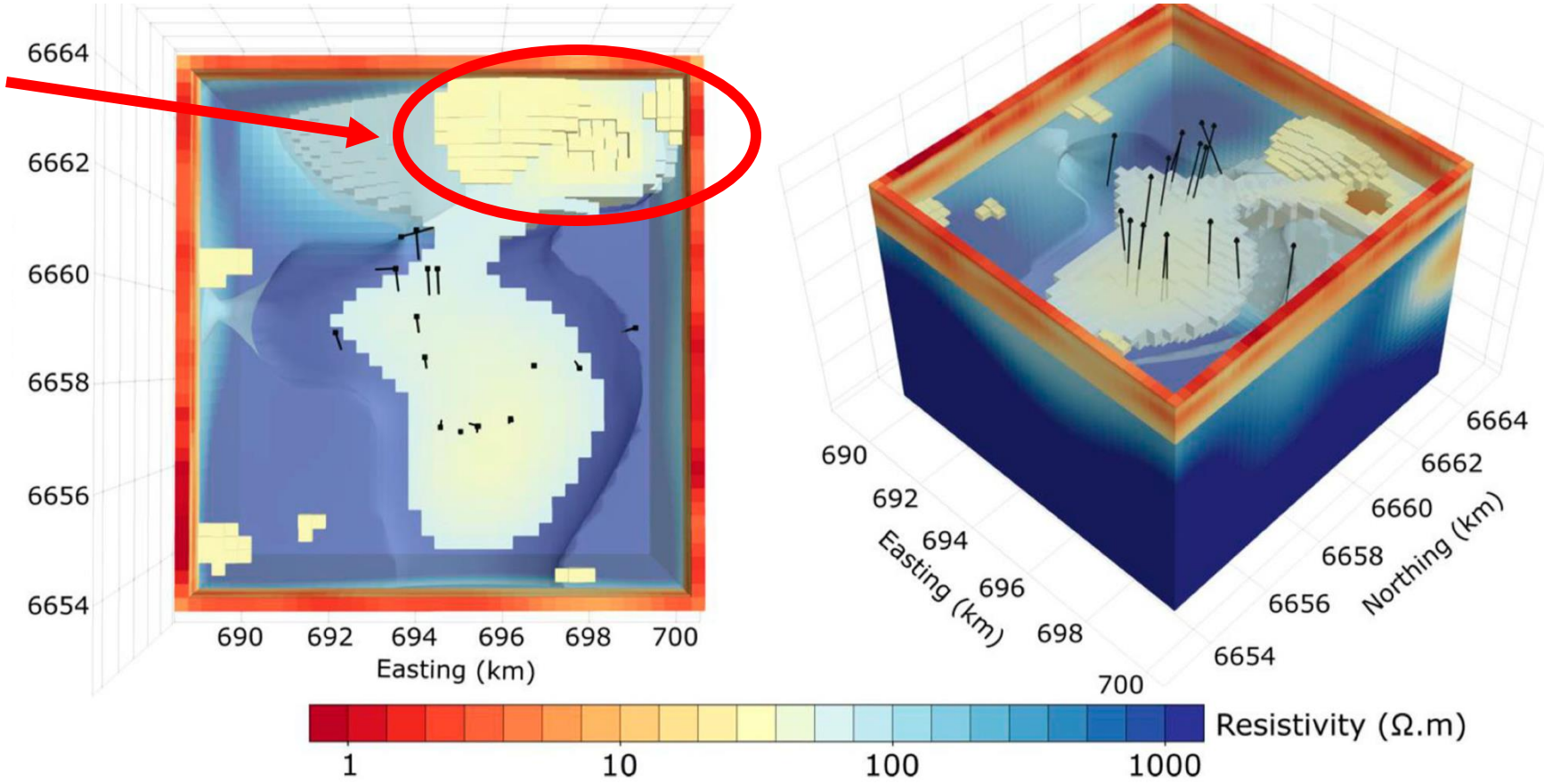

Magnetotelluric imaging of an iron-oxide copper gold (IOCG) deposit under thick cover

Ben Kay [a], Graham Heinson [a], Goran Boren [a], Ying Liu [a,b], Simon Carter [a,c], Gerrit Olivier [d,e], Tim Jones [e], Rebecca Abel [f], Lisa Vella [f] and Louise McAllister [f]

Bayankhongor Au–Cu metal belt, central Mongolia

Imaging the Whole-Lithosphere Architecture of a Mineral System—Geophysical Signatures of the Sources and Pathways of Ore-Forming Fluids

Matthew J. Comeau[1], Michael Becken[1], and Alexey V. Kuvshinov[2]

An extensive data set of 342 MT measurements has been acquired across central Mongolia over a total area of more than 450 km by 700 km.

Measurements were acquired on an array with a nominal spacing of 50 km by 50 km, as well as along denser profiles, with a spacing of 1–10 km.

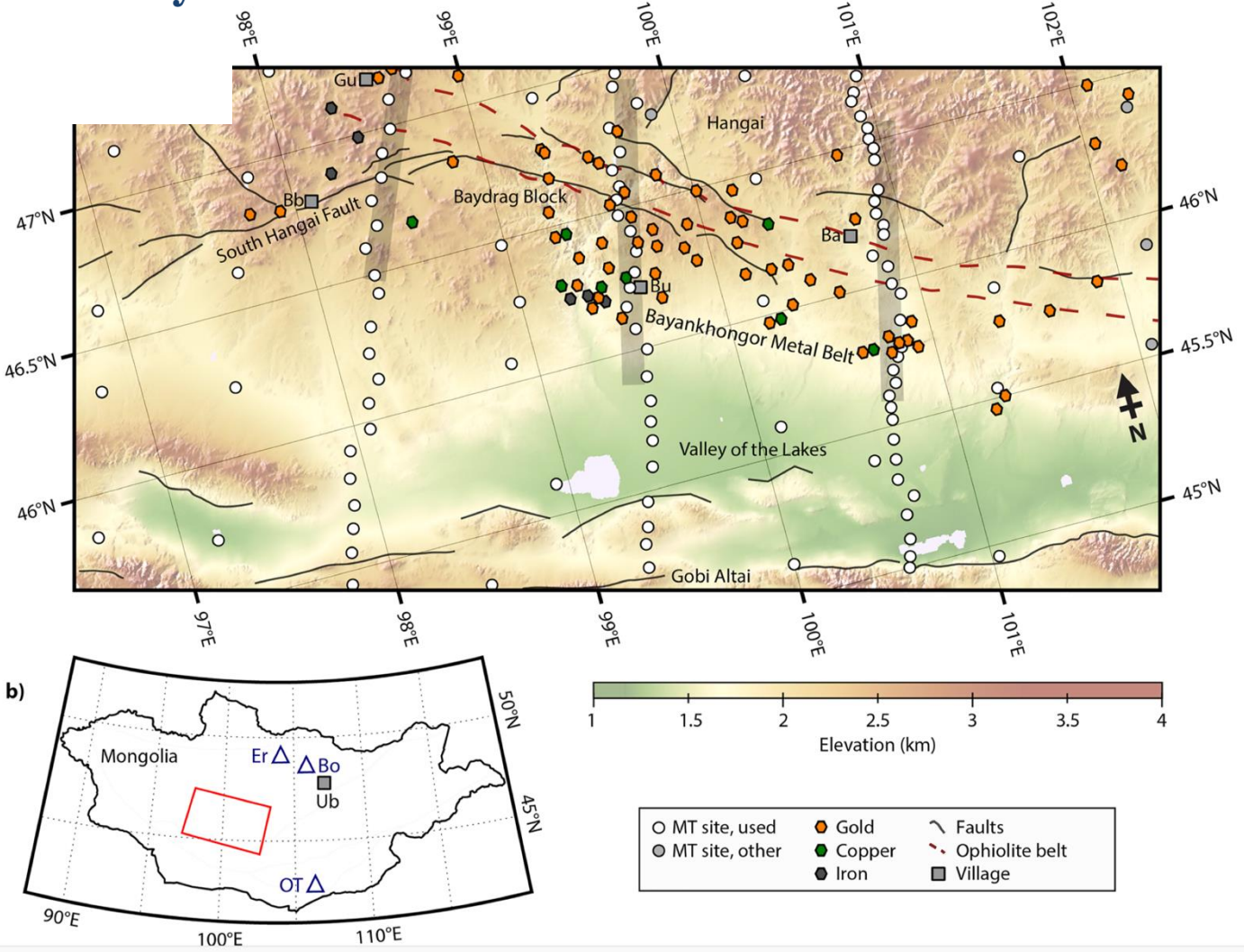

Bayankhongor Au–Cu metal belt, central Mongolia

Imaging
System—
of Ore-F

Matthew J. Co

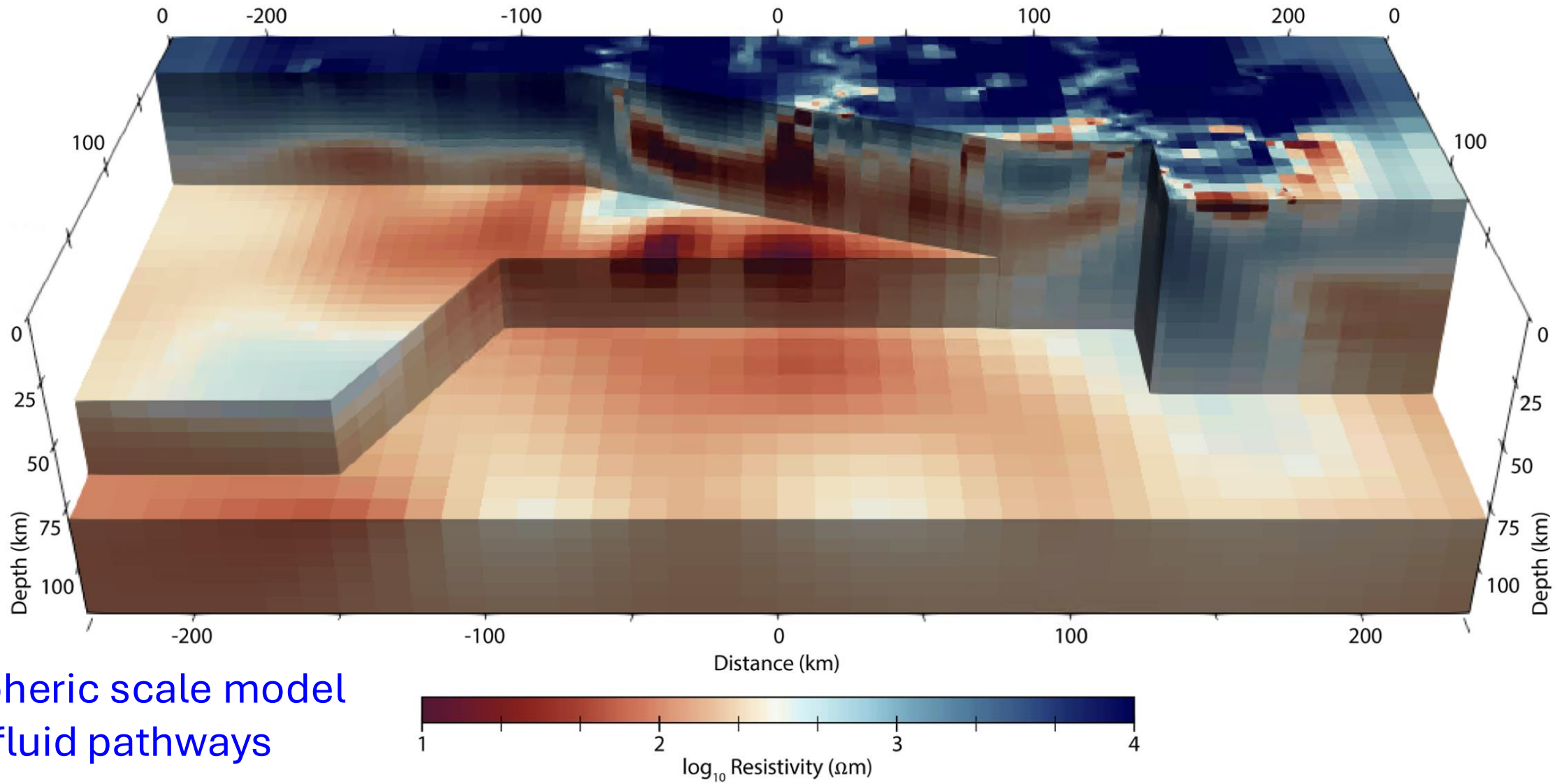

Lithospheric scale model shows fluid pathways

Examples of deposit-scale mapping by AMT

There have been many hundreds of high-resolution commercial AMT surveys over mineral deposits, but the vast majority of these are confidential.

One public example is the mapping of the Eastern Deeps at Voisey's Bay by AMT down to 1700 m.

The Voisey's Bay nickel deposit (Labrador, Canada) is a world-class magmatic Ni-Cu-Co sulphide orebody hosted in Proterozoic mafic intrusions, consisting of several zones (Ovoid, Eastern Deeps, Reid Brook) formed by sulphide segregation and accumulation at conduit–chamber margins.

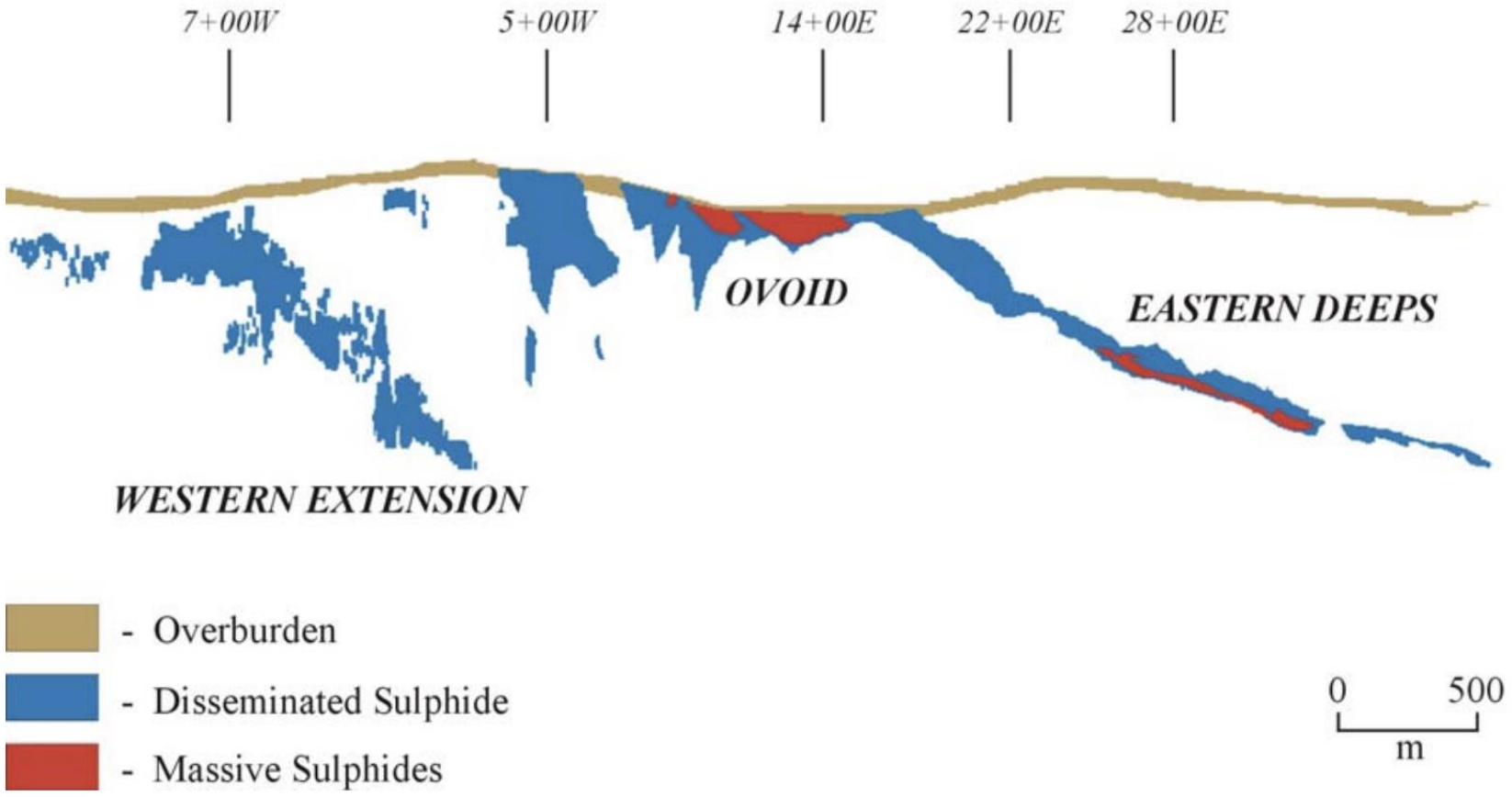

Other examples of AMT mapping of mineral deposits

Well-documented public-domain examples where **audio-magnetotellurics (AMT)** was used to map or help target mineralization (thousands of examples are confidential!)

Voisey's Bay (Eastern Deeps), Labrador, Canada — Ni-Cu-Co sulfides. AEM-constrained 2D inversion of AMT outlined the Eastern Deeps response and aided depth targeting.

McArthur River, Saskatchewan, Canada — unconformity-type U. AMT used for exploration around the deposit.

Shaxi copper deposit, Anhui, China — porphyry Cu. AMT defined 3D electrical structure in the mining area.

Layikeleke, Xinjiang, China — buried porphyry Cu. 3D AMT inversion mapped conductive architecture of the system.

Jianbeigou, Qinling belt, China — Au polymetallic. AMT combined with field geology to delineate structures guiding mineralization.

Zhugongtang, China — Fe-polymetallic. AMT imaged conductivity structure across the deposit area.

Cimabanshuo, Tibet, China — porphyry Cu. 3D inversion of AMT over porphyry system (reviewed among recent case studies).

Baohuashan, Jiangsu, China — deep Cu-Mo porphyry. AMT used to investigate deep targets beneath cover.

Darnley Bay area, NWT, Canada — base-metal potential. AMT case study demonstrating exploration workflow and results.

Sunnyside profile, Great Basin, USA — concealed targets under cover. USGS AMT profile released to test detection of mineralized bodies beneath thick overburden.

Re-processing/re-analysis/re-modelling of legacy MT data

There is value in re-processing, re-analysis and re-modelling of legacy AMT/BBMT/LMT data using modern methods

Example: A client was going to spent $5M on a drill program based on 15-year-old MT data and model.

My re-analysis and re-modelling of the legacy AMT data showed that the “anomaly” to be drilled was a data problem, and when that problem was corrected, there was no anomaly.

For a very small outlay (<1%), that client was saved $5M (and a lot of embarrassment!)

Same argument for having an independent review of any project AMT data and models prior to an extensive (and expensive) drill program

NSEM Quo Vadimus??? General

General:

MT really hasn't changed in decades. We are still doing single-station MT and calculating single station impedances **Z**.

We should be using a base station to give us the full Tipper matrix **T** and calculating inter-station horizontal magnetic field transfer functions **H**

Theoretically, ALL of these, **Z**, **T** and **H**, contain the same information and will give us the same subsurface.

BUT, in the presence of noise all of them will be differently sensitive and have different resolution properties, so will improve resolution

Also, **T** and **H** are unaffected by galvanic distortion of the electric field

NSEM Quo Vadimus??? Instrumentation

Instrumentation:

Need to get a LOT more sensors on the ground, preferably e-fields.

- Cheaper equipment (need to manufacture thousands of systems)
- Quicker installation (capacitive electrodes for high freqs)
- Drone deployments of e-fields – copy the Lunar Magnetotelluric Sounder (LMS)?

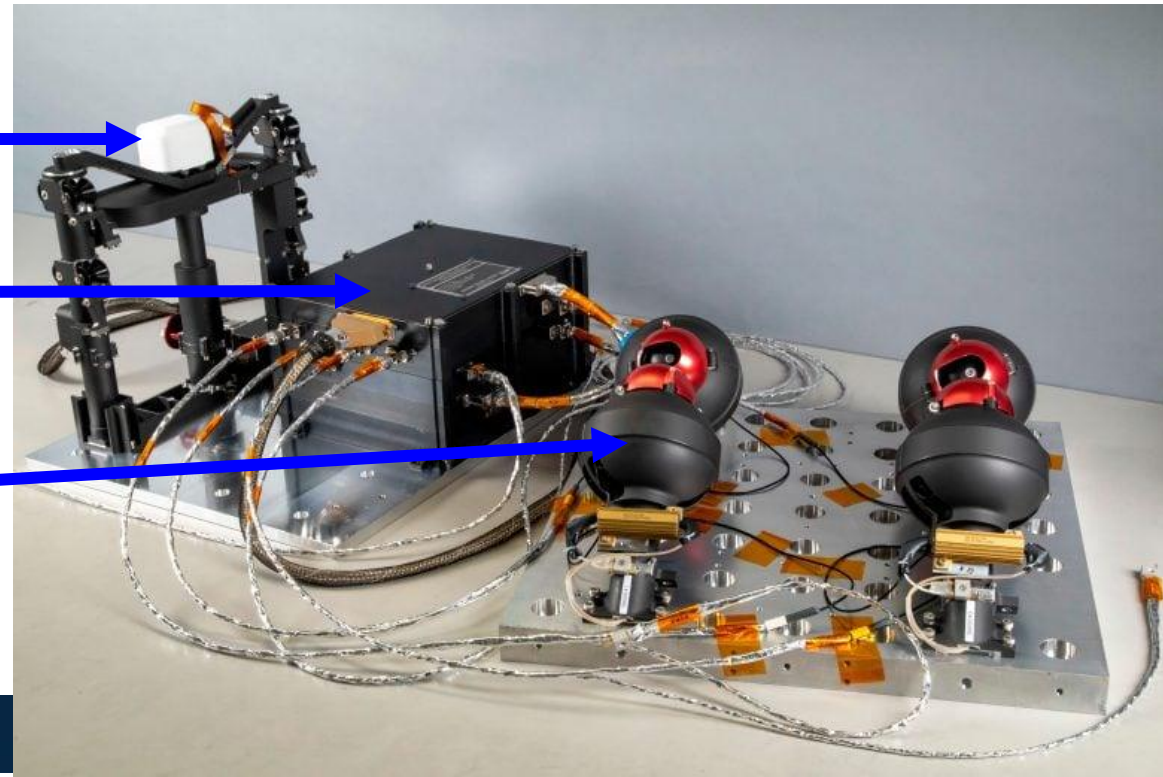

NSEM Quo Vadimus??? Processing

Processing:

Need to see a new quantum leap in our processing.

- Robust methods advanced in the 1980s (LTS: Jones and Joedicke, 1984; M-regression: Egbert and Booker, 1986; Chave et al., 1987; D^+: Larsen et al., 1996)

Jones et al. (1989)

Method	Description	Source
1	conventional spectral analysis	Bahr
2	conventional spectral analysis	Auld
3	conventional spectral analysis	Jones
4	weighted cascade decimation	Jones
5	remote reference	Chave
6	robust cascade decimation	Jones
7	robust	Egbert
8	robust remote reference	Chave

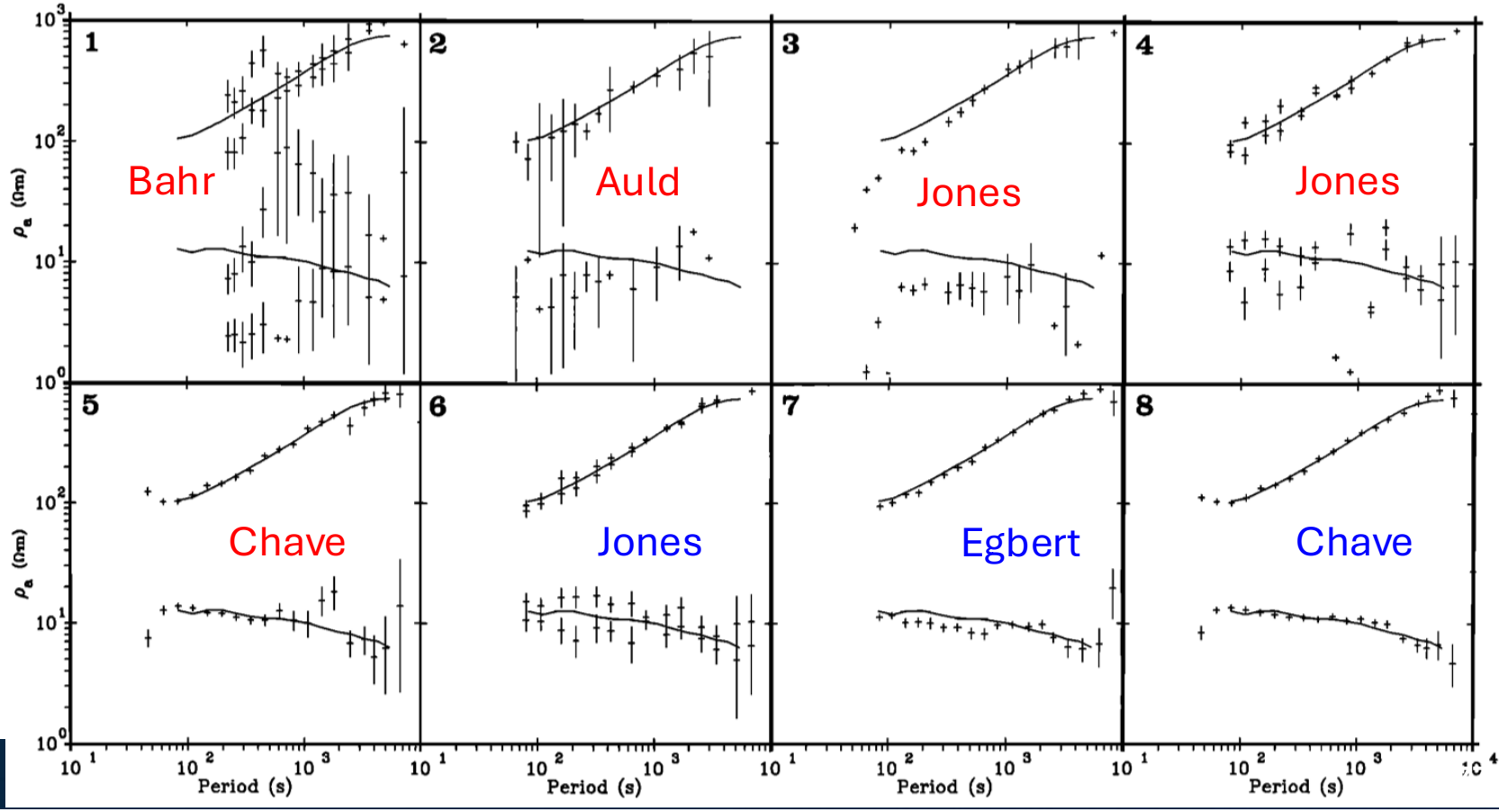

NSEM Quo Vadimus??? Processing

Processing:

Need to see a new quantum leap in our processing.

- Robust methods advanced in the 1980s (LTS: Jones and Joedicke, 1984; M-regression: Egbert and Booker, 1986; Chave et al., 1987; D^+: Larsen et al., 1996)
- BUT as cultural noise becomes more pervasive and as we want to acquire NSEM data within brownfields areas, we need to have another quantum leap in processing
  - Tried wavelets with some success (Garcia and Jones, 2008) →
  - Perhaps an ideal issue for AI?

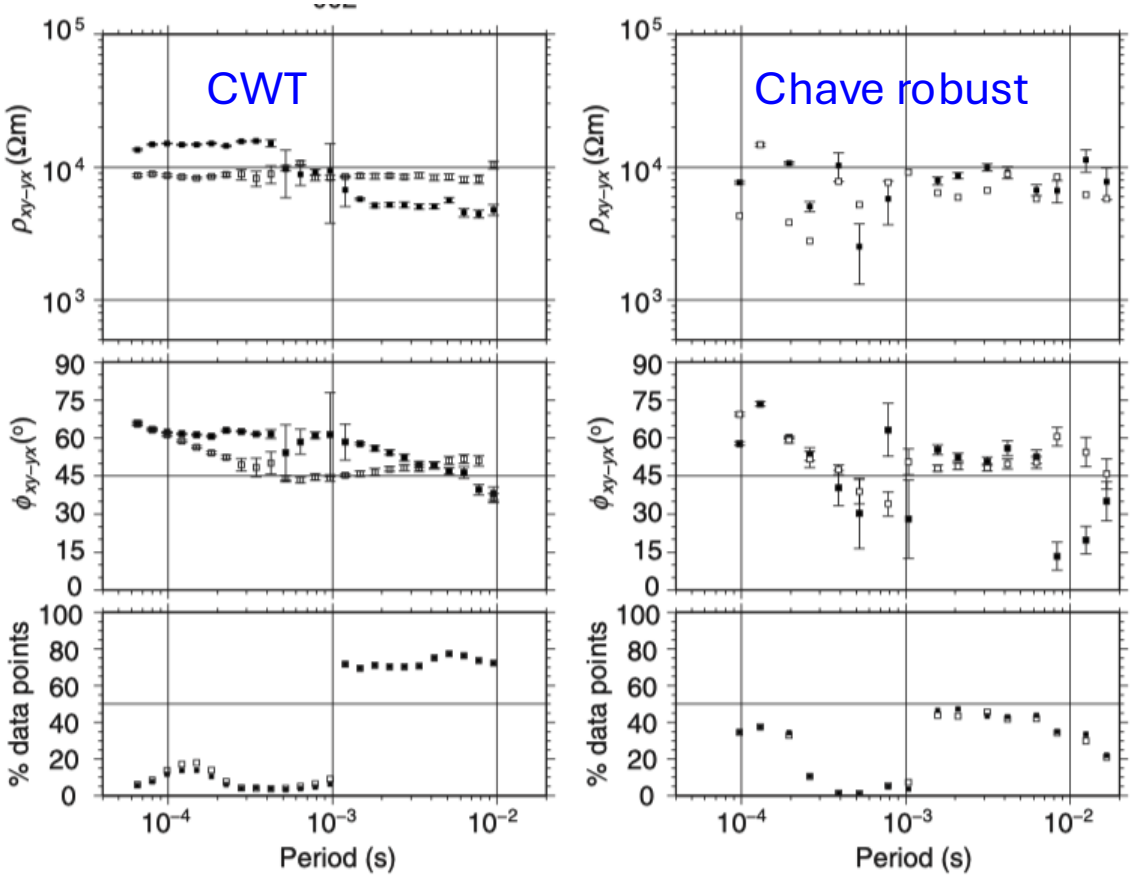

NSEM Quo Vadimus??? Analysis

Analysis:

Need to see a new quantum leap in our analysis of MT and Tipper estimates.

- Understanding the effects of galvanic distortion (primarily but not exclusively of the e-fields) by near-surface inhomogeneities brought us a long way in the late-1980s.
    - The Groom-Bailey approach, and the multi-site, multi-frequency extension by McNeice and Jones, gave us tools to determine the dimensionality and directionality within the statistical errors of the data
- BUT, we now need more tools to discern possible anisotropy effects

NSEM Quo Vadimus??? Modelling/Inversion

Modelling/Inversion:

Need to see a new quantum leap in our modelling and inversion of MT and Tipper estimates.

- We have come a LONG way in the last two decades, with a number of robust 3-D NSEM inversion codes now available (some freely, some commercial)
- BUT, the subsurface is not made up of isotropic rectilinear blocks or even isotropic cells within unstructured meshes
- Also, the numerical accuracy of the forward solutions for more and more complexity within the subsurface begs the need for a suite of control models
- Also, also, everything is just too slow, and deterministic
- We need unstructured mesh probabilistic inversion approaches in 3-D with general anisotropy
    - Have to wait for quantum computing…

Conclusions

1. Natural source EM methods have significant advantages over controlled source EM methods.
2. Magnetotellurics can contribute to exploration for minerals at all scales, from regional to local to deposit scale.
3. Airborne natural source EM (ANSEM) methods can rapidly cover large areas, but are only useful if:
    1. the target responds at the frequencies of the methods
    2. the target geometry is such that it generates sufficiently large anomalous magnetic fields (e.g. spheres have low anom. mag fields)
4. Combining ANSEM with some MT sites improves subsurface resolution significantly
5. There is value in re-processing/re-analysis/re-modelling of legacy data

Acknowledgements

- Very many thanks to SAGA for the invitation to present this paper
- I am indebted to all of my mentors, all of my peers and colleagues, and all of my students over my 50+ year career. I have learned something from everyone.
- I especially thank Professor Graham Heinson for providing the Olympic Dam example
- And thank you, the audience, for listening to my presentation.